REMOTE SENSING AND GIS ASSISTED INTERPRETATIONS FOR TECTONO-GEOMORPHIC EVOLUTION OF SAMBHAR LAKE IN THAR DESERT, RAJASTHAN

a thesis submitted

in partial fulfilment of the requirements

for the degree of

Master of Technology

by

Vasanth Kumar Madapuram

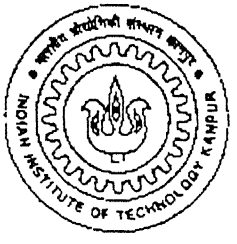

to the

DEPARTMENT OF CIVIL ENGINEERING

INDIAN INSTITUTE OF TECHNOLOGY, KANPUR

March, 2000

CERTIFICATE

It is certified that the work presented in this thesis entitled **"REMOTE SENSING AND GIS ASSISTED INTERPRETATIONS FOR TECTONO-GEOMORPHIC EVOLUTION OF SAMBHAR LAKE IN THAR DESERT, RAJASTHAN"** has been carried out by **Mr. Vasanth Kumar Madapuram** (Roll No. 9810331) under our supervision and has not been submitted elsewhere for a degree.

Rajiv Sinha

(Rajiv Sinha)
Asst. Professor
Department of Civil Engineering
Indian Institute of Technology
Kanpur-208016.

Onkar Dikshit

(Onkar Dikshit)
Asst. Professor
Department of Civil Engineering
Indian Institute of Technology
Kanpur-208016.

Acknowledgements

I extend my profound sense of gratitude to my inspiring guide, Dr. Onkar Dikshit for his clear insight and valuable guidance on various image processing concepts that were required for the present work. He was always ready to share his ideas on various aspects whenever it was required. I also thank him for providing me very good resources for my work. I enjoyed great liberty and freedom of thought with him during my work.

I am deeply beholden to Dr. Rajiv Sinha, whose timely cooperation and constructive suggestions made this work successful. He always helped me whenever I got into confusion with some geological issues. His clear insight into the problem has helped me a great deal in arriving at important conclusions in the present work.

Also, I thank all the teachers at IITK who have helped me enrich my knowledge.

I thank Vikrant Jain for the exchange of ideas I have had with him in regard to my work.

I am greatly indebted to Sudhir, Suresh, Maruthi, Reddy, Monika, Sridhar, Satya Pavan for their immeasurable help and cooperation during the making of this report.

Thanks are also due to Aditya and Amit who made my working very comfortable especially, during the last stages of my work when I was fully occupied with the system.

My heart full thanks to Mishraji and Ram Kishan for the loving, caring and sharing they have shown during my stay here.

Finally, I thank all other friends of mine who painstakingly stood by my side through thick and thin.

Vasanth Kumar. M

CONTENTS

LIST OF PLATES

LIST OF FIGURES

LIST OF TABLES

ABSTRACT

The Sambhar lake spreading over three districts, namely Jaipur, Ajmer and Nagaur of Rajasthan forms the eastern fringe of the Great Indian desert and is bounded by neotectonically active Aravalli range. There are many speculations in connection with the evolution of this lake. An attempt has been made to study the physical aspects of this lake's evolution. Diverse information about this terrain regarding the topographic parameters (height, slope, aspect etc), the aeolian and fluvial landforms (buried channels, sand dunes, other active drainage, fluvial deposits etc) and structural aspects (lineaments, faults) was obtained from the satellite imagery of IRS-1B LISS-II by the use of advanced image processing techniques like thresholding. A detailed methodology has been proposed to generate various thematic layers of aforementioned information. The information obtained in this way was interpreted in a GIS environment in the light of the past research in this area to understand the various processes that could have been responsible in the physical evolution of the Sambhar lake. The main important physical aspects of evolution of Sambhar lake enquired into are (a) cause for development of an elongated depression, (b) maintenance of such a depression subsequently, and (c) source of water and sediment for the depression to form a lake. The first aspect concerns itself with the 'tectonic' part and the remaining two aspects are related to the 'Geomorphic' part.

INTRODUCTION

1.1 General

Arid and semiarid lands, make up over one third of the landmasses of the earth (Dregne, 1986) where rainfall is scarce to non-existent. In terms of aridity, there are major differences between deserts. Every desert is unique, and even in the same desert some places are different from others. Therefore, it is rather improper to make generalizations about various conditions in it and each area must be considered separately and dealt with as a microcosm. The deserts were not always as dry as there are today. Wet periods alternated with dry episodes throughout the Quaternary. The basic features of the terrain in deserts and semiarid lands are formed by water erosion in the geological past. These features are often overlooked in the study of what is presently an arid/semi-arid, wind-sculptured environment. Thus, for a better understanding of any desert environment, a clear insight into its geological past is essential.

Wind is the major agent of erosion and deposition in today's deserts. Features of wind erosion and deposition must be fully understood. Rainfall may seldom occur in deserts but may then be violent and lead to widespread fluvial-lacustrine processes. In semi-arid lands, fluvial activity also plays a predominant role. Few landforms due to fluvial activity include fans, dry river channels and lakes. The desert lakes (playas) are generally salty, shallow and temporary and constitute sources of mineral wealth such as salts formed by evaporation.

The saline lakes are as much a part of the desert landscapes as the sand dunes are. Both the features develop under the conditions of aridity. While the sand dunes form through aeolian process, involving wind action, the major constraint for the evolution of saline lakes is the low to very low precipitation with correspondingly very high rate of evaporation. Few important aspects of evolution of the saline lakes are: physical evolution concerning mainly the cause of lake depression and that being filled by some

drainage activity and chemical evolution concerning the cause of salinity and the chemical imbalance of the lake water. Topographically, the saline lakes occupy the most depressed part of the isolated basins. Another characteristic feature of the saline lakes is the centripetal drainage system of ephemeral type. Aridity being the prime factor in the development of saline lakes, it may be pertinent to inquire when actually such a condition had set in. Remnants of fluvial lakes occupy closed basins in arid regions characterized by internal drainage. In such climatic regions the rivers, if present, never reach the sea. These are termed endorheic areas because they are under-drained by streams. In arid and hyper-arid regions, the buried channels are of added importance, owing to acute water scarcity conditions. The realm of desert limnology, by definition, coincides with regions where closed basins are found (Cole, 1979). Sambhar, Didwana and some other lakes of Rajasthan are characterised by endorheic drainage, with negligible depth, containing only quarternary deposits (Biswas *et. al.*, 1982).

A variety of aspects related to lakes have been looked into in the past few decades. However, very little attention has been centered on the geological aspects of lakes. All lakes are transitory in the geologic record because the very nature of the lake basin, a topographic low completely surrounded by higher areas, ensure s its inevitable destruction. Thus, many lake basins, often during the short life span of a man, pass through a recognizable cycle of destruction, from lake to pond, marsh, swamp or to dry land (Reeves, 1968). Reeves suggests that, from a geologic standpoint, future research will focus on: the refinement of dating techniques, further documentation of various genetic types, morphologic and depositional responses of the lakes to climatic changes, morphologic changes in playa lakes with time, factors controlling specific locations, the influence of regional structure, the relationship of incipient playa basins to large playa lakes, and the relationship of playa basins to large alkaline lake basins (Reeves, 1997).

1.2 The Sambhar Lake Ecosystem

Sambhar lake ($26^0 52'$ N – $27^0 02'$ N, $74^0 54'$ E – $75^0 14'$ E) is some what elliptical in shape with its long axis running east-northeast to west-southwest. Several brackish and freshwater wetlands (mostly man-made) are scattered around the lake: Devadani (Devyani) tank to the east, large ponds near Jhapok village, Lake Phulera to the south of Sambhar lake, and numerous waterbodies along the course of Mendha river are

notable examples. These satellite wetlands range in size from less than a hectare to a few hectares, and are generally shallow – often less than a metre depth.

Most of the Sambhar lake basin lies in Jaipur and Nagaur districts, and only a small portion in Ajmer district. To the northwest and west of the basin, the Aravalli ranges rise abruptly to heights exceeding 500 m (highest peak: Patalia Dungar, 742 m), with outcrops in the form of hillocks scattered along the northern and western periphery of the lake. In fact the Sambhar lake basin which occupies a depression in the Aravalli schists, appear like a valley within the Aravalli ranges. It is a shallow lake, reaching only about 3 m at its deepest, with an average depth not exceeding 0.61 cm. The maximum length of the lake basin is 22.5 km, while the width ranges from 3.2 km to 11.2 km. The lake bed (360 m above sea level) is almost flat, with a slope of less than 10 cm per km.

The lake has an extensive catchment spread over 7560 sq km, most of which lies to the north and northeast of the lake, extending up to Sikar district. It is fed by four ephemeral streams, Mendha, Rupangarh, Kharian and Khandel, besides numerous rivulets and surface runoff. River Mendha, the largest feeder stream, originates in Sikar district and thus moves southwest and west before entering the lake from the north. The river drains an area of about 3600 sq km (about half of the total catchment of Sambhar lake), most of which is a sandy, undulating plain, framed to the north, west, and east by residual Aravalli outcrops. Remote sensing studies, using Landsat False Colour Composites(FCC), have shown that the Mendha has changed its course in the bygone years, as well as in the recent past. The catchment area is subjected to sand encroachment and to land transformation by agricultural activity. Several paleochannels lie buried beneath the sand. For instance, some segments of the Anokhi and Ranoli – two major tributaries of the Mendha – have disappeared under sand during the last two decades (Saint *et. al.*, 1989). Aeolian processes, particularly the movement of sand, thus play a major role in the catchment, influencing the runoff and river flow entering the lake. One view is that the gaps in the Aravallis (Sambhar gaps) allow the movement of windblown sand from the west of the range, its deposition in the area being the cause of increasing desertification (Dhabariya, 1984).

River Rupangarh (Rupnagar), also draining into Sambhar, rises in the south near Ajmer city and runs northeast to enter the lake from the south. Its catchment, spreading over

625 sq km, is mostly rocky. The Kharian is a smaller stream entering the lake from the northwest, while the Khandel, another small ephemeral stream, drains a limited area to the east of the lake before debouching into the Sambhar basin.

The Sambhar lake area is situated over a transitional area with arid climate at the west and semiarid climatic zone towards the east of it. The Aravallis demarcate the boundary between the western arid and eastern semi-arid climatic zones, and the lake lies just to their east. The climate of the region is therefore typical subtropical monsoonic. The year is marked with distinct summer, rainy, and winter seasons. The mean monthly maximum temperature during summer rises to above 40^0C whereas the mean minimum winter temperature remains about 11^0C. The rainfall which annually averages 54 cm, occurs almost entirely during the period July to September. All these climatic data nevertheless, suggest that the study area belongs to a semi arid region

The commercial utilization of natural resources i.e, salt of Sambhar lake marks the industrial importance of the area. The Sambhar lake produces over 2 million tons of salt per annum. In a major attempt to revive the Sambhar Salt Limited the Rajasthan government recently opened a large part of the lake for private organizations for a better exploitation of the salt resources. The adverse impact of industrial growth in the area on the delicate ecological system of the lake has also been a matter of extensive debate among the ecologist and the environmentalists.

This area is equally important for scientific research work and economy of the country. Within the scientific community the geographers are turned on by this typical piece of transitional climatic zone sandwiched between arid and semi-arid climatic zones. The Sambhar lake has drawn considerable attention from the ecologists as a natural laboratory to study the ecological diversity. It has the distinction of a "wetland of international importance" under Ramsar convention (1971). The problem of algal growth in the salt pans and reservoirs of the Sambhar lake is providing a tool for interdisciplinary study like bio-geochemistry. The geological interest into Sambhar lake has been strongly focussed on the origin of hyper-salinity in lake water.

1.3 Defining the Problem

Sambhar lake is located in a typical semi-arid environment. This area provides a unique opportunity to study both fluvial and aeolian processes and resultant forms. The study

of physical evolution of Sambhar lake would require understanding of the various structural and geomorphologic processes in this terrain. Such an understanding is required because Sambhar lake is of great national importance in view of its impressive biological diversity and commercial importance for salt production and hence we need to know lot of information about it to protect or maintain it safely. Also, such a study would be a good contribution to the field of desert limnology in understanding the evolution of some other set of saline lakes with like similar conditions. Besides this, the information generated from such a study can be also used while planning some developmental activities in this area.

To have a better understanding of this unique semi-arid landscape and the physical evolution of the Sambhar lake, the various aspects that need to be studied here are: the topographic parameters (height, slope, aspect etc), the aeolian and fluvial landforms (buried channels, sand dunes, other active drainage, fluvial deposits etc) and structural aspects (lineaments, faults).

As regards how these aforementioned details are to be extracted, all the conventional methods of study suffer from some limitations. This area being very vast requires an enormous effort to study using the conventional methods. One cannot study a small part and ignore the rest, because what ever happens in one part affects some other place. To fully study various aeolian and fluvial landforms in this desert area one must traverse very long distances in an exceedingly harsh environment.

However, these aforementioned shortcomings may be overcome to some extent by employing satellite remote sensing techniques. Satellite images provide a very useful tool to study deserts and semiarid land like the Sambhar terrain because of their large area coverage and the amount of information they reveal about these terrains. The processes of wind action, erosion and deposition are generally clearly manifested in images obtained from satellite. Natural colors of desert surfaces in satellite imageries are meaningful and could be used to distinguish formations and areas of active erosion. For instance, in desert sands, the darker the red color the older the deposit and/or the farther away from its source. Thus, remote sensing is an appropriate technology for the present study because of the synoptic view of the region it offers.

1.4 Objectives of the Present Work

The main objective of the present work was to understand the tectono-geomorphic evolution of the Sambhar lake through interpretation of various lineaments, drainage activity, land cover and three dimensional topographic information extracted by applying some image processing techniques on satellite imagery in a GIS environment.

1.5 Brief Overview of the Past Work

Some of the earlier researches in the Sambhar area have focussed on the regional geological setting (Sen and Ramalingam, 1976), geomorphology (Sharma, 1987) and neo-tectonics (Dassarma, 1988). The important issues of this area that have attracted the attention of various researchers are the physical and chemical evolution of the Sambhar lake. Various theories on the evolution of this lake have been propounded in literature. An integrated approach by using all the past work done in this area can give a very good picture about the physical evolution of the Sambhar Lake.

In regard to the geological observations, it has been found that the Aravalli series underlie the Sambhar lake basin and surround it on almost all sides. The Aravalli range itself is not continuous here, but is composed of residual hills with several gaps. Micaceous schists overlain with limestone nodules buried in clay form the basin bottom. Above these spreads a thick layer of sand which, in turn, is covered by a 20 m-thick layer of saliferous silt. High terrace sand and clay deposits are also found on the Aravalli outcrops around the lake basin. The origin of salt in the lake has been a subject of considerable debate among geologists and chemists. Chemical weathering of the Aravallis, resulting in the production of soluble sodium salts and their drainage into the Sambhar basin, is the most widely accepted explanation.

Coming to the geomorphological observations, the Sambhar area is a classic example of manifestation of aeolian, fluvial and lacustrine processes and landforms. Of these wind action is certainly predominant while surface water processes assume importance during the monsoon period. The effect of lacustrine process is marginal as the lake is shallow in nature; maximum depth being slightly more than 1 m during monsoon, and is practically devoid of any current and tidal action. A keen study of various landforms in this region provides numerous evidences of neotectonism.

The drainage in this area is essentially structurally controlled, showing preferred directions along NE-SW, E-W and NW-SE. The rejuvenated faults and fractures control the overall drainage pattern of the area. A number of lakes including Sambhar lake occur in the eastern fringes of the wind gap and also across disorganized river courses. The river Mendha flows straight along NE-SW stretches for major part of its course and shows N-S alignments particularly just before merging into the lake. All paleochannels of the Mendha river show the initial dominance of NE-SW lineaments, and subsequent superposition of N-S through river capture. Differential uplift and tilting of N-S oriented blocks have been largely responsible for segmentation, ponding, disorganisation of rivers and formation of several saline lakes in the eastern fringe of the Aravalli range (Dassarma, 1988). Most of the river channels display contrasting morphologies in adjacent segments, locally grafting relict meander loops of Roopangarh river to insurgent straight headway of river Mendha.

Sundaram and Pareek (1995) reported that the Quarternary landforms in the northern and eastern proximity of the Sambhar lake are products of depositional, structural and erosional processes. The depositional landforms are made up of fluvial and lacustrine and aeolian facies. The structural and erosional landforms are carved out of Pre-Cambrian and hard rocks. Of the two lacustrine facies the older is marked by the presence of saline deposits and the younger by saliferrous sediments. The depositional facies have evolved in a sequence which indicate slow variation in a predominantly arid climate. The presence of fluvial sediments forming the lake base contradicts the earlier observations which suggested an aeolian base for these lacustrine sediments.

Various theories are mentioned in literature about different aspects of evolution of saline lakes in the Thar desert. Riverine connection theory (Aggrawal, 1957; Ghose, 1964, 1968) explains that some of the lakes in the Thar desert are having some riverine connections in the form of surface and subsurface streams, thus feeding the saline lakes. Palaeo-channel segmentation theory (Ghose, 1977) suggested that due to change of climate from a wetter to a drier phase during the early Quaternary period in the desert, the drainage system disorganized, resulting in an increase in aeolian activity and consequent sand dune formation across the major valleys. The sand dunes thus formed acted as barriers segmenting the major valleys into sandy inland basins. The subsequent reestablishment of the wetter phase turned those inland sandy basins into fresh water

lakes, but another dry phase (the present one) increased the concentration of salts in them and created the present situation of saline flats. Another important theory that is of more relevance in the present case is the one based on neotectonism and lineament control (Sinha-Roy, 1986; Dassarma, 1988). Some of the saline lakes like Sambhar lake in Rajasthan ere located exactly at the intersection of major lineaments. Sinha-Roy opine that Sambhar lake originated as a pull-apart structural depression due to strike-slip faulting along curvilinear planes. However, Dassarma suggested that the pull-apart depression at Sambhar could be due to rotational movements of the fault-bounded blocks. Aeolian process of Wind-scouring theory (Kar, 1989) explains the cause of depressions of smaller dimensions in the desert terrains to be due to the process of deflation of sand bodies and their subsequent transformation into ephemeral lakes during the rains. The Stream-Trap theory (Kar, 1990) discusses that in some regions of the desert, due to the presence of isolated hills, two longitudinal obstacle dunes flanking the hill have formed with a vortex in the middle. Some of the major streams got obstructed by these dunes and got trapped in between these dunes thus resulting in a lake formation in that area.

1.6 Scope of the Present Work

The scope of the present work can be detailed as under:

1. To scan all the relevant topographic sheets of the study area and make a mosaic out of it.

2. Georeferencing the mosaic of scanned topographic sheets to make a base map followed by georeferencing and resampling of the satellite imagery with respect to the base map.

3. Generation of a sliced DTM, slope map, aspect map and a three dimensional view of the terrain by digitizing point height information from the topographic sheets with subsequent interpolation and slope and aspect calculations.

4. Generation of the lineament map of the terrain and the Rose diagram lineaments using various edge detection filters and thresholding techniques on satellite imagery.

5. Generation of a map showing the lakes, surface streams, rivers, abandoned channels, phantom channels etc., of the study area through visual interpretation and digitisation.

6. Generation of a land cover map by means of Maximum Likelihood classification of four bands of satellite imagery of the study area.

7. Interpretation of all the information generated from the thematic layers to understand the geomorphic and tectonic evolution of the Sambhar lake.

1.7 Organisation of the Thesis

The present thesis is organised into seven chapters. Chapter-1 gives an overview of the entire work taken up. Chapter-2 presents the location map of study area and details of data and software used for the present work. Chapter-3 introduces the geology, geomorphology and neotectonics of the Sambhar surroundings and also the various theories of evolution concerning some saline lakes of Rajasthan. Chapter-4 discusses about some remote sensing and image processing concepts as required for the present work. Chapter-5 details the entire methodology that has been followed here for the generation of various thematic layers. Chapter-6 presents the results of the present work along with some discussions and interpretations that arise from them. This chapter also discusses the results of thresholding technique employed here, which was found very important for extraction of lineaments. It also formulates the structural and geomorphologic evolution of the Sambhar lake. Finally, Chapter-7 gives the summary and conclusions of the present work and some future recommendations made.

STUDY AREA, DATA AND SOFTWARE USED

2.1 Geographical Setting of Study Area

The study area for this present work is centered around the Sambhar lake. It falls between latitudes $26^0 48'$ N – $27^0 14'$ N and longitudes $74^0 50'$ E – $75^0 32'$ E spanning in five Survey of India toposheets $45\frac{L}{16}$, $45\frac{M}{4}$, $45\frac{J}{13}$, $45\frac{N}{1}$ and $45\frac{N}{5}$. It spreads over three districts of Rajasthan namely Jaipur, Ajmer and Nagaur. Sambhar is the largest inland saline lake of India covering approximately 225 sq. km. of area. It is about 80 km. west of Jaipur and around 60 km. northeast of Ajmer. Most of the Sambhar lake basin lies in Jaipur and Nagaur districts, and only a small portion in Ajmer district. The Sambhar lake is a hallow in a vast stretch of almost flat sand body and is located in a gap of the Aravalli range. To the northwest and west of the basin, the Aravalli ranges rise abruptly to heights exceeding 500 m (highest peak: Patalia Dungar, 742 m), with outcrops in the form of hillocks scattered along the northern and western periphery of the lake. In fact the Sambhar lake basin which occupies a depression in the Aravalli schists, appears like a valley within the Aravalli ranges.

Sambhar is a shallow lake, reaching only about 3 m at its deepest (Brijgopal and Sharma, 1994), with an average depth not exceeding 0.61 m. The maximum length of the lake basin is 22.5 km, while the width ranges from 3.2 km to 11.2 km. The lake bed (360 m above sea level) is almost flat, with a slope of less than 10 cm per km. (Brijgopal and Sharma, 1994). The climatic setting of the study area is transitional with an arid zone to the west and semi-arid zone to the east.

2.2 Data used for the Study

The digital remote sensing data of IRS-1B LISS-II used in the present work has been acquired from NRSA, Hyderabad. Linear Image Self Scanning (LISS) pay load of Indian Remote Sensing Satellite IRS-1B consists of three solid state cameras: low resolution (72.5 m) LISS-I, and medium resolution (36.25 m) LISS-IIA and LISS-IIB.

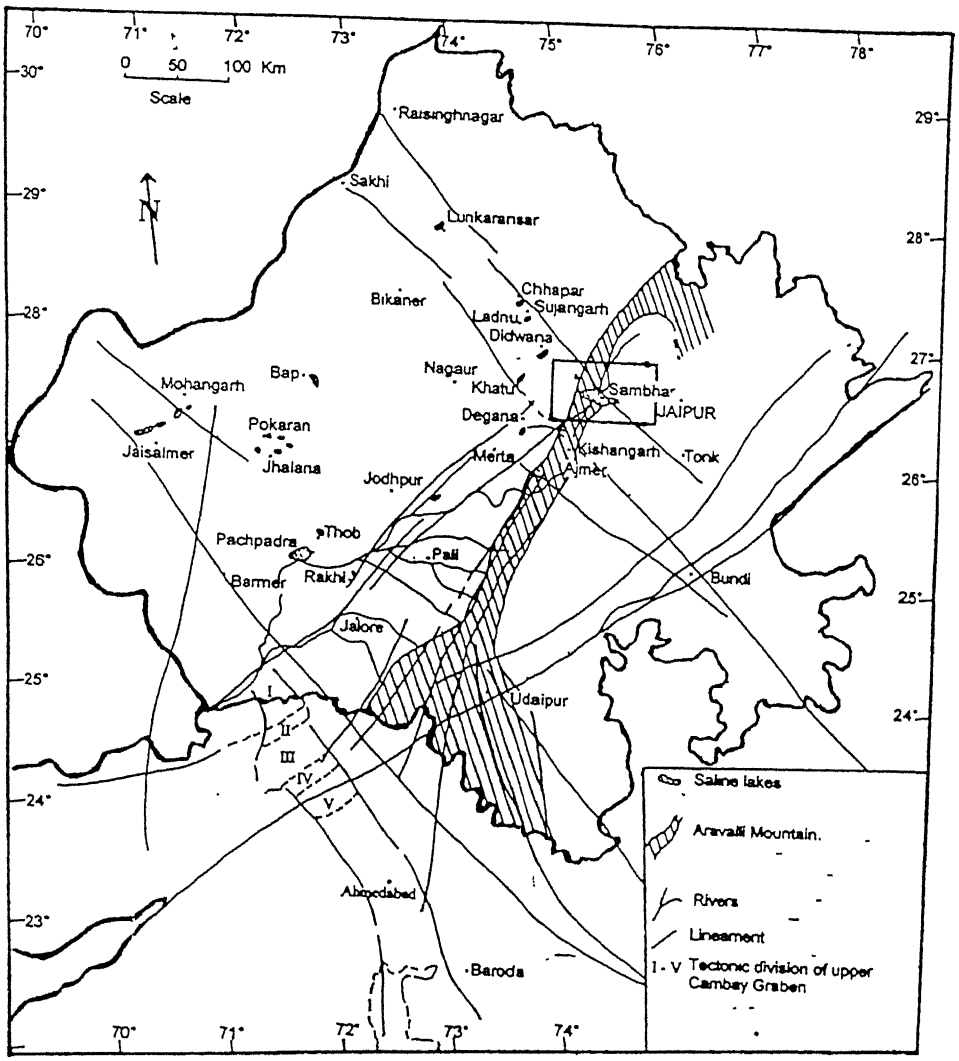

Fig-2.1 Location map of the study area

LISS-I provides a swath of 148 km, while the composite swath of LISS-IIA and LISS-IIB is 145 km. IRS satellites are placed in a 904 km polar sun-synchronous orbit with an orbit period of 103 minutes. The satellites return to their original orbit trace every 22 days enabling repeated collection of data over the same place and at the same local time. The detailed specifications of the data used are listed in Table 2.1

Table 2.1 Specifications of the data used

Satellite	IRS 1B
Sensor	L2A
Path – Row	30-49
Sub-scene	A1
Date of pass	21 Nov. 1995
Inter pixel distance (meters)	36.25
Inter line distance (meters)	36.25
Band Nos.	1 2 3 4

LISS cameras observe radiance reflected from earth's surface in four bands of the following wavelengths: 0.45 μm to 0.52 μm (band 1), 0.52 μm to 0.59 μm (band 2), 0.62 μm to 0.68 μm (band 3) and 0.77 μm to 0.86 μm (band 4). Table 2.2 lists the major characteristics of IRS bands and their applications.

Table 2.2 IRS spectral bands and their principal applications

Band No.	Spectral range (μm)	Spectral location	Principal applications
1	0.45 – 0.52	Blue	Sensitive to sedimentation, deciduous/ coniferous forest cover discrimination
2	0.52 – 0.59	Green	Green reflectance of healthy vegetation
3	0.62 – 0.68	Red	Sensitive to chlorophyll absorption by vegetation, differentiation of soil and geological boundary
4	0.77 – 0.86	NIR	Sensitive to green biomes and moisture in vegetation, land water contrast.

2.3 Details of Software Used

In the present work, some image processing and GIS operations are employed on the satellite images so as to extract relevant information from them. This was done mostly through some readily available commercial software which facilitate this. However, some other advanced image processing issues as thresholding and some edge filters

required separate coding of algorithms in "C" language. Table 2.3 summarizes the software used in the present work.

Table 2.3 Details of software used in the present work

S.No	Software	Purpose	Remarks
1	Software along With UMAX scanner	Scanning of topographic maps in pieces and later stitching them to make a mosaic of five topographic sheets.	Scanning Software
2	IDRISI	a) Extract four bands out of raw satellite data in BIL format from NRSA. b) Displaying output after the execution of the "C" programs written for the present work.	Commercial image processing and GIS software from Clarks Lab, USA
3	ILWIS2.2	General Image Processing and GIS operations.	Commercial image processing & GIS software from ITC Netherlands.
4	"LoGf.c"	Laplacian of Gaussian filter	
5	"Morphf.c"	Morphological filter	Haralick et al(1987)
6	"Kirshf.c"	Kirsh filter	Robinson (1977)
7	"Thresh.c"	Global and Local thresholding of edge images	Otsu (1979), Kittler and Illingworth (1985)
8	"Resample.c"	Multi-resolutionizing the given image	Richards ()

GEOLOGY AND GEOMORPHOLOGY OF SAMBHAR LAKE REGION

3.0 Introduction

Sambhar lake is one of the largest saline lakes in Rajasthan. It is located in the gap of the Aravalli range about 80 km west of Jaipur. It holds a unique distinction amongst the saline basins of Rajasthan, of having maximum thickness of Quaternary deposits and being the principal source of salt. The Quaternary thickness is about 20 m to 50 m and the total lake area is about 230 sq. km.

This area attracts the attention of many researchers because it gives a unique opportunity to study both fluvial and aeolian processes and resultant forms. Earlier researches in this area have focussed on the regional geological setting (Sen and Ramalingam, 1976), geomorphology (Sharma, 1987) and neo-tectonics (Dassarma, 1988). The chemical aspects of this lake have also been explored to some extent (Godbole, 1952). Some of the researchers tried to trace the sedimentation history of this area (Sundaram and Pareek, 1995). Diverse ideas have been put forward to explain the physical and chemical evolution of the Sambhar lake. The following sections present an overview of the available geological and geomorphological information on the Sambhar lake region.

3.1 Regional Geology

Sambhar lake is located southeast of the Aravalli mountain Range. Hence, it is very important to understand the structural and stratigraphic features of this mountain range. The geology of the area around the Sambhar lake has been described by Hacket (1880), Heron (1917), Sen and Ramalingam (1976) etc. Hacket was the first to write a geological paper on this mountain range about hundred years ago.

As regards the structural aspects, the Aravalli mountain range of Rajasthan and northern Gujarat comprises a number of fold belts of early and middle Proterozoic

age. Beginning around 250 million years back, the records of the Proterozoic events in the Aravalli mountain range can be traced as late as 500 million years before present. These Proterozoic fold belts, like other proterozoic fold belts of the world, evolved through the development of a series of basins in which sediments and volcanics were laid down in several successive groups bounded by unconformities.

The stratigraphic units forming this mountain range include several unconformity-bound metasedimentary and metavolcanic units deposited successively over an ancient basement of plutonic rocks and para-gneisses. As a cover unit, Heron (1935, 1953) recognised the "Aravalli system" as the oldest formation overlying the Banded Gneissic Complex (Roy, 1988), and the Bundelkhand gneiss (renamed by Pascoe, 1950, as the Berach granite) with a profound unconformity (Sen, 1988). The "Raialo series" and the "Delhi system" are the two other cover sequences recognized by many researchers. Table 3.1 shows the stratigraphic succession of the Precambrian rocks of the Aravalli mountain range as recognised by Sen (1988).

Table 3.1: Lithostratigraphic framework of the Aravalli Mountain Range

MALANI VOLCANICS	
ERINPURA GRANITE	
MAFIC AND ULTRAMAFIC INTRUSIVES IN THE DELHI FOLD BELT	
CHAMPANER GROUP	
SIROHI GROUP (?)	
DELHI SUPERGROUP	AJABGARH GROUP ALWAR GROUP RAYANAHALA GROUP
//UNCONFORMITY////////////////////////////	
ARAVALLI SUPERGROUP	UPPER – ARAVALLI GROUP LOWER – ARAVALLI GROUP
//UNCONFORMITY////////////////////////////	
MEWAR GNEISS	PRE – ARAVALLI GRANITE GNEISSES, AMPHIBOLES, METASEDIMENTS, AND GRANITIC ROCKS

(After Sen, 1988)

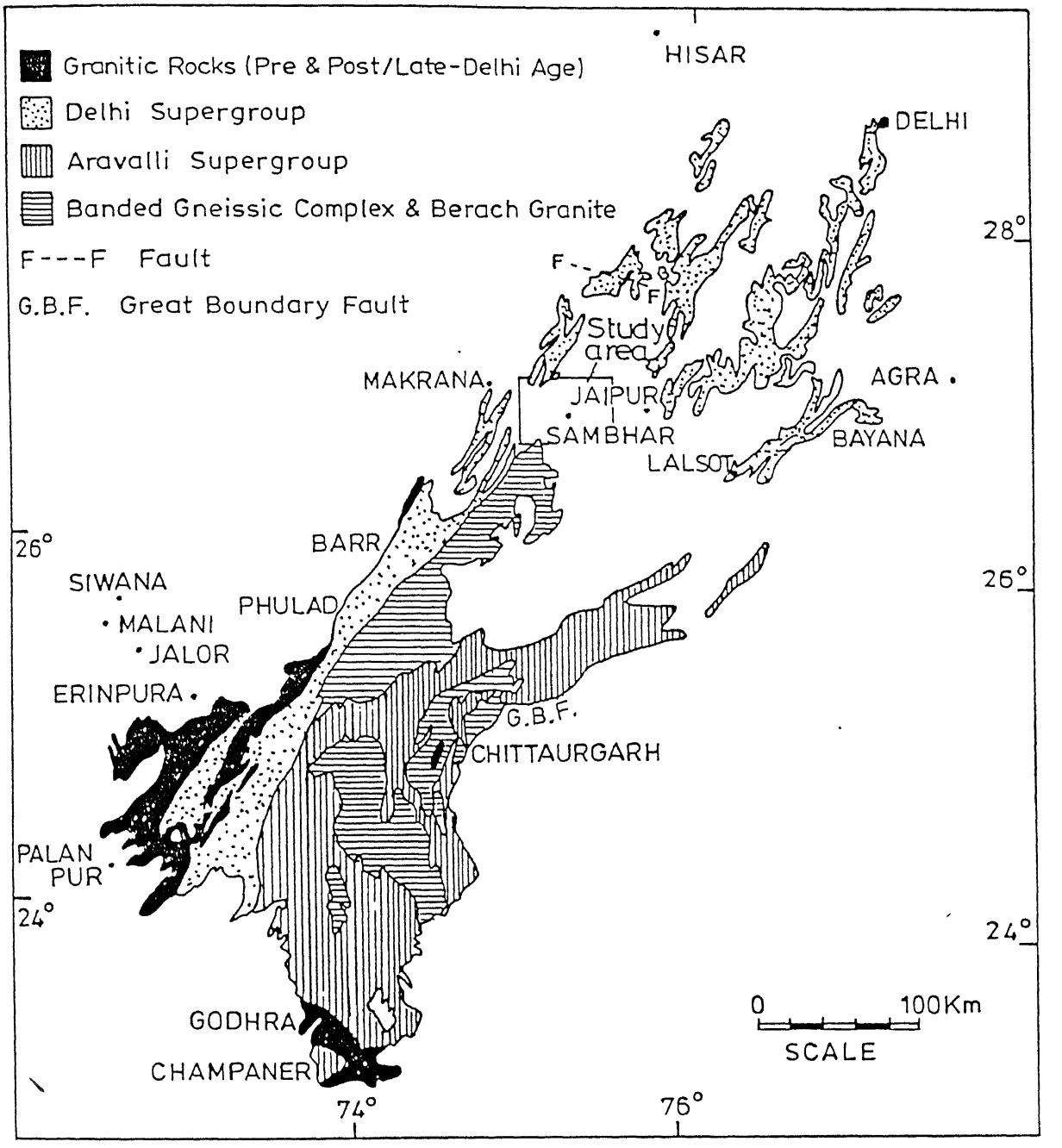

Fig-3.1 Map showing the distribution of the Precambrian crystalline rocks in the Aravalli mountain belt and its surrounding plains along the study area (Simplified after the published maps of the Geological Survey of India)

A clear idea of the lithology of Aravalli mountain belt and its surrounding plains within the study area can be had from the published map of the Geological Survey of India (Fig. 3.1). This map reveals that the major parts of the Sambhar lake region are covered with Quaternary deposits. Hence, these Quaternary deposits conceal the structural and stratigraphic features of this area. Nevertheless, it has been recognized that most of the outcrops west to this region belong to the Delhi super group, and the BGC and the Berach granite are towards the south of the area.

From the aforementioned map, it is clear that the Delhi super group, which constitutes the main edifice of the Aravalli range, occupies a narrow linear stretch in this part of the central Rajasthan. Sharma (1988) described the lithology of the Delhi supergroup rocks of this region as indicative of lower greenschist facies of regional metamorphism. The regional schistosity is considered synkinematic with folding on NE-SW axis and accompanied by low-grade crystallisation of the metasediments (Basu, 1982: Gangopadhaya and Pyne, 1980; Singh, 1982).

The Banded Gneissic Complex (BGC) exposed towards the south of the Sambhar area is considered as underlying the supracrustal of the Aravalli and Delhis, and is characterized by polymetamorphic mineral assemblages. The mineral assemblages comprising the rocks of the region suggest high-pressure conditions during which the upper stability of muscovite had been reached (Sharma, 1988). Geothermometric and geobarometric estimations by Sharma (1988) suggest a pressure of 5.5-6 kb and temperature range of 600^0-700^0C. The mineral assemblage comprising biotite-sillimanite- "melt", in which melt is coarse-grained quartz, plagioclase and microcline (Sharma, 1988).

Three phases of folding have been recognized in the Delhi rocks (Mukhopadhaya and Dasgupta, 1978; Naha et al, 1984; Roy and Das, 1985). Two of these folding episodes appear temporally very close to each other (Banerjee and Mitra, 1977; Roy, 1988), both forming during the Delhi orogeny. Temporal reactions between the crystallization and deformation suggest that the metamorphism of the supergroup rocks of this region was broadly coeval with these two phases of deformations, and the crystallization outlasted the second deformation (Roy and Das, 1985). This part of

the Delhi basin is characterized by several fossil grabens, horsts and grabens (Singh, 1988). The neotectonically active "Sambhar-Jaipur-Dausa Wrench fault" has been presumed to be a palaeotransform fault separating the "north Delhi basin", which opened earlier from "south Delhi basin" opening at a later date (Roy, 1988).

3.2 Geomorphology

"Geomorphology deals with the study of landforms and landscapes, including their description, type and genesis"(Gupta, 1991). Landform is the end product resulting from the interaction of the natural surface agencies and the type of rock (Bloom, 1969). It depends on three main factors such as (a) climatic setting, including its variation in the past (b) lithology and structure, and (c) the time span involved.

The Sambhar area is a classic example of manifestation of aeolian, fluvial and lacustrine processes and landforms. Of these wind action is certainly predominant while surface water processes assume importance during the monsoon period. The effect of lacustrine process is marginal as the lake is shallow in nature; maximum depth being slightly more than 1 m during monsoon, and is practically devoid of any current and tidal action. A close observation of various landforms in this region provides numerous evidences of neotectonism.

The Aravalli range, trending diagonally from the northeast to southwest, opens out in a fan like fashion in Jaipur and Alwar districts. The hill ranges are abruptly truncated both in the east and west, and show linear mountain fronts over long distances. The hill tops have preserved relict erosional surfaces at different levels with many of the hills showing first order topography, preserving anticlinal hills and synclinal valleys (Dassarma, 1988). Described as the ridge and valley province, the Aravalli range in this part breached transversely to form a number of wind gaps including one near the Sambhar lake.

An extensive pediplain truncates with the rocks belonging to the older sub divisions of the crust including the basement in this area. The middle part of the pediplain is covered up with menacing aeolian sand shield and dunes of various mor[illegible] types. Remnants of an earlier planation surface occur as narrow linear stretches of different elevations on hill tops and rise in stepped terraces from the adjoining plains

(Dassarma, 1988). The surfaces are longitudinally bounded by NE-SW and N-S faults and fractures, fortified with scarps and truncated by E-W cross faults. Effect of post planation uplift and faulting are manifested in the abundance of spectacular hanging valleys all of which show three distinct steps in their rise (Roy and Sen, 1983).

The effect of warping is discernible in the local segmented blocks bounded by longitudinal and cross faults (Roy and Sen, 1983). The anticlinal hills present in the area attain a maximum height at the middle and steadily decline in elevation both northward and southward by about 400 m till it is truncated by cross faults. A striking parallelism exists between the axes of warping and axes of folding in the area so much so that the maximum and the minimum elevation of the warped surface locally coincide with culminations and depressions of early fold axes where these are crossed by the folding (Sen and Sen, 1983; Roy, 1983). Relevant in this context is the description of the fold formation as "broad warps" and "unaccompanied by internal deformation" (Roday, 1979), as "mild", "extremely local" and "non penetrative" (Roy, 1983) and as "broad open cross-folds" which generated "wider spaced fractures" (Sen and Sen, 1983). In the present case, the prevalence of N-S fractures and scarps parallel to the compression axis, the general rejuvenation of NW-SE striking faults fully bears out a N-S directed compression axis (Ghosh and Vishwanath, 1991). Faults trending E-W and parallel to the axis of warping are possibly of tensional origin.

The drainage in this area is essentially structurally controlled, showing preferred directions along NE-SW, E-W and NW-SE. The rejuvenated faults and fractures control the overall drainage pattern of the area. A number of lakes including Sambhar lake occur in the eastern fringes of the wind gap and also across disorganized river courses. The river Mendha flows straight along NE-SW stretches for major part of its course and shows N-S alignments particularly just before merging into the lake. All paleochannels of the Mendha river show the initial dominance of NE-SW lineaments, and subsequent superposition of N-S through river capture. Differential uplift and tilting of N-S oriented blocks have been largely responsible for segmentation, ponding, disorganisation of rivers and formation of several saline lakes in the eastern fringe of the Aravalli range (Dassarma, 1988). Most of the river channels display contrasting morphologies in adjacent segments, locally grafting relict meanderal loops

of Roopangarh river to insurgent straight headway of river Mendha. As free meandering suggests absence of tectonic control, the cumulative evidences of meandering and recurrent river captures along successive preferred directions suggest periodic impulses (Williams and Clarke, 1995).

Quaternary sedimentation is mainly restricted to the marginal fault troughs fringing the uplifted western and eastern margin of the Aravalli range. The formation of the troughs and their rapid filling during the quaternary period indicate normal faulting accompanying block uplift; the drowning of the sediment suggests continuation of movements (Blatt, 1980). The deposition of linear alluvial valleys in successive parallel stretches suggests sedimentation in stepped graben in the Mendha valley. The successive linear basins simulate stepped grabens formed by a series of antithetical faults heading towards the main fault (cf. De Sitter, 1956). The linear and parallel valleys in the Mendha basin may indicate sedimentation either in Ridel shears formed oblique to the regional NE shear or in successive grabens formed by fault antithetic to the normal component of the original fault (Ghosh and Viswanatham,1991).

3.3 Neo-tectonic Activity

The structural, geomorphological, pedological and stratigraphic features of any area are affected by the neotectonic activity in that region. Hence, these features serve as good evidences for the tectonic activity in the area. A summary of the structural, geomorphological, pedological and stratigraphic evidences in support of neotectonic movements in northeast Rajasthan has been furnished by Dassarma (1988).

The structural evidences comprise truncated hill fronts with fault scarps, in alluvium and silcretes, and post orogenic bending, shattering and dragging of ridges with rotational effects to form transverse wind gaps. The pedological features include relict silcrete and calcrete skins on topographic highs, and anomalous depths of oxidation in contiguous blocks on opposite sides of the NE-SW trending faults (Dassarma, 1988). The important geomorphological features suggesting neotectonic activity in the area are swarms of parallel structurally controlled paleochannels, lineament-controlled river captures, river diversions, ponding and formation of salt lakes across disorganised channels and anomalous terracing in adjacent rivers. The stratigraphic

evidence of neotectonism includes differential accumulation of sediments in contiguous blocks with local "drowned" Quaternary topography.

Sen and Sen (1983) suggested a post-Neogene uplift of the Aravalli range as a horst which, according to them, took place through re-activation of older lineaments, principally the Great Boundary Fault in the east and Sardarsahar Fault in the west. Anhert's work (1970) on the relationship of denudation, relief and uplift suggests that if the uplift is only isostatic, then the main relief of any terrain will probably be reduced to 10 percent of its original value after 30 million years. Thus, assuming the Aravalli range as an absolutely stable region at least since Mesozoic, the present mean relief of 300 m would imply a relief of 3,000 m in Paleocene. Such high relief would suggest that the present topographic and geomorphic features of the Aravalli range to be interpreted as rejuvenated feature of late Tertiary or early Quaternary age.

A possible driving force for the post-orogeny movements could be during the late Pliocene early Pleistocene time when the continental crusts of the Indian and Eurasian plates became locked (Sen and Sen, 1983). The differential movement caused rotation of some of the blocks along reactivated faults, ripping open in the process linear depression to form Quaternary sedimentation basins and lakes. The absence of sediments earlier than Quaternary in all these depressions provides stratigraphic evidence for recent movements (Roy and Sen, 1983). The movements were perhaps impulsive as suggested by anomalous terracing and ephemeral meandering phases of paleochannels.

As regards the Sambhar lake, it is said to be located at the intersection of some major lineaments (Sinha-Roy, 1986) as shown in Figure 3.1. Role of rotational movement was suggested for the formation of the conspicuous wind gaps, transverse to the Aravalli mountain range between Sambhar lake and Kantli river where a series of NE-SW, NW-SE and N-S faults intersect (Figure 3.2) each other (Dassarma, 1985). A comparison of lineaments indicated by Mendha stepped grabens suggests a relative clockwise rotation of the crustal block east of the Aravalli orographic axes. The rotational process has also pulled apart a series of marginal depressions in the eastern fringes of the gaps to form the Sambhar and some other smaller lakes with linear boundaries.

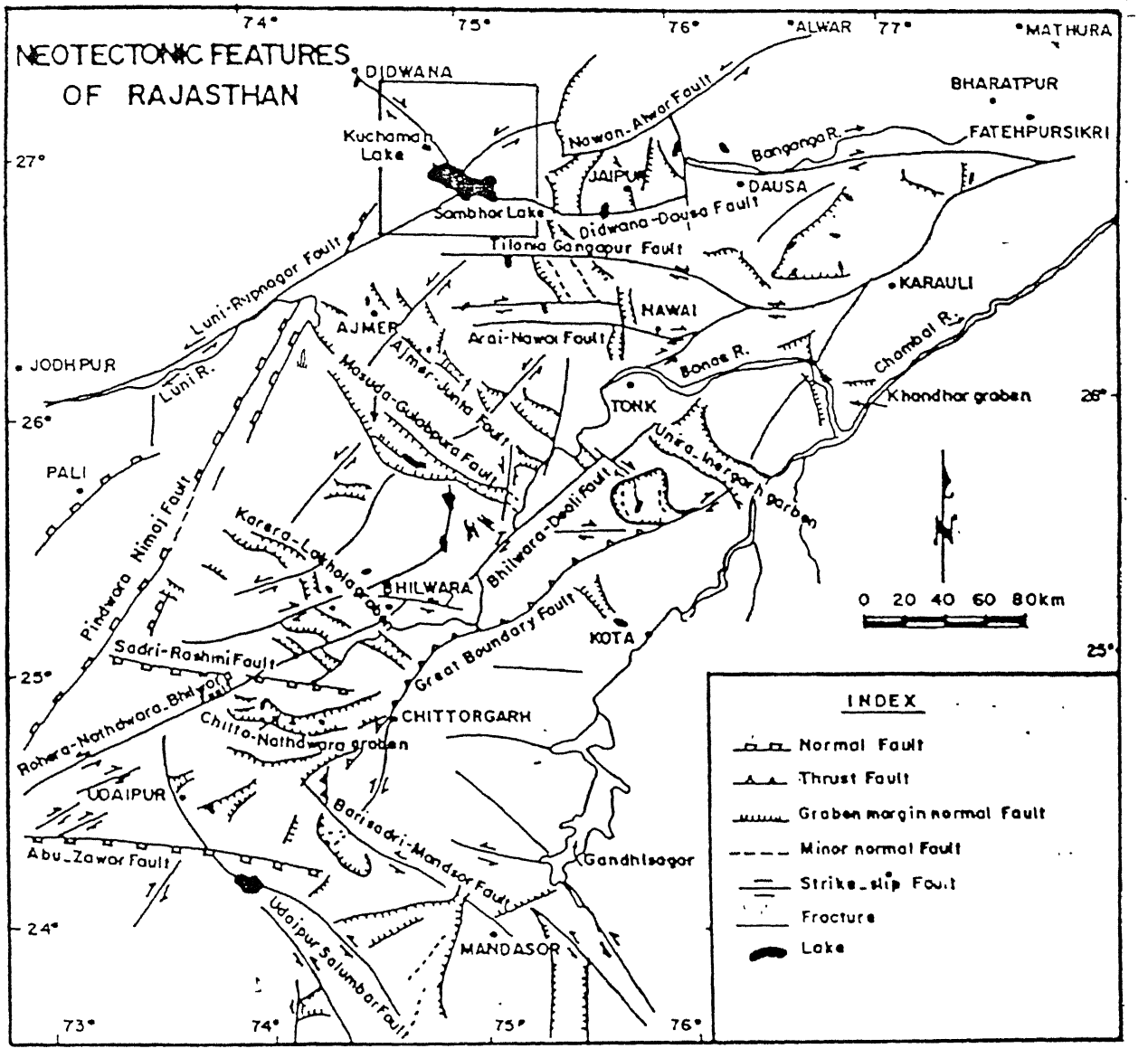

Fig-3.2 Neotectonics features in Rajasthan highlighting the Sambhar terrain (after Sinha-Roy, 1986)

3.4 Climate and other Anthropogenic Activity

Climatically, the study area is situated over a transitional area with arid climate at the west and semiarid climatic zone towards the east of it. Mainly monsoon and the physiography of the area, i.e. the Aravalli range, govern the total climatic factor of the area. The southwest monsoon that originates in the western part of the Indian Ocean as the Southeast trade wind, is drawn north of the equator by a low-pressure area over north-west India. As it crosses peninsular India, part of it swings north and then west over the Ganges plain, to lose the last of its moisture on the eastern slope of the Aravalli range. The average annual precipitation over this region is 550 mm to 650 mm and sometimes up to 800 mm. Another cause of low annual precipitation around this area is the relatively warm dry, anticyclone air that overlies the near surface air of the southwest monsoon (Pramanik and Ramanatham, 1952). This absorbs any moist air that rises along Aravalli range and results in the dissipation of any cloud and decreases the likely load of rain over this region. The southwest monsoon is though replaced on the autumn by light winds of northeast monsoon, but having had a continental route before reaching this area. The annual rainfall intensity as estimated by the meteorological department is 17.5 mm (Sharma, 1990). The average annual temperature of this region is 23^0C, the maximum being 45^0C. All these climatic data nevertheless, suggests that the study area belongs to a semi arid region.

A characteristic feature of the climate is the extreme temporal variability in precipitation. The rainfall record of more than a century of this area showed that both the total annual rainfall and its period of occurrence and intensity during the season exhibit wide variations, resulting in frequent spells of drought and flood. The rainfall, which has often been as low as 16 cm (in 1939, for instance) exceeded 100 cm in 1892, 1893, and 1917. According to the data compiled by Aggarwal (1951), as much as 15 cm rain had fallen during July and 31 cm rain within five days in September 1884, causing severe floods. Heavy rainfall in the years 1892 and 1917 was, however, relatively evenly spread over the rainy season. Again, in 1929, more than 44 cm and 51 cm of rain at Jhapok and Nawa settlements respectively, occurred five days within the last week of July. Another example of intense rain was recorded in July 1949 when more than 13 cm rain fell within three hours and again about 17 cm within 24

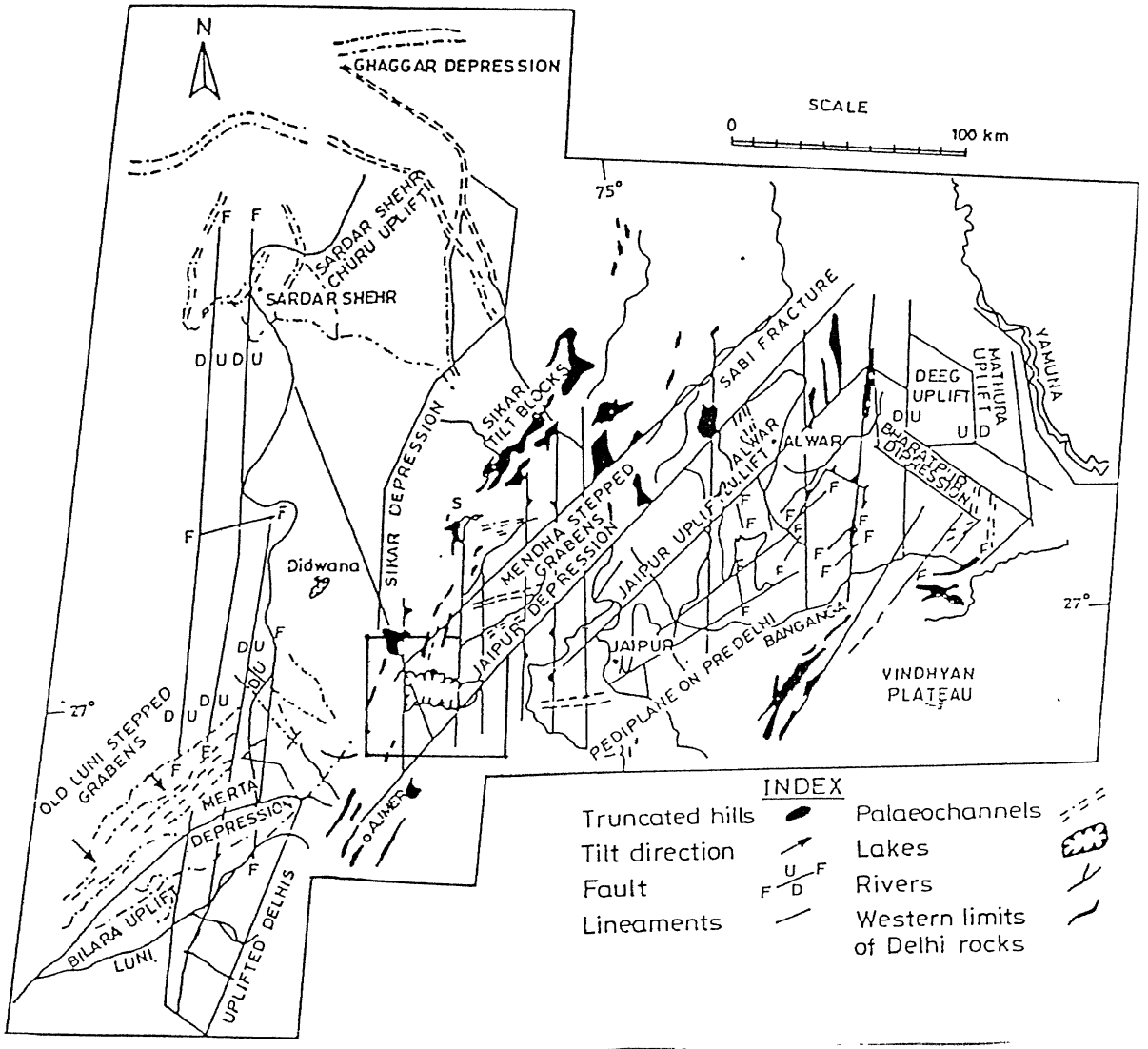

Fig 3.3 Neotectonic map of northeastern Rajasthan: prepared from Landsat imagery followed by field checks (Dassarma, 1988)

hours. In contrast, during dry years, rainfall was often well distributed over the whole basin, registering only 3 – 5 cm in a month. Flash floods which have become fairly regular in recent decades – in 1968, 1971, 1974, 1975, 1977, 1981 and 1983 – were due not to excess rain but to high intensity of rainfall on certain days.

Many anthropogenic activities are noted in the northeastern part of Aravalli hills from Sambhar lake upto Jaipur city. In the past few decades it has become evident that the processes of desertification have been very much enhanced in this region mainly through rapid increase of human and animal population. The major anthropogenic activities accentuating desertification process are deforestation, overgrazing, unplanned cultivation, expansion of urban settlements, quarrying and engineering constructions (Sharma, 1988). The removal of vegetation cover from the stable dunes by these activities makes them unstable and this reactivation results in vast land being encroached by drifting sand (Raghav, 1988). After complete removal of the vegetation by the aforementioned activities such patches appear on the satellite imagery and air-photos as blurred, bright patches, more or less star shaped. In the case of more intensified land use the above mentioned patches merges into large areas. Aerial photographs and satellite imagery showed a clear pattern of ripple and barchan dunes that have developed in such areas. Also, the adverse impact of industrial growth in this area on the delicate ecological system of the lake has been a matter of extensive debate among the ecologists and the environmentalists.

3.5 Evolution of Saline Lakes in Rajasthan - an Overview

There are two aspects of evolution for the saline lakes – *Physical* and *Chemical*. The former concerns itself with the cause of lake depression and the later with the cause of salinity of the water collected in the lake depression. Several theories have been proposed by the researchers in the past to explain the origin of the saline lakes as well as their associated salinity. However, there is still a lack of consensus among the research workers.

As mentioned earlier, the saline lakes are essential features of the desert regions all over the world. This very fact implies that the aridity must be the prime factor in the evolution of saline lakes. Other than the factor of aridity, the most important

component in the evolution of saline lakes is the formation of depressions with the associated centripetal and ephemeral drainage pattern. "The saline depressions of some of the lakes in Rajasthan are morphologically similar to the playa lakes, which are broad and shallow depressions occasionally getting inundated with water" (Roy, 1999).

Before taking up the task of inquiring into the details of evolution of any particular saline lake, it is necessary to closely scrutinize the existing theories of evolution pertaining to various other saline lakes, as that would apprise of the various phenomena that can come into play in their formation. The present review is confined to the 'physical' evolution of the saline lakes of Rajasthan and does not include the purely 'chemical' evolution. In many cases, however, the chemical evolution is strongly linked to the physical evolution. The available literature indicates the following for the physical evolution of saline lakes of Rajasthan.

1) Riverine-Connection theory (Aggrawal, 1957; Ghose, 1964, 1965).
2) Palaeo-Channels Segmentation theory (Ghose *et al.* 1977).
3) Theory based on Neo-Tectonism and Lineament Control (Sinha-Roy, 1986; Dassarma, 1988).
4) Aeolian Process or Wind-Scouring theory (Kar, 1989).
5) Stream-Trap theory (Kar, 1990).

3.5.1 Riverine connection theory

For almost all the major saline lakes in the Desert regions of Rajasthan there are indications of riverine connections. Aggarwal (1957), emphasized for the first time a riverine connection for the salt lakes at Pachpadra and Didwana, and indicated that the courses of the streams through these lakes were blocked by sand dunes. Subsurface flow of water, carrying soluble salts from the drainage area of the streams, however, continued towards the lakes and thus enriched the salinity of the lakes. A riverine connection hypothesis was also put forward by Ghose (1964, 1965) when he mapped the buried stream courses at Pachpadra depression at the confluence of two streams. According to him the region was formerly endowed with a well-integrated drainage system. The streams carried enormous silt load and deposited the finer materials at

their confluence, which eventually blocked their mouths. With the onset of aridity, scanty rainfall could not keep these streams live (Ghose, 1964). Yet, subterraneous flow of water, carrying dissolved salts from the catchment, continues along the courses. The through flow is, however, restricted at the confluence because of silt particles and results in subterraneous water-logging, capillary rise of water, evaporation and gradual increase in salt concentration (Ghose, 1964).

3.5.2 Palaeo-channel segmentation theory

This theory is a slight modification of the aforementioned concept of riverine connection theory. Some studies based on the stratigraphic records of the lakes indicated that change of climate from a wetter to a drier phase during the early Quarternary period disorganized the drainage system, resulting in an increase in aeolian activity and consequent sand dune formation across the major valleys. The sand dunes thus formed acted as barriers segmenting the major valleys into sandy inland basins. The subsequent reestablishment of the wetter phase turned those inland sandy basins into fresh water lakes, but another dry phase (the present one) increased the concentration of salts in them and created the present situation of saline flats (Ghose *et al.* 1977). All through these phases subsurface flow of water through the buried courses and intermittent surface run-off enriched the basins with salts derived from the catchment area. Thus, while morphological changes in the terrain, in response to changes in climate during the Quarternary, are thought to be responsible for the creation of inland basins and lakes, the distribution of salts in them depended upon their geo-chemical properties and solubility.

3.5.3 Theory based on Neotectonism and Lineament control

This theory explains the evolution of some other saline lakes in the Thar desert based on the Neotectonism and lineament control of saline lakes. Several possible relict palaeochannels of the Saraswati and the Drishadvati river systems as also that of the present Luni follow a NE-SW trend. This is the trend not only of the Aravalli Mountain but also of a set of major lineaments in the region, which controlled the palaeo-drainage pattern in Rajasthan (Dassarma, 1984; Kar, 1988). On the other hand, the NW-SE trending lineaments have guided the stream channels that descended from the Aravalli mountain (Dassarma, 1984). Although the tracing of lineaments is highly

impeded by the thick cover of sand in the desert region, detailed studies made in northern Gujarat, specially in the Kutch region, helped to elucidate the significance of the two lineaments (NW-SE and NE-SW) in controlling the Quarternary geomorphology of the region (Biswas, 1971; Sridhar *et al.* 1997). In the area between the Luni basin and Gulf of Cambay the neotectonic movements along NW-SE and NE-SW trending sets of lineaments produced a series of rhomb-shaped alternating horsts and grabens. From south-east of the Luni basin, the structures have been identified as the Sanchor graben, Tharad high, Palyak depression. Deodar high, and Patan depression. In contrast to the 'highs', the grabens are the zones of very thick Quartenary sediments (Chandra and Chowdhary, 1969; Raju, 1968). A very similar situation seems to have developed in the desert region of western Rajasthan. There is a strong possibility that most of the NE-SW oriented saline lakes are situated in the rhombic blocks of grabens bounded by the NE-SW trending lineaments (Rai, 1990).

The isopach map of the Pokaran lake located in the western part of the desert not only indicates presence of a thick E-W trending sediment prism in the north, but also a sharp change of thickness across the NE-SW trending eastern boundary of the lake (Rai, 1990). This suggests that the Pokaran lake evolved as a graben (or possibly a half graben) between NE and SW trending faults. A striking feature in the spatial distribution of the major salt lakes at Sambhar, Kuchaman, Didwana, Chappar, Sujangarh and Lunkaransar, is that these lakes are confined within a narrow belt bounded by the NW-SE trending depression in the basement rocks, which is further segmented by NE-SW running sets of lineament faults. The discovery of two important NW-SE trending subsurface ridges (or horsts), the Delhi-Lahore ridge and the Jaisalmer-Muri ridge, by geo-physical studies, implies the existence of linear grabens sub parallel to these structures. Confirmation of the existence of NE-SW trending faults (lineaments) in western Rajasthan also comes from the mapping of a series of NE-SW trending lineaments (showing vertical movements) in the Luni basin by Dassarma (1988), Kar (1988), and Tiwari and Gangadhar (1997).

Intersection of two sets of lineaments divided the western Rajasthan crust into a number of rectangular blocks. Differential movements along these blocks seem to have controlled the Quartenary tectonics of the region (Roy, 1999). Known as 'block

tectonics', this type of tectonic movement operated in the same way as in the case of eastern Kach region of northern Gujarat, at least during the late Quarternary. Such neo-tectonic activities have considerably influenced not only development of the landform patterns but also in disorganizing the drainage network. This geomorphic-tectonic process, which was involved in shifting and segmentation of dried stream channels, eventually led to formation of many playa depressions and saline lakes. In addition to the block tectonic model, segmentation of most of the NE-SW trending channels could have been due to movements along NW-SE trending lineaments. Upliftment and tilting of lineament bounded blocks appear to be the most effective mechanism that caused segmentation of channels, drainage reversal and ponding (Dassarma, 1984, 1988).

The largest saline lake, the Sambhar, which is situated astride the NE-SW trend of the Aravalli Mountains, appears to have evolved by a process different from what has been suggested above. According to Sinha-Roy (1986), the Sambhar originated as a pull-apart structural depression due to strike-slip faulting along curvilinear planes. According to him, the lake is situated at the junction of two lineaments. Dassarma (1988), however, suggested that the pull-apart depression at Sambhar could be due to rotational movements of the fault-bounded blocks.

The distribution pattern of lake Sediments in the Sambhar basin provides indication of deposition in a recent to sub-recent graben formed over a fluvial channel (Sundaram and Pareek, 1995). It is, however, difficult to prove whether the down sagging was due to the formation of pull-apart basin, either due to movements along curvilinear planes, or due to rotation of fault-bounded blocks. Detailed structural studies may be necessary to conclusively prove the actual mechanism of neo-tectonic movement, which led to the formation of such a large depression. However, the trends of the lineaments as well as the known patterns of neo-tectonic movements along some of these lineaments, might suggest rotation of a NE-SW trending rhombic depression to the present position.

3.5.4 Aeolian process or Wind-scouring theory

This theory explains the formation of some of the saline lake depressions to be due to aeolian process. In a desert terrain, the depressions of smaller dimensions commonly form by the process of deflation of sand bodies. These depressions turn into ephemeral lakes during the rains. With the onset of dry season, water is evaporated, leaving a thin veneer of salt encrustation. There may be annual repetition of the process. The formation of such depressions by the process of deflation is a very common feature in the sand dune-infested terrain. However, the depressions formed by this process are transient in nature and are subsequently covered with sand dunes. For the initiation of some saline lakes in the rocky tract of Jaisalmer region, Kar (1989) suggested a theory of wind scouring of limestone by the quartz-dominated sand-particles, which ultimately created the basins for water accumulation.

3.5.5 Stream-Trap theory

Some of the saline lakes in the Thar desert seemed to have a different genesis than those conceptualized above. Few observations with such lakes are as follows: Some of the saline lakes within the desert, especially in its eastern part, are flanked by a hill or upland at their southwestern margin (e.g. at Chhapar, Ladnu, Didwana, Khatu). It was also observed that the alignments of the lakes under such situation are roughly NE-SW and the alignment is in close conformity with the prevailing wind direction over the area, i.e. SW to NE. In other words, the lakes appear to have formed at the wind-shadow zone of the hills. While the hills and associated obstacle sand dunes form the southern margin of the lakes, longitudinal sand dunes have formed along their flanks and continue almost parallel to each other for quite a long distance beyond the lake's northeastern margin. Ultimately, the dunes from both the flanks converge and form a roughly elliptical inland basin. The deepest part of the lakes generally lies more towards the hillside end rather than towards the northeastern margin. During the rainy season (July to September) the lakes collect water from the hills through small rills and gullies, but significant contribution comes from the northeastern end also.

Based on the aforementioned observations a new theory called the stream trap hypothesis was formulated by Kar (1990) to explain the evolution of such saline lakes. During the arid phase a lot of dune building activity took place. The wind direction

was roughly from the southwest, as at present (attested by the trends of the high stable dunes). The isolated hills, because of their peculiar locations, created vast wind shadow zones to their lee, while sand deposition went on towards their windward slope as obstacle dines. As the hill obstructed the path of the sand laden wind, a horseshoe vortex developed around it in the manner sketched by Allen (1968, 1985) and swept the sand and the minor vortices along both the flanks of the hill. The 'wind-shadow zone' downwind of the hill, became a zone of divergence where a slow deflation process began to be established, while zones of convergence marked the flanks of the hills and downwind therefrom. As a result, the sand grains began to be deposited along the hill flanks and entrained downwind. Therefore, a set of two parallel longitudinal dune systems gradually developed from the hill downwind, keeping the wind-shadow corridor relatively free from sandy undulations. As the longitudinal dunes from the hill flanks gradually advanced and met a stream bank per chance, overwhelmed it and blocked its ephemeral surface flow, the stream found it increasingly difficult to cut through the dunes and flow along its original course, but to follow the inter dunal corridor and be guided by the flanking dunes to end in a lake at the base of the hill. In other words, the sandy ridges formed a trap for the stream flowing away from the hill. Subsequent monsoon rains established this pirated course more firmly and fed the lake with water and sediment. As mentioned earlier, a slow deflation by the eddy currents at the back of the hills, in the wind-shadow zone, did also help in the creation and maintenance of the lake depression.

As suggested by lake stratigraphy (Singh *et al.* 1972, 1974; Ghose *et al.* 1977, Wasson *et al.* 1983) the dry phase was followed by a wetter phase and the lakes recorded increased fresh water contribution. Consequently the salinity level of the lakes decreased. This indicates that the dune systems which effectively turned the streams towards the isolated hills got firm anchorage and the streams, even with their higher discharge, had to feed the lake, rather than seek other courses out of it through the dunes. Some minor shifting of the courses did, however, take place, as attested by the situation in the Didwana area, but the dunes again guided all such shifted courses to the lake. At Didwana such shifting of courses led to the creation of a smaller elongated lake, named the Singhi Talav.

OVERVIEW OF VARIOUS ANALYTICAL TOOLS USED FOR THE PRESENT STUDY

4.0 Introduction

Keeping the broad objectives and the problem definition of the present work in mind, a critical review of literature on remote sensing and image processing concepts has been taken up. One of the important objectives of the present work is to procure Structural and Geomorphological information of the study area from the satellite imagery. Hence, there is a need to evaluate the various capabilities of remote sensing data from the past studies in the light of the aforementioned requirements. Remote sensing data can be utilized for any application only when some appropriate image processing concepts are used. In view of this, selection of appropriate image processing techniques is also of utmost importance. The various concepts of remote sensing and image processing with reference to the requirements of the present work have been explained in the present chapter.

4.1 Remote Sensing as a Tool

"Remote sensing is the practical tool of measuring properties of materials expressed by electromagnetic waves, reflected or emitted, from large areas without having the measuring device in contact with the object" (Elghawaby, 1987). The application of remote sensing in the field of geology can then be explained simply as the study of earth's characteristics utilizing electromagnetic radiation, which is either reflected or emitted from land surface in waves ranging from ultraviolet to microwave. Remote sensing investigations may be said to have a two-fold purpose - to allow viewing of the ground features in a different perspective, on a different scale, or in a different spectral vision, and to reduce the amount of fieldwork involved for covering the entire study area.

Multispectral remote sensing data has shown tremendous potential for applications in various branches of geology – in geomorphology, structure, lithological mapping,

mineral and oil exploration, stratigraphical delineation, geotechnical, ground water and geo-environmental studies etc.

It should be appreciated that even when soil and vegetation cover is appreciable, remote sensing data has its value in providing information on sub-surface geology, at least to some extent. The type of bedrock and structure control the type of soil, soil moisture and vegetation, which can give indirect information on the geology of the area. The geological information needed to be extracted from space images by analysis and interpretation can be summarized in (a) the identification of surface features of different lithological or landform units, and (b) the delineation of lineaments either signifying structural fabric and fractures or non-tectonic natural or cultural patterns.

The rock attributes (i.e. structure, lithology, rock defects etc.) and physical processes (i.e. climatic setting, weathering and erosional agencies) operating in a region over a time, govern the nature and appearance of landscape – relief, topography, drainage and soil, vegetation etc. This in turn influences image-characters. The main task in remote sensing image interpretation is to decipher geological parameters from minute observations on elements of image interpretation, using the vital clues provided by geotechnical elements. The elements of image interpretation include color or tone, size, shape, texture, site, association, shadow and pattern.

Much advancement is noticed in the field of remote sensing nowadays which make it a good tool for various geological applications. The advent and deployment of scanners with more spectral channels upgrade the methods of interpretation. The various enhancement techniques used in deriving information from imageries have improved remarkably. Various Band Ratioing techniques facilitate easy interpretation of structural linear and curvilinear elements of specific surface features, showing more significant results with structural elements governing mineral or energy resources. The ratio display techniques improve the discrimination of lithology and provide a more detailed description of the regional structures. Addition or subtraction of the ratios is often tried to bring out the main required feature or structure. The inversion of one ratio and its addition to another one may show most of the features being studied. Faults could be inferred from one-spectral band image. Also, foliation or cleavage

trends can be visible on satellite imagery but the study of the same area by ratio composite imagery may provide further structural features. Integration of remote sensing data with geophysical and geochemical data on digitized ratio composite maps, is the prospective methodology for better lithological and structural maps.

"Remote sensing investigations should not be considered as an alternative to field investigations. On the other hand, remote sensing data interpretation must be supported by field data – field observations, sampling, analysis and even subsurface exploration to a limited depth – for reliable inferences" (Gupta, 1991).

4.2 Geomorphological Studies

"Geomorphology involves the study of a number of parameters, namely extent and steepness of the slopes, their variations, shape, size, pattern, whether the slopes are barren or covered with soil or vegetation, type of surface material, whether the slope is stable or unstable etc., and mutual relations of the slopes and their genesis" (Gupta, 1991).

One of the widest applications of remote sensing data has been in the field of geomorphology, because (1) Remote sensing data products give direct information on the landscape, the surface feature on the earth, and therefore facilitate geomorphologic investigations. (2) Landform features can be better studied on a regional scale using synoptic coverages provided by remote sensing data, rather than in the field. (3) Stereoscopic ability permits evaluation of slopes, relief and forms; vertical exaggeration in stereoviewing brings out minor morphological details. The data in the VNIR broad band range have been used extensively for geomorphological investigations, as they provide higher spatial resolution and are able to bring out differences in topography, vegetation, soil, moisture, drainage etc.

Although the land surface features are stable, their manifestation and detection on remote sensing images are predominantly influenced by temporal surface parameters, namely, soil moisture, vegetation, land cover, drainage (dry/wet channels) etc. Therefore, it is important that the data sets be suitably selected to provide adequate temporal coverage. In many cases, landforms are characteristic of a particular type of terrain. As landforms are directly observed on the remote sensing data products, an

efficient photo-interpreter must have a sound knowledge of geomorphological principles and processes.

Landform Mapping generally deals with the homogeneity and instability of the material with reference to the old and present conditions. The indication of instability are mostly slides, tears, angularity or gentleness of slopes and hills, while the homogenates are categorized as planes, terraces, valleys, plateaus, hills, mountains and so on. It must be noted that the dip and strike of bedding planes, foliation and other structural elements make clues for the shape of landform unit, even it is not stereoscopic. As it is said before the land has a highly complex and varied surface. Each type of rock, fracture, and erosional and depositional feature bears the imprint of the conditions that controlled it. Geologists may ask about the importance of such type of mapping for their aim. To describe the earth's materials and structures, it is necessary to understand the geomorphology and to recognize the surface expressions of materials and structures.

The element most useful in terrain studies is topography because most landforms are erosional or depositional and are produced by modified geomorphologic agents – water, wind and ice, topography is modified by one or more of these agents. To identify various landforms the interpreter must be guided by understanding of the lithological and structural influences, the activity of subareal agents, the effects of past and present climates and the influences exerted by organisms. The two important categories of landforms are those produced by erosion, deposition and solution and that produced by tectonism. These have been elaborated here under.

4.2.1 Fluvial Environments and Landforms

"Running water is one of the most prominent agents of landform sculpturing, whose effects are almost everywhere to be seen. Huge quantities of sediments or rock material are removed, transported and dumped from one place to another by the rivers, thus modifying the land surface configuration"(Baker, 1996). The fluvial landscape comprises of valleys, channelways and drainage networks. The important issues of concern here with regard to the "Fluvial" landforms are "the drainage and rivers, their dynamics, the various fluvial deposits, and the effect of tectonics on drainage".

Drainage pattern is the spatial arrangement of streams and is in general very characteristic of the terrain. The drainage networks possess a geometric regularity of different types, which reveal the character of the geological terrain, and also help in understanding the fluvial system. A drainage system that develops on a regional surface is controlled by the slope of the surface and the types and attitudes of the underlying rocks. Drainage patterns, which are easily visible on photographs and images, reflect to varying degree lithology and structure of the region. The various depositional landforms include fans, cones, alluvial plains, flood plains, natural levees, river terraces, meander scars, channel fills, point bars, backswamps and deltas etc. Depending upon the dimensions involved, the landforms can be identified on aerial and satellite remote sensing data.

Understanding of controls exerted by the lithology and structure on a stream course is valuable in the interpretation of remote sensing data. Change in rock type along a stream can be inferred from segmental changes in valley width, degree of channel incision, valley or channel trend and habit and deposits in the valley floor. "Local bending or segmental gradient changes in a stream valley may be caused by local warping or by faults transverse to the stream course" (Elghawaby, 1977b). Compressional stress usually yields a series of nearly parallel folds, the spacing and the form of which depend on the type and thickness of the folded strata and the intensity of stress. A general parallelism of trunk stream denotes parallel folds. These geologic drainage relations must be taken into consideration during interpretation because they help better understanding of geologic setting of the region under investigation.

An important application of remote sensing data is in change detection of dynamic features, such as in changes in planform and migration of rivers, and delineation of paleochannels and palaeohydrology. The delineation of the palaeochannels and palaeohydrology has been discussed in great detail in the next section.

4.2.2 Aeolian Environments and Landforms

'Aeolian' landforms are commonly noticed in Deserts. The landforms in deserts are created by erosion, transportation and deposition, chiefly by wind action. The aeolian

terrain is marked by scanty or no vegetation and little surface moisture. Therefore, on VNIR photographs and images, the area has very light phototones. The various landforms can be distinguished on the basis of shape, topography and pattern. Aeolian erosional processes lead to the formation of a variety of landforms such as yardangs (sculptured landform streamlined by wind), blow-outs (a deflation basin), desert varnish (dark shiny surficial stains) etc. Remote sensing data can help monitor changes in deserts, their landform movement etc., and locate oases and buried channels. Two of the important features of the desert environment are sand dunes and buried channels. As the present work involves extracting buried channels in the study area, a more detailed coverage of it has been given under.

4.2.2.1 Sand Dunes

The transportation action due to wind removes loose sand and silt particles to distant places. Dust storms are aeolian turbidity currents. Loess deposits are homogeneous non-stratified and unconsolidated wind-blown silt. They are susceptible to gullying and may develop pinnate and dendritic drainage patterns. The dry Loess slopes are able to stand erect and form steep topography. Aeolian deposition leads to sand sheets, various types of dunes such as crescent, linear, star, parabolic and complex dunes and ripples. "The dunes occur in bundles or as individual (linear) dune-forms. Some of the latter form as a result of topographic impediments. As the wind moves across the surface, it forks at a topographic high and breaks into two components. As the two components meet again in the lee of hill, the two winds collide with each other and start unloading the sand. This continues to happen and the dune grows to several kilometers in length" (Farouk, 1987). The crescent-shaped or barachan dunes are more common in a desert, which reflect the direction of the wind, by its two arms. Further, after an active phase of appreciable movements, the dunes may get 'stabilized'.

4.2.2.2 Identification of Buried Channels

The streams draining through any region respond to the climatic fluctuations in the area as drier and wetter phases during the Quaternary. They also strongly respond to the neotectonism of the area, which may lead to gradual migration of the streams. In a region of marked climatic shifts and tectonic events such as the deserts of Rajasthan, it is common to find the palaeo-course of rivers buried under aeolian sand cover.

Initially, aerial photographs were used to study the lost and disorganized courses of some such rivers. With the availability of spaceborne multispectral data from Landsat, SPOT and the Indian Remote Sensing (IRS) series of satellites, palaeochannels can also be detected and mapped using satellite images. The availability of RADAR imagery from the European Remote Sensing Satellite (ERS-1/2), high resolution optical sensor data of Indian Remote Sensing Satellite (IRS-1C) and advanced digital image processing systems for data analysis have provided opportunities to explore with new tools and techniques.

Remote sensing techniques for identifying palaeochannels in parts of the Thar desert have been utilised by many investigators, particularly to trace the old courses of the mighty Vedic river, " Sarasvati" since the past two decades (Rao, 1991). However, there is a need to improve/update the interpretation at a large-scale (1:50,000) using synergic application of multi sensor, multi temporal data sets, digital enhancements and conduct systematic field validation.

The palaeochannels are usually associated with dense and vigorous vegetation cover, which exhibits characteristic spectral response pattern in the optical region of the electromagnetic spectrum. In the event of the presence of mineral matter of varying thickness over palaeochannels, it may not be possible to detect them since the spectral response measured from such a terrain by an optical sensor is basically from the surface.

Some of the image processing techniques found helpful for extraction of palaeochannels are Edge detection, Thresholding, Statistical Classification, Stretching and Color Composites (Sastry *et. al*, 1999). 'Merging' of satellite data from different sensors, especially the optical and the microwave, also proved advantageous in the identification of the buried channels. Some of the aforementioned methods were found to be inadequate in some cases e.g. conventional edge detectors failed due to the density of the sand dunes. A number of major and minor edges were detected and they are found to act as noise for accurately tracing palaeochannels. Classification gave fuzzy and incomplete results. Therefore, an attempt was made to multi-resolutionise (space-scale environment) and use image pyramids to maintain

locational accuracy and aid easy identification by Sastry et. al (1999). This step is called as the 'Pyramidal Processing'. The technical basis of this processing is elaborated here under.

A pyramid follows a hierarchial architecture *i.e.* it is a multi-layered data structure representing data at exponentially decreasing resolutions. It is constructed by combining adjoining pixels using a specific mathematical function. An element of pyramid is callednode or cell which in reference to an image is characterised by pixel dimension (x, y) and its level, k. Each node is linked or related to nodes either as $k-1$, its children (child block) or $k+1$, its parent (s). The pyramidal, therefore, consists of a stack of images in which each node except the base (input image/parent) has at least one child and that each node except the apex has at least one parent. Pyramids can be constructed for a wide range of image properties like range, colour, texture etc. using a variety of mathematical functions and different forms of architecture. Depending on the nature of the signature to propagate upwards, a suitable pyramid is chosen. One of the most significant advantage of multiresolution pyramidal processing is that the increasing order of subsampling in spatial and frequency domain leads to detection of definite edges while false edges are eliminated. For example in the subsampling by a factor of 2 the 2D signal is combined with a smoothing process i.e. by using a Gaussian operator so as to remove the high frequencies. In the resulting subsampled image, the number of pixels is reduced by half in each direction and therefore is 4 times smaller than the original. The filtering cum sampling process thus generates a set of images of decreasing sizes at different levels i.e. I (original/input) through V. The hierarchical architecture of a pyramid is analogous to human vision i.e., it perceives high resolution and high precision measurement of light reflected from the object and is able to identify objects of interest from its surroundings.

"IRS-1C LISS III data using 'digital enhancements' has helped in the identification of hitherto unknown palaeochannels, circular features and lineaments in parts of the Thar desert. These features have not been observed in corresponding multidate Landsat MSS, TM and IRS LISS II data. 'Pyramidal processing' has been found to be useful in the identification of a circular feature and a few palaeochannels not visible in other digitally enhanced products of IRS LISS III data" (Sastry, 1999).

Faint traces of Palaeochannels can be identified by looking for weak but consistent signature of moisture and vegetation through interdunal depressions and transverse sand dunes. Although the FCC of Level I showed some faint traces of Palaeochannels, these faint signature could be enhanced well in the Level IV of Pyramidal processing.

After identification of the palaeochannels reconnaissance field visits can be made and thus leading to intensive site selection. The final detailed field validation of palaeochannels may include Sediment Sampling, Ground water sampling, Geophysical Surveys, and Exploratory Drilling.

4.3 Structural Studies

Remote sensing tools are dependable tools in investigating geological problems specially those related to structural aspects. Experience with space imagery has demonstrated the exceptional value of synoptic view for displaying extended structural elements such as closed anticline, dome, fault zone, regional joint pattern, folded belts and intrusive bodies (Short and Lowman, 1973). Where the rock is exposed, the surface expression of tectonic elements of the crust is often better in the images. Also new lineaments of considerable magnitude and extent can be picked out in the images because of their breadth and continuity. Integrating the structural information derived from satellite images with the lithological distribution, landuse, landform, drainage pattern etc; a better understanding of the structural evolution of the region can be developed.

4.3.1 Delineation of Structural Elements

'Faults' are one of the important structural elements. One of the greatest advantages of remote sensing data from aerial and space platform lies in delineating vertical to high-angle faults or suspected faults. Low-angle faults are difficult to interpret, since the images provide planar views from the above. Such faults have strongly curving or irregular outcrop and can be inferred on the basis of discordance between rock groups. e.g., in the attitude of beds, degree of deformation, degree of metamorphism etc. The other important structural element is 'lineament'. The linear alignment of features on photos and images, are one of the most obvious features on high-altitude aerial and

space images, and therefore the use of the term lineament has proliferated in remote sensing geology literature recently. The lineaments and faults can be identified more clearly based on the information given in Table 4.1.

Lineaments can be easily identified on multispectral images by means of various tools of image interpretation and Image processing concepts. The manifestation of a lineament is dependent on the scale of observation and the dimensions involved. Lineaments of a certain dimension and character may be more clear on a particular scale, for which reason tectonic features of the size of hundreds of kilometers need to be studied on smaller scale images. On a certain photo or image, both major and minor lineaments are invariably observed. The major lineaments frequently correspond to important shear zones, faults, rift valleys, and major tectonic structures or boundaries. On the other hand, minor lineaments or micro-lineaments correspond to relatively minor faults, or joints, fractures, bedding traces etc. These are expressed as soil tonal changes, vegetation alignments, springs, gaps in ridges, aligned surface rags and depressions etc., and impart the textural character in a larger scene.

Table 4.1 Various possible lineaments and faults in a typical terrain (after Gupta, 1991).

Lineaments	Faults
(1) Shear zones/faults	(1) Displacement of beds or key horizons
(2) Rift valleys	(2) Truncation of beds
(3) Truncation of out crops	(3) Drag effects
(4) Fold axial traces	(4) Presence of scarps
(5) Joints and fracture traces	(5) Triangular facets
(6) Alignment of fissures, pipes, dykes, plutons	(6) Alignment of topography including saddles, knobs etc.
(7) Linear trends due to lithological layering	(7) Off-setting of streams
(8) Lines of significant sedimentary facies change	(8) Alignment of ponds or closed depressions
(9) Alignment of streams and valleys	(9) Spring alignment
(10) Topographical alignments – subsidences and ridges	(10) Alignment of vegetation
(11) Alignment of oil and gas fields .	(11) Straight segments of streams
(12) Occurrence of geysers, fumaroles and springs along a line	(12) Waterfalls across the stream courses
(13) Linear features seen on gravity, magnetic and other geophysical data	(13) Knick points or local steepening of stream gradients
(14) Vegetation alignments	(14) Disruption of channels and valleys, etc.
(15) Soil tonal changes etc.	
(16) Natural limits of distribution of certain earth surface features	

There are two ways of extracting lineaments - visual or through digital interpretation. The lineaments can be mapped on the original/simpler data products, as well as on processed/enhanced images. On an image, the lineaments can be easily identified by visual interpretation using tone, colour, texture, pattern, association etc., as elements of photo-interpretation. Visual interpretation of the lineaments involves some degree of subjectivity, i.e. the results may change from person to person. Alternatively, the automatic digital techniques of edge detection can also be applied for lineament detection. They can be applied in the form of isotropic and anisotropic filters of various sizes. The anisotropic filters enhance linear information in certain preferred directions. The edge detection techniques are, however, still under development, with numerous variations being possible, and lead to many artifacts or non-meaningful linears, which crop up due to illumination, topography, clouds, shadows etc. Therefore, the visual interpretation technique is preferred and extensively applied.

The lineaments mapped on a remote sensing image commonly exhibit spatial variations in trend, frequency and length. For statistical analysis, the lineaments are often grouped in ranges of angles (commonly 10^0 interval) in plan. The counting of lineaments for numbers and length measurement can be carried out manually, although it is tedious. Once the data of all the lineaments is read, it can be reformatted and processed to provide statistical information on trend, number and length (cumulative and average) etc. of lineament distribution. Further, the lineament data can be processed to generate contour maps and images for frequency or intersection density etc.

4.4 Image Processing Concepts

The image-processing concepts that were utilized extensively in the present work are the Thresholding and Classification techniques. Hence, a detailed elaboration of both of these techniques has been given in the sections to follow. The details of Thresholding include its purpose, various methods and some research work in this area. As regards Classification, it is a vast subject and numerous mathematical approaches for this have been developed and extensive discussion of this subject can be found in various image processing literature. The discussion given herein about them is rather rudimentary.

4.4.1 Thresholding of Edge Images

In any edge detection procedure, the final edge map is generated only after thresholding the image. "Image thresholding involves removal of grey level values below a certain threshold value". Edges are obtained by the application of some edge operator. This process is followed by application of a threshold on this edge detected image to obtain a resultant thresholded edge map.

Selection of a proper threshold value is always critical. If we select a very high value as threshold then most of the detected edges in the image are removed. On the other hand, if we select a very low threshold value, many spurious edges will also be included in the final edge map. Therefore, an automatic threshold selection is desirable than selecting a threshold value arbitrarily.

Considerable literature is available for the selection of automatic threshold values (Otsu, 1979, Kapur et al, 1985, Weszka., 1978). Majority of threshold detection methods use image histogram to optimize a certain criterion function. The threshold value obtained fro m this histogram is assumed to separate image into the background and object information. For a bi-modal histogram, the threshold value may be taken at its valley bottom. The selection of valley bottom as threshold value is justified in the sense that here the probability of misclassification of object as background and vice versa is minimized. Further, when we threshold at the bottom of valley, the results are relatively insensitive to our exact choice of the threshold value, since grey level values at a valley bottom are relatively unpopulated. However, in reality the histograms of edge images from natural scenes are rarely seen to possess distinctive bimodal nature. This creates additional problem in extraction of suitable threshold.

4.4.2 Classification

"The overall objective of image classification procedures is to automatically categorize all pixels in an image into land cover classes or themes" (Lillesand and Kiefer, 1987). Normally, multispectral data are used to perform the classification and indeed, the spectral pattern present within the data for each pixel is used as the numerical basis for categorization. That is different feature types manifest different combinations based on their inherent spectral reflectance and emittance properties.

The various methods of classification may be broadly categorized as Supervised, Unsupervised and Hybrid methods. Spectrally oriented classification procedures are more emphasized in various image processing literature. This emphasis is based on the relative state-of-the-art of these procedures. They currently form the backbone of most classification activities.

Another area that is continuing to receive increased attention by remote sensing specialists is that of classification accuracy assessment. There is no simple, standardized, generally accepted methodology for determining classification accuracy. There are two commonly employed approaches. They both involve comparing the results obtained from a digital classification to the "known" identity of land cover in test areas derived from reference data. The test areas are typically represented by one, or combinations, of the following: (1). Homogeneous test areas selected by the analyst. (2). Test pixels or areas selected randomly.

The concept of *contingency table* is used as an aid in assessing training area classification accuracy. It should be remembered that such procedures only indicate how well the statistics extracted from these areas can be used to categorize the same areas! If the results are good it means nothing more than the training areas are homogeneous, the training classes are spectrally separable, and the classification strategy being employed works well in the training areas. This aids in the *training set refinement* process but it indicates little about how the classifier performs elsewhere in the screen.

Test areas are areas of representative, uniform land cover that are different from, and considerably more extensive than, training areas. They are often located during the training stage of supervised classification by intentionally designating more candidate training areas than are actually needed to develop the classification statistics. A subset of these may then be withheld for the postclassification accuracy assessment, again using *contingeny table* to express the results.

METHODOLOGY FOR GENERATION OF THEMATIC LAYERS

5.1 Introduction

While doing the present work the main interest was to extract various information from the satellite imagery by laying special emphasis on the "Geomorphologic" and "Structural" aspects of the study area. The important themes on which attention has been focussed are height, slope and aspect of the terrain, lineament and faults, drainage network in the area, various aeolian, lacustrine and fluvial landforms in the area and the lacustrine processes. In order to extract the aforementioned themes from the satellite imagery, various image processing techniques have been used in a GIS environment in the light of the literature review presented in previous chapters.

This chapter explains in detail how the various thematic layers of interest have been generated. In this work the entire methodology has been divided into seven steps. Figure 5.1 shows the break-up of the various steps followed here. 'Step-1' concerns extracting four bands from the raw satellite data and converting the five topographic sheets of the study area into digital form. In 'Step-2', ground coordinates are attached to imagery and digital topographic sheets followed by geometrical correction of the satellite data by means of georeferencing and resampling operations respectively. 'Step-3' involves the use of some visual enhancement techniques so as to get some preliminary information of the terrain. 'Step-4' deals with acquiring topographic information by generating DTM, slope and aspect map of the terrain. 'Step-5'extracts the structural information (lineaments and faults) of the study area through spatial enhancement involving edge filters and thresholding techniques. 'Step-6' concerns itself with the identification of the surface and subsurface drainage in the area by means of some special interpretation keys and pyramidal processing. Finally, 'Step-7' deals with extracting some of the geomorphologic features from the satellite

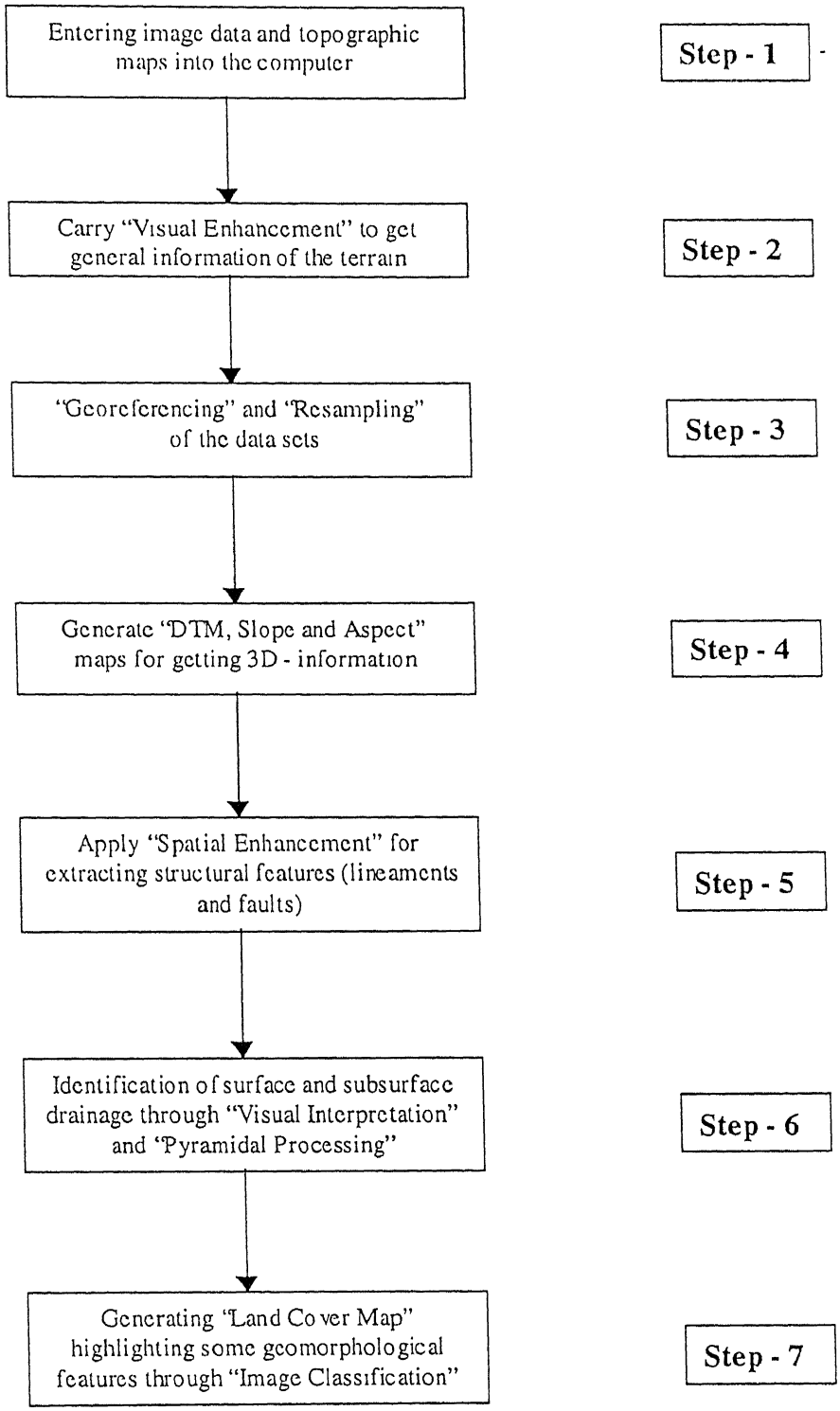

Figure 5.1 Block diagram showing various steps followed in the present methodology

imagery in the form of land cover map developed by doing image classification. Each of the aforementioned steps has been explained separately in great detail in the subsequent sections.

5.2 Data Selection and Entry into Computers (Step – 1)

This step deals with the data sets used for the present study, their suitability, and the way they are entered into computer. Satellite imagery and the topographic sheets are the important data sets used here. The imagery gave a very good regional coverage of the entire region around Sambhar Lake. "It was observed that for the semi-arid regions, the imagery immediately after the rains (post monsoon) impart the maximum information, particularly those obtained from the optical sensors. This is because of the distinct signature due to vegetation and moist pockets. The haze in the imagery is considerably reduced as the dust in the atmosphere present during hot summer season gets settled after the rains and thus leads to improved contrast" (Rajawat *et al.*, 1999). Hence, it has been ensured that the date of pass of the satellite while capturing the present imagery falls in post monsoon (i.e. 21 Nov. 1995, in the present case).

The raw image data thus procured was in Band Interleaved by Line (BIL) format. The four bands spectral data was extracted from this raw data by using IDRISI initially and was later imported into ILWIS for further processing.

Five topographic sheets of the study area have been obtained from SOI and as they are in hard copy form it was required to convert this into digital form. This was accomplished by scanning all the sheets in piece-wise form using UMAX flatbed scanner at 150 dpi, 256 colors and then later *stitching* them using 'Presto Image Folio' software to form a mosaic (Plate-24). This digital form of the topographic sheets was used later while registering the satellite image, extracting height information from it and also for picking up various training and testing areas during classification stage etc.

5.3 Visual Enhancement for General Information (Step – 2)

At this stage, various visual enhancement operations have been employed on the satellite imagery to get some preliminary information of the study area. The enhancement operations taken up in this step are shown in the Figure 5.2. Each of this techniques are separately explained here under:

a) *Contrast Stretching*: The raw satellite imagery did not show a good contrast between various features appearing on it. Hence, there was a necessity to apply contrast stretching on this imagery. Linear stretching with 2% saturation was applied in the present case.

b) *Histogram Equalization*: By doing histogram equalization on the raw satellite imagery, the entropy of the image, a measure of the information content of the image, was increased. The underlying principle is that each histogram class (0-255) in the displayed image must contain an approximately equal number of pixel values, and the histogram of these displayed values will then be almost uniform (Mather, 1987).

c) *Band Ratioing*: Band ratioing is an extremely useful procedure for enhancing features on the multispectral images. It is used to reduce the variable effects of illumination condition and topography (Gupta, 1991). The new digital image is constructed by computing ratio of DN values in two or more input images, pixel by pixel. Band ratioing was employed in the present study mainly to extract the vegetation pattern in this area. The ratio such as $\frac{X_4 - X_3}{X_4 + X_3}$, where X represents the DN values of individual bands, are most commonly used because of large difference in spectral values of vegetation in band4. Contrast stretching and enhancement are applied on the ratioed image finally for easy distinction of vegetation. Besides this, some other band ratioing operations have been carried out, viz. *Band1/Band2, Band2/Band3 and Band3/Band4.*

d) *Multiple Band Enhancement*: An important aspect of remote sensing is that it provides data in multiple spectral bands which can be super-imposed over one another to deduce information not readily seen on a single image (Gupta, 1991). Two important multiple band enhancement techniques considered here are False Color Composite (FCC) and Principal Component Transformation (PCT).

(1) *Principal Component Transformation*: This is a technique designed to remove or reduce the redundancy in multi-spectral data. It has a two-fold purpose, as an enhancement operation prior to visual interpretation of the data and as a

confirming them with the scanned topographic sheet. Besides this, it also helps in drawing various interpretations by overlaying the vector layers on raster layers both sharing a common georeference.

Table 5.1 Variance – Covariance Matrix

	Band1	Band2	Band3	Band4
Band1	42.66	32.66	50.73	35.82
Band2	32.66	27.69	44.72	31.09
Band3	50.73	44.72	87.08	70.75
Band4	35.82	31.09	70.75	94.06
Mean	44.46	30.60	47.61	51.22
Std.Dev	6.53	5.26	9.33	9.70

Table 5.2 Correlation Matrix of the bands

	Band1	Band2	Band3	Band4
Band1	1	0.95	0.83	0.57
Band2	0.95	1	0.91	0.61
Band3	0.83	0.91	1	0.78
Band4	0.57	0.61	0.78	1
Mean	44.46	30.60	47.61	51.22
Std. Dev	6.53	5.26	9.33	9.70

Table 5.3 Transformation coefficients for PCA

	Band1	Band2	Band3	Band4
PCA1	0.384	0.326	0.626	0.595
PCA2	0.502	0.370	0.215	-0.752
PCA3	0.647	0.092	-0.706	0.275
PCA4	0.428	-0.865	0.253	-0.068
Variance	208.68	34.71	7.19	0.91
%Variance	82.98	13.80	2.86	0.36

Table 5.4 Choice of bands for FCC based on OIF

S.No	Band Combinations			OIF*
1	Band1	Band3	Band4	11.73
2	Band2	Band3	Band4	10.55
3	Band1	Band2	Band4	10.11
4	Band1	Band2	Band3	7.84

In the present work, georeferencing was carried out in two stages. Firstly, the scanned topographic sheets were georeferenced followed by registeration of the satellite data with respect to this base map. Transformation equations were used here for the

purpose of georeferencing both the scanned topographic sheet and the satellite imagery. These equations were also useful for geometric correction of the satellite imagery. An affine transformation shown below was used in the present work.

$$X = a_0 + a_1 R_n + a_2 C_n$$
$$Y = b_0 + b_1 R_n + b_2 C_n$$

Where R_n is row number and C_n is the column number of the image. To define the transformation, it will be necessary to compute the coefficients of the polynomials (e.g. a_0, a_1, a_2). For the computations, the various points collected are given in Table 5.5 and Table 5.6. The overall accuracy of the transformation is indicated by the average of the errors in the reference points. It is also called as a Root Mean Square Error (RMSE) or Sigma, and is kept less than 1 pixel in this study.

After geo-referencing, the image still has its original geometry and the pixels have their initial position in the image, with respect to row and column indices. A new image was created from this by means of resampling it, applying nearest neighbourhood interpolation method (Mather, 1987). The interpolation method is used to compute the radiometric values of the pixels in the new image based on the DN values in the original image. This newly obtained image is geometrically corrected.

It is to be noted here that all the image processing operations in the subsequent steps were carried out on the georeferenced images but not on the resampled images. The reason being it is a good practice to work with undisturbed raw grey level values of the image than with the changed radiometric values after resampling (Lillesand and Kiefer, 1994).

Table 5.5 Points used for Georeferencing of Scanned Topographical Sheet

S.No	X	Y	Row	Col	Drow	Dcol
1	-78406.8	3018128	1161	4935	-0.45	-0.03
2	-55213.9	2979975	5515	7832	0.53	-0.15
3	-113349	2982675	5514	1066	0.07	-0.31
4	-111724	3019512	1180	1058	-0.43	-0.34
5	-103699	3010052	2249	2041	1.72	0.18
6	-87124.3	3009259	2250	3970	-0.16	0.04
7	-87995.5	2990743	4428	3968	-0.76	0.39
8	-104595	2991533	4426	2036	-0.4	0.4
9	-80124.3	2981099	5518	4933	-0.12	-0.19

Sigma = 0.647 pixels

Table 5.6 Georeferencing of Satellite Images with Toposheet as Base map

S.No	X	Y	Row	Col	DRow	DCol
1	-105938	3006641	646	105	-0.46	1.19
2	-108152	3006428	664	46	-0.76	0.18
3	-108534	3006736	659	34	0.31	0.35
4	-110014	3002273	787	21	0.09	-1.11
5	-97508.7	3001761	730	361	0.53	0.61
6	-97261	3004901	643	348	-0.77	0.74
7	-96643.1	3006542	596	355	-0.21	1.52
8	-82541.5	2994116	850	808	0.5	-1.55
9	-83664.8	2994407	848	776	-0.1	-1.62
10	-84170.2	2990154	965	791	-0.13	0.14
11	-83031.3	2989079	988	827	0.5	-1.14
12	-79292	2990252	935	920	0.25	-0.95
13	-76857.3	2985897	1038	1014	0.21	0.4
14	-76986.2	2984591	1074	1018	0.42	-0.37
15	-77020.5	2986467	1024	1005	0.57	-0.64
16	-80169.2	2984257	1101	935	0.32	-0.19
17	-61359.7	2972742	1300	1515	-2.72	3.34
18	-98239	3001233	748	344	0.19	-0.15
19	-61503.9	2971855	1326	1516	-1.37	2.61
20	-58776.9	2973858	1257	1577	-1.08	3.16
21	-63575	2976440	1216	1429	-0.07	-0.03
22	-108643	2984134	1266	173	-0.03	-0.04
23	-94913.5	2987782	1090	518	0.04	0.06
24	-101973	3023961	159	101	0.06	0.01
25	-89407.4	3022152	136	449	0.01	-0.07
26	-80323	3010163	406	768	-0.1	0.04

Sigma = 0.785 pixels

5.5 DTM, Slope and Aspect map for three dimensional Information (Step – 4)

The purpose of this step was to extract the height, slope and aspect of the terrain, which was useful to identify the various deformations in and around Sambhar lake. The various wind gaps in the area and the drainage trend were also visualized through this operation. The sequence of operations carried out in this step are given in the Figure 5.2.

a) Firstly, the area common to the satellite image and the scanned mosaic of topographic sheets was extracted by means of some overlaying operations. The common portion was covering most of the terrain around Sambhar lake except some portion on the northeast side.

For the generation of DTM, height information was obtained from the topographic sheet were digitized and a DTM was obtained by means of interpolating the random

height data using weighted nearest neighbourhood interpolation facility in ILWIS. The final DTM after interpolation gave some localized peaks because of some limitations of the interpolation method employed here. Therefore, a 3 x 3 mean filter

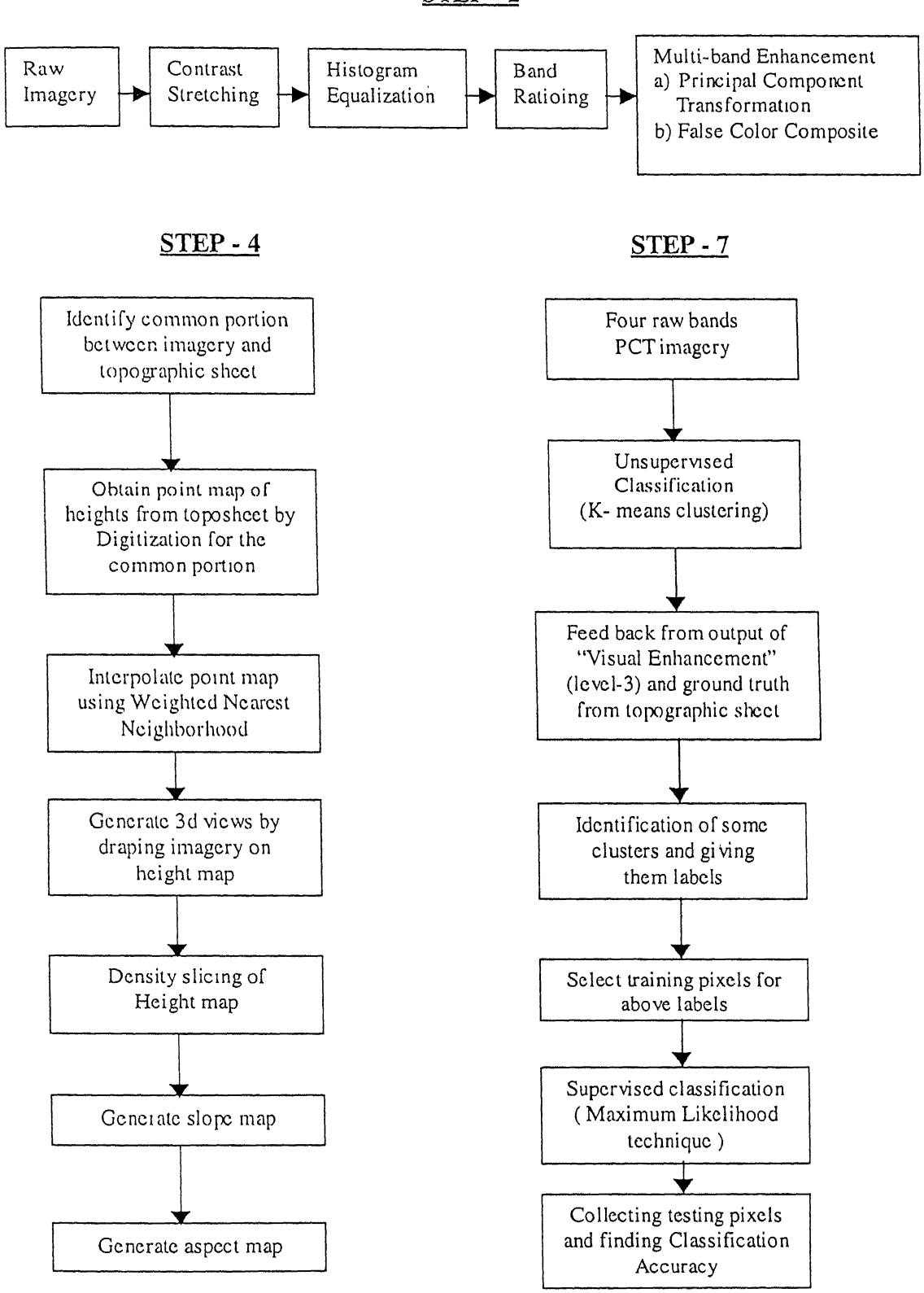

Figure 5.2 Sequence of operations carried out in 'step-2', 'step-4' and 'step-7'

was applied on the DTM for smoothing the image. A 3D view of the study area was obtained using the 3D display capabilities of ILWIS. The standard FCC (Plate-6) was draped over the DTM obtained previously. A wire mesh plot was also obtained. While displaying the view was adjusted in a manner as to get a good view of the wind gap in this area and also to see the depressions in the area. The results are presented in the next chapter.

b) A slope map (Plate-12) giving the inclination at a point was calculated from the previous height map using a function from ILWIS " *slopedeg=RADDEG (ATAN((HYP(Dx, Dy))/pixelsize))* " where *Dx* and *Dy* are horizontal and vertical gradients obtained by applying linear directional filters. *RADDEG* is a function used to convert from radians to degrees. *ATAN* calculates the arctan ($\tan^{-1}$). *HYP* (hypotenuse) calculates the positive root of the sum of a square Dx plus Dy. This map was needed to understand the terrain nature and the drainage characteristics.

c) Also, an aspect map (Plate-13) showing the direction of slope was calculated from the height map using the function from ILWIS "*aspect=RADDEG(ATAN2(Dx, Dy) + pi)*". *ATAN2* returns the angle in radians of two input values *Dx* and *Dy*. This map was needed mainly to know the direction of flow of the drainage.

5.6 Spatial Enhancement for Generating Lineament and Fault Map (Step – 5)

The objective of this step was to generate a lineament and fault map so that the structural evolution of Sambhar lake could be more clearly understood. Spatial enhancement techniques were applied to extract various edges out of the satellite imageries to identify various lineaments and faults. The sequence of operations carried out in this step are clearly detailed in the Figure 5.3.

a) The choice of band for applying edge filters is generally based on the criterion that it should have maximum information present in it. In the present case, from the correlation matrix (Table 5.2) of all the four bands it was observed that band 3 was highly correlated with all the rest of the bands and hence having most of the information of the other bands contained in it. Based on this band 3 was selected in the present work for applying various edge filters. The choice of band 3 was

also directed by the fact that visually more linear features could be seen on this band.

b) The process of edge detection involves convolution of various windows based operators with the image. The various edge filters used in the present study are Sobel, Kirsh, Laplacian of Gaussian (LoG), Morphological, Laplacian subtracted from the original image, Frei-Chen, Prewit and other directional filters. The details of various aforementioned filters along with their masks are given in the Appendix-II. The final edge images comprise of both minor and major edges as well. It was very difficult to identify lineaments and faults from this. Hence, thresholding was carried out next to suppress spurious edges and retain major edges.

c) Two important steps here are firstly to identify a suitable threshold separating spurious edges from important edges and then to binarize the edge image based on this threshold. In the present work, both global and local thresholding was carried out. The thresholding criteria have been taken from Otsu (1979) and Kittler and Illingworth (1985). The details of thresholding, various types, criterions and the algorithm that were followed in the present work are given in Appendix-2. In *global thresholding*, a single threshold was obtained and based on this the grey values below this threshold were made zero and the rest to 255. *Local thresholding* was done by dividing the image into 8, 16, 32, 64 parts in row and column direction, as is the common practice followed by many, and finding the threshold pertinent to each individual part and binarizing each part separately based on this. Some interesting observations emerge from the algorithm that was followed here and these are elaborated in the next chapter. Some of the thresholded images are also shown in the next chapter.

d) Before identifying various lineaments and faults from the edge images, some feedback was required from the visually enhanced images obtained at 'step – 2'. This includes information on vegetation pattern, rivers and other drainage and sharp tonal changes of the surface features in the imagery noticed after carrying out spectral and multi-band enhancement. The details as to how this information helps in giving idea of various lineaments and faults are discussed in the next chapter showing the particular locations in the study area where it holds good.

STEP - 5

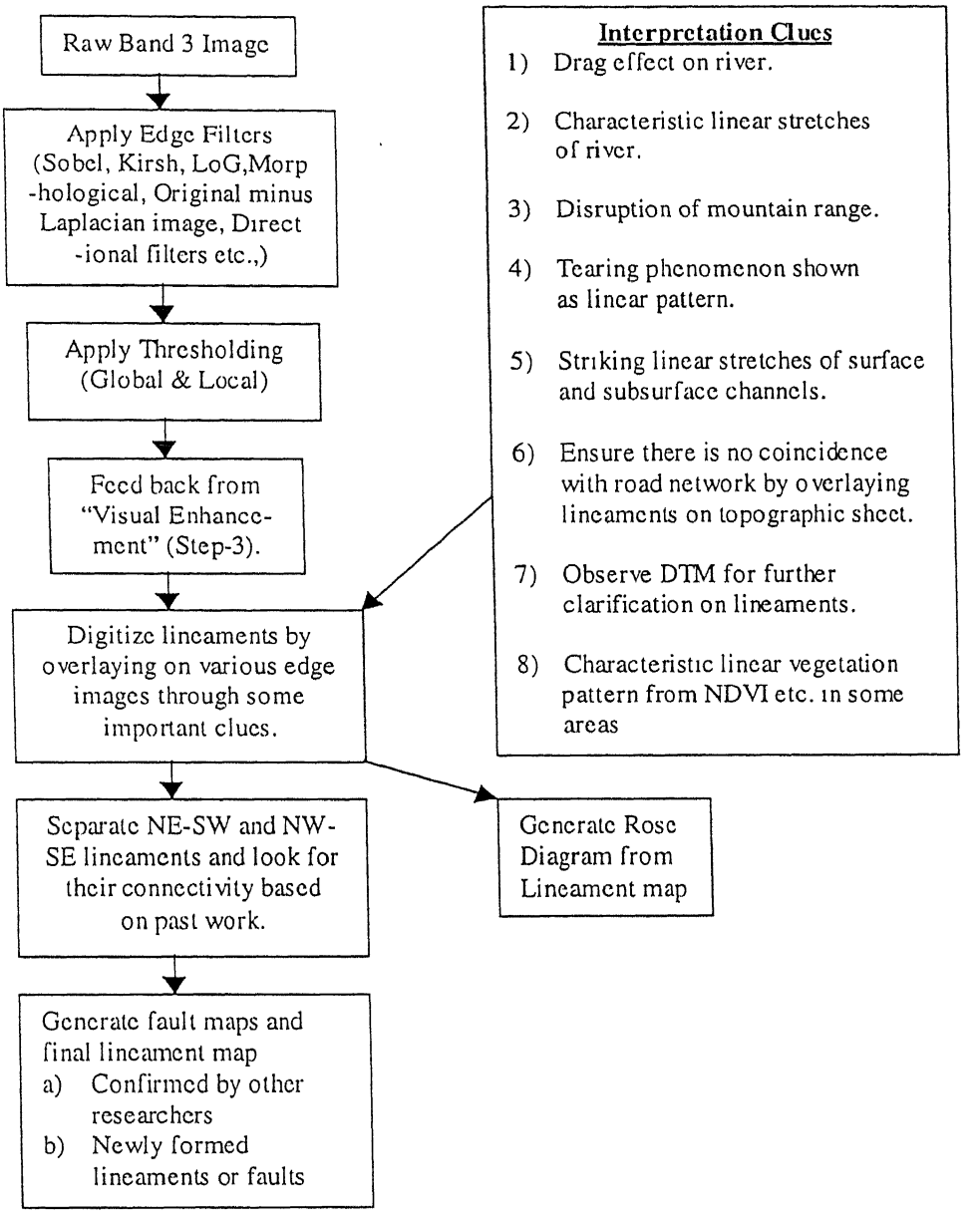

Figure 5.3 Sequence of operations carried out for extracting Lineaments & Faults (step-5)

e) The lineaments are digitized mainly from the edge images obtained after applying 'Sobel' and the 'Laplacian minus Original' filter. Digitization was done by overlaying the same vector layer on various images of concern. Some of the edges were also identified from the thresholded images of 'Kirsh', 'LoG' and 'Sobel'

filters. Some lineaments were also observed in the ratioed image of band1 and band2 (Plate-5). The visual interpretation keys used in the identification of various lineaments and faults are given clearly in Fig –5.3. Some of the lineaments that are identified are shown in the next chapter. Finally, the Rose diagram of the lineaments was obtained with the help of ILWIS.

f) The lineaments in NE-SW and NW-SE directions are separated from the vector layer obtained earlier. The connectivity of various fragmentary lineaments has been looked for in each of the aforementioned individual directions based on the orientation of various minor lineaments. The neotectonic maps showing lineaments of this area given by Das sarma (1988) and Sinha-Roy (1986) were also kept in mind while doing this.

g) The final lineament map prepared from digital processing of the remote sensing data includes many of the lineaments identified by earlier works (Dassarma, 1988 and Sinha-Roy, 1986) as well some new lineaments based on the present interpretation.

5.7 Identification of Surface and Subsurface Drainage (Step – 6)

Various image transformation techniques have been of tremendous value for identification of buried channels in the study area along with the surface drainage network. Besides these, the various lakes in this area and some high moisture zones were also identified. The various operations in this step are shown in the Figure 5.4.

a) The FCC of PCT generated in visual enhancement stage (step-2) i.e. by loading PCT!, PCT2, PCT3 on R, G, B planes was used initially to identify the high moisture zones in the area (shown in Plate-10). These zones were then digitized into a polygon map, which was very useful for interpretation of surface and subsurface drainage. Besides this, the FCC was also used to identify all the water bodies in the area which were digitized separately.

b) The various high moisture zones identified earlier were observed to be located in topological depressions as inferred from the DTM .

c) Some other feedback was obtained from the output obtained at the visual enhancement stage. This includes the contrast stretched images of band3 and band4 giving very good contrast between land and water bodies. vegetation activity in the area from NDVI map, some lineaments from band ratioed image band1/band2 and PCT3, and some information about aeolian activity as given from the FCC generated by loading band1/band2, band2/band3, band3/band4 on R, G, B planes.

Shastry *et al.* (1999) in his findings reported that pyramidal processing techniques are favorable for identification of some of the buried channels from IRS-1C PAN data. This concept is based on multi-resolutionizing the image at different decreasing reso lutions and then identifying the buried channels at different levels of resolution from a stack of multi resolution images. This technique was reported to be somewhat similar to how human being visually identifies various features. This technique has been implemented here and a stack of images of FCC generated from PCT3, PCT2, PCT1 loaded on R, G, B planes has been made by resampling the original image with a resampling ratio of 1/2, 1/4, 1/8 i.e at 4 levels totally including the original image. The choice of the above FCC of PCT images is guided by the fact that visually more surface and subsurface features were found in it. The results and the important observations that emerge in this stage are presented in the next chapter.

d) The vector layers of high moisture zones and various water bodies digitized earlier were overlayed on the FCC of PCT images referred in the previous stage. Most of the surface and subsurface drainage were extracted from this combined layer in the light of the feedback information from visual enhancement stage mentioned before. The identification is completely based on visual interpretation. The various interpretation keys used in the present work are detailed in the Figure 5.4.

e) Thus, the final thematic layer was generated by digitizing the surface and subsurface drainage along with various water bodies and high moisture zones in the area.

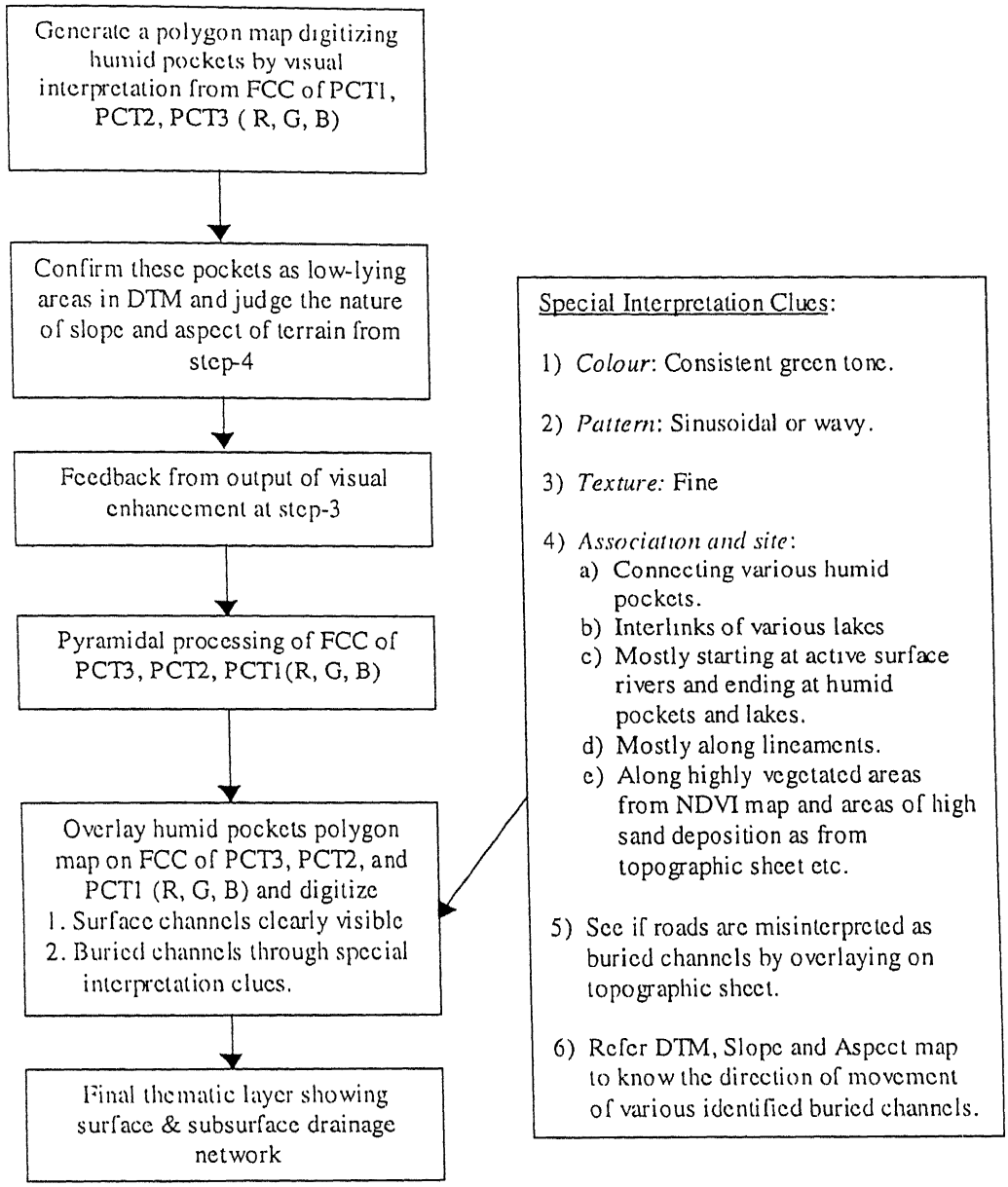

Figure 5.4 Sequence of operations for extracting surface & subsurface drainage (Step-6).

5.8 Generating Land Cover Map for Geomorphologic Information (Step – 7)

In this step, in order to extract some geomorphologic information from satellite images classification was carried out. "Multispectral classification is the process of sorting pixels into a finite number of individual classes, categories of data, based on their data file values. If a pixel satisfies a certain set of criteria, the pixel is assigned to the class that correspond to that criteria" (Lillesand and Kiefer, 1987). The various operations that were carried out to generate a final land cover map with some geomorphologic details are given in the Figure 5.2.

a) In this work classification has been taken up for two different input data sets separately - all the four spectral bands at one time and the first three PCT images the other time.

b) Initially unsupervised classification using K-means clustering (Mather, 1987) was applied on the input data set mentioned earlier. The only input given was the number of clusters that were to be identified in the data set. This was roughly taken as double the total number of actual classes that were to be obtained. After this the algorithm examines the unknown pixels in an image and aggregates them into number of classes based on the natural groupings or clusters present in the image values. The classes that result from this classification are spectral classes. Because they are based solely on the natural groupings in the image values, the identity of the spectral classes will be initially unknown. Thus the classified data has to be compared with some form of reference data to determine the identity and informational value of the spectral classes.

c) For the reference data on various classes in the image some feedback was acquired from the output of "visual enhancement" (step – 3) and also from the scanned topographic sheet. This included the sparse vegetation identified using NDVI map, the lake processes (different algae and depth categories) as observed from FCC generated out of band4, band3, band2 loaded on R, G, B planes, and the aeolian activity as inferred from FCC generated out of band1/band2, band2/band3 and band3/band4 loaded on R, G, B planes etc. From the topographic sheet, information on the green cover of this area and sand dune activity etc., were obtained besides the geographical location of various important features of interest.

d) Based on the feedback acquired as mentioned above, some of the resultant clusters from unsupervised classification were identified and suitable labels were attached to them. Table 6.1 gives the details of various classes identified and selected for further supervised classification.

e) Before going for further classification, some training pixels were selected from the input data set for each class type listed above. The idea was to assemble a set of statistics that describe the spectral response pattern for each land cover type to be classified in the image. It was ensured that a minimum number of $10n$ to $100n$ pixels was used as a representative sample for each class, n being the number of spectral bands taken (Lillesand and Kiefer, 1987). The various training statistics are presented in Table. 6.2

f) Based on the training samples taken previously for various classes of interest, supervised classification has been carried. Maximum Likelihood classification technique is used here (Mather, 1987). The final results and the output image are shown in the next chapter.

g) Collecting testing pixels and finding classification accuracy. Finally, classification accuracy assessment has been done. This involved comparing the results obtained from a digital classification to the known identity of land cover in test areas derived from reference data. With the help of the ground truth information from the topographic map, some testing areas are selected as representative samples. It is ensured that these pixels don't coincide with the training pixels. With this a confusion matrix (Mather, 1987) is generated to assess the classification accuracy using a facility in ILWIS2.2 software. The confusion matrix is presented in Table 6.3.

RESULTS AND DISCUSSIONS

6.0 Introduction

In the previous chapter various steps taken up in the present methodology for generating some thematic layers have been elaborated. This chapter presents the outcome of these steps. This includes various images acquired at different steps and the interpretations that arise out of them. The interpretations from the visually enhanced images are dealt separately from that of the other individual thematic layers. Finally, based on these interpretations, some discussions are given in regard to geomorphologic and structural evolution of the Sambhar lake.

6.1 Observations on Visually Enhanced Images

Visually enhanced images comprise contrast stretched images, band ratioed images, FCC, PCT etc. Some preliminary information of the terrain could be derived from these images as given under.

6.1.1 Contrast Stretched Images

In the contrast stretched image of Band1 (Plate-1) the fresh alluvial sediments and the salt encrusted lands are appearing as brightest tone while the aeolian and the old alluvial sediments are showing lighter tone. Stretched image of Band3 (Plate-2) being sensitive to chlorophyll highlights the vegetation as dark gray patches. It helps in differentiating soil types and delineating geological boundaries. In this band fresh and salt encrusted sand is represented by the brightest tone while old sand is represented by lighter shades of gray. The manmade structures are delineated from their distinct pattern and contrasting tone with the surrounding. Most of the information about the terrain was obtained from this one band itself. Stretched image of Band4 (Plate-3) is elaborating the land water contrast. The green biomass and moisture being sensitive to this spectral range appeared as distinct patches of darker tone in the image.

6.1.2 Band Ratioing

NDVI is an important band ratioed image here highlighting the sparse vegetation cover present in this area. Plate-4 shows the sliced NDVI image with 5 classes in it. In this image, sparsely distributed patches of green tone are having very high NDVI and are densely vegetated areas. Few open-scrub forests, as identified from the topographic sheets, belong to this category. These are located mainly on the southern and eastern side of Sambhar lake and also on the northwestern side close to the Aravalli hills. The sand deposits with high vegetation cover is shown in blue color indicating high NDVI. These are mainly located in regions radially farther away from the Sambhar lake. Medium NDVI values shown in black occur mostly on the northeast and south east of Sambhar lake. Soils with very low to no vegetation cover comes under this category. The salt encrustated soils showed low NDVI values in pink color while the water bodies indicated very low NDVI values shown in yellow color.

The ratio image *band1/band2* highlights some of the lineaments and the palaeo-channel zones in the study area very clearly along parallel lines oriented themselves in NE-SW direction (Plate-5). Besides this, many other band ratioed images referred to in the earlier chapter didn't give any significant information. However, on generating FCC with these, some important information could be derived. These particulars are given under the next heading.

6.1.3 False Color Composite

The standard FCC (Plate-6) generated by loading Band4, Band3 and Band2 on Red (R), Green (G), Blue (B) planes respectively coupled with geometric corrections provided a regional view with respect to geology, topography, drainage and vegetation in different shades of colors. The shades of dark brown on the west of Sambhar lake represent greatest height corresponding to quartzite and quartzoschist ridges and light brown colour on the northeast and southeast of the lake represents sand dunes and sand mounts of different heights. Most of the drainage seen on the image are dry channels and are depicted by the shades of white. Apart from the Sambhar lake, a few smaller lakes are also seen on its south which seem to be connected by one of the old channels. Sparsely vegetated cover is represented by different shades of red color. The different parts of lake are well depicted in this FCC.

The leftmost part is the main lake body showing different shades of blue color while the reservoir and the bittern part showing light blue and green colors respectively are the central and rightmost parts of the lake. In the main lake body, darker the blue tone deeper is that particular portion of the lake. Besides this, the salt pans on the north and south of Sambhar lake and also some of the shallow water bodies in the study area appear in sky blue color.

The True Colour Composite (Plate-7) obtained by loading band3, band2 and band1 on R, G, B planes respectively also shows a better contrast between different land covers. Most of the features interpreted earlier in the standard FCC could also be traced very well in this image. The Aravalli ridges are represented by narrow elongated zones of deep brown colour. While the alluvial fans developed on the footslopes are represented by medium shades of brown. Drainage and salt encrusted sand are represented by brightest tone. The dark brown colors in this image represent the older sand deposits with sparse vegetation cover and some moisture in it. The light brown tone represent younger or fresh sand deposits. Some of the relatively older sand deposits appear in an intermediate brown tone. This image shows the central and the rightmost part of the Sambhar lake in green and red tone indicating the presence of green and red algae. The presence of a specific algae type is related to the salinity of the water. This additional information could not be directly visualized from the standard FCC (Plate-6). Further, few striking parallel lines with a characteristic tone, aligned in NE-SW direction were picked up on this image which were interpreted as lineaments. Some pale blue shades showing zones of palaeo-channel were also observed on this image.

An FCC has been also generated by loading the band ratioed images *Band1/Band2, Band2/Band3, Band3/Band4* images on R, G, B planes respectively, which reflects the land cover distribution in the area. This image (Plate-8) has very high information content compared to the standard FCC and the True Color Composite. It summarizes almost all the previous interpretations. It shows sparse vegetation cover in its natural tone. The area with salt pans and the shallow lakes around Sambhar lake show an intermediate blue-green tone. All the sand deposits appear in reddish brown color and salt encrusted lands appear in metal gray shade. The alluvial deposits and other fluvial deposits were also clearly visible in a light yellowish tone around the Aravalli hills and along some stream courses in the area. The different parts of the lake showed

different colors – green color in the main reservoir indicates green algae, red color in the bittern part indicates red algae, and the various colours in the main body of lake are due to varied depths in it.

6.1.4 Principal Component Analysis (PCA)

Out of four principal component images generated, PC3, although seemingly noisy, indicated very clearly a set of seven parallel lineaments (marked as A, B, ...G on Plate-9). The one labeled as 'D' could not be easily marked elsewhere in other images (Plate-9). An enhanced colour composite (Plate-10) was produced by loading the images PC1, PC2, PC3 in planes R, G and B respectively. In this, narrow linear patches of dark tone represent the Aravalli hills. However, the main objective here was to extract clearly all the water bodies, moisture zones, present and past drainage network from this image. All the lakes are shown in dark red color and the high humid zones in this area as light red color. The high humid zones in the Sambhar terrain are shown as regions bounded by thick blue lines in Plate-10. Besides this, the present and the past drainage network could also be traced from this image which is detailed in one of the subsequent sections.

6.2 Observations on Various Thematic Layers

The various thematic layers that are generated in the methodology stage are DTM, slope and aspect map, lineament and fault map, surface and subsurface drainage, land-cover map. The interpretations on each of these individual thematic layers are presented herein.

6.2.1 DTM, Slope and Aspect map

Plate-11 shows the sliced DTM with different colors assigned to various height ranges. It can be seen from this image that greater magnitudes of heights are concentrated around the Aravalli mountain range and the remaining part of the terrain has little variation in height. Pediplains are observed around these hills as bands of different colors. Sambhar lake is seen to be located in the central depression thus resulting in centripetal drainage into the lake. Many other saline lakes and high moisture zones are observed to fall in the topographic depressions as observed in this image. An elongated depression shown as a band of low heights in this image is found aligned in NE-SW direction along the Mendha and Rupangarh river. This observation

is supported by Dassarma (1985) who referred it as 'Mendha stepped graben'. The entire portion on the southeast of Sambhar depression is a low-lying area, which is manifested as large and frequent moisture zones.

The slope and aspect maps (Plates-12 and -13) show the slope in degrees and the direction of slope respectively. From Plate-12 it was found that the entire region is more or less a plain terrain with a gentle slope towards the Sambhar lake and other topographical depressions. The aspect map confirms this by indicating the slope direction to be towards all the saline lakes and other low-lying areas in the region. Steep slopes were observed only in regions just around the Aravalli hills.

The FCC generated by loading band4, band3 and band2 on R, G, B planes respectively is draped over the DTM to get a 3D-view of the terrain (Plate-14). The entire terrain appears as a saucer-shaped feature with Sambhar lake located at its centre and all the drainage network debouching into the lake. However, few isolated points of larger heights are seen because of the limitations of the interpolation technique employed here. Two wind gaps are clearly observed in this 3D-view, one on the northeastern side of the Sambhar lake and the other on the southeastern side. The visualization of these features has proved to be of immense value in understanding the aeolian transport and deposition in the region thereby explaining the geomorphic evolution of the Sambhar lake as elaborated in the subsequent sections.

6.2.2 Lineament and Fault maps

Among all the edge filters Sobel filter gave visually good results (Plate-15). The labels A, B.....F indicate some of the important lineaments conspicuous on this image. Besides this, another image that gave good results is the edge-enhanced image (Plate-18). All other filters referred to in chapter 5 gave a bit noisy edges. After applying thresholding on all the edge images it was found that the binary images obtained still contained some noise and missed some minor lineaments of interest. Plate-16 and -17 show the images after thresholding the edge images obtained by applying Sobel, and Frei-Chen filters.

The interpretation clues that were helpful in tracing the lineaments are as follows:

1. Some of the lineaments were conspicuous as drag effects on Mendha and Rupangarh river (Fig-6.1 and –6.2),
2. Some characteristic linear stretches of Mendha (labeled as 'D' in Plate-15) and Rupangarh (Fig-6.2) river were also identified as lineaments,
3. The linear stretches of mountains in this area were also identified and at some places a sudden disruption of the range is observed to be due to some faulting (Fig-6.3),
4. Some striking linear stretches of subsurface channels and some minor surface streams as found in top left portion of true color composite (Plate-7) were identified as lineaments. Labels 'E' and 'F' shown in Plate-15 give another example of surface streams following the conspicuous linear stretch.
5. Tearing phenomena can be observed as a linear pattern from three-dimensional topographic view of the terrain (Plate-14) on the eastern side of Sambhar lake.
6. PC3 and *Band1/Band2* images show a set of seven parallel lineaments in the form of a tonal variation. The lineaments labeled as 'D' and 'G' in these Plate-9 and -5 are not clear in other images.

Plate-16 shows various lineaments that have been digitized in the aforementioned way. The Rose diagram (Fig. 6.4) for this lineament map showed most of the lineaments to occur in NE-SW, NW-SE and Eastern direction. Using the neotectonic maps (Dassarma, 1988; Sinha-Roy, 1986) as ground truth the connectivity of all fragments of lineaments was established which were then joined as single major lineaments. Plate-18 shows lineaments in three different colors; yellow and magenta lines are those confirmed as major lineaments through maps of Dassarma (1988) and Sinha-Roy (1986) respectively, and those shown in blue are the newly identified lineaments in the present work. The directions of faulting could not be identified here because that would require interpretation of even more wider coverage of the terrain and some field data. Further discussions on these lineaments in view of the structural evolution of the Sambhar lake are presented in section 6.4.1

6.2.3 Surface and Subsurface Drainage

The surface drainage network in this area can be clearly identified from FCC generated by loading PC1, PC2, PC3 on R, G, B planes respectively (Plate-10). In this

Fig . 6.1 Drag effect on Mendha river

Fig-6.2 Drag effect on Rupangarh river

Fig. 6.3 Shattered Aravalli hills with minor faulting across.

FCC, the surface drainage shows a hazy appearance. Although the surface drainage network is dried up, there was clear indication of fresh fluvial sand, which appeared in white colour, and this sand is encrusted with salt in some areas giving it a bright shiny appearance. Most of the surface drainage in this area originates from the Aravalli hills. Apart from the surface drainage, Plate-10 also clearly indicates various lakes and other water bodies in the area in red shade. Some humid pockets are also highlighted on this image as regions of light red tone enclosed by thick lines of blue and these helped in the location of buried channels at later stages. The interpretation clues used for the identification of buried channels are discussed next.

Plate-19, -20 and -21 are three windows extracted from the FCC image shown in Plate-10 to highlight the buried channels along with some labeling. In Plate-19 , at 'A', a buried channel connecting two small lakes is clearly visible as a wavy pattern showing consistent green tone. The area around 'C' shows a palaeo-channel connecting a small lake and the high moisture zone shown as enclosed by thick blue line. The area around 'B' is the region with many buried channels in consistent darker green tones and sinusoidal pattern connecting the Rupangarh river. The point 'D' indicates a wavy pattern linking the lake below 'A' to the high moisture zone below 'E'. The area around 'F' also shows many such channels. At 'E' few palaeo-channels with only a part of their entire stretch visible are shown. On the same lines, some paleochannels are identified in Plate-21 at 'B, C, D' to the northeast, 'E, F, H' to the southeast and at 'A' to the east of Sambhar lake where some palaeochannels connect the high moisture zones along the fracture on the eastern side of Sambhar lake. Another Plate-20 shows buried channels below the Mendha river. The points labelled as 'A' and 'C' indicate regions where some wavy patterns in green tone originate from Mendha and end at high moisture zones shown just below. Further, few more buried channels at 'B, D, E' extend from these zones to northeast of the Sambhar lake.

The DTM, Slope and Aspect maps (Plates-11, -12, -13) help in judging the direction of flow of these channels and identify the low-lying areas. The orientation of most of the buried channels is observed to be parallel to the trends of lineaments in the study area (Fig-6.5). Moreover, most of these channels are mapped in the areas of extensive aeolian cover and also in the region where the sand dunes are found fixed with sparse vegetation (Plate-4) e.g. the area northeast of Sambhar lake. Some of these buried channels follow the drainage lines of the present day rivers and finally terminate in

lakes or low-lying areas or as dead ends. The entire trace of the buried channels was visible in some cases while only a fragment could be traced at times.

6.2.4 Land Cover map

Plate-22 is the image showing 15 clusters of different colors obtained after carrying out unsupervised classification on all the four raw bands. Based on the ground truth information available from topographic sheets, appropriate class names were associated with these clusters. Some of the important classes identified at this unsupervised stage are given in Table 6.1.

Table 6.1 Class labels attached to the clusters obtained during unsupervised classification

Cluster No.	Class identity of the cluster based on ground truth from topographic sheet
1	Older sand deposits (aeolian)
2	Shallow/medium depths of the Sambhar lake and shadow of the hills
3	Younger or fresh sand deposits (aeolian)
4	Sparse distribution of vegetation
5	Salt pans and fresh sand deposits
6	Shallow depths of the lake and young/fresh sand deposits
7	Older sand deposits fixed with sparse vegetation (aeolian)
8	Open scrub
10	Salt encrusted soils and sand
13	Deeper parts of the Sambhar lake

Apart from the clusters listed above, the remaining clusters (e.g., cluster nos. 9, 11, 12, 14 and 15) were too sparsely distributed and could not be correlated to any existing physical class. Thus, based on the information derived in the above manner, supervised classification was carried out next. Plate-23 shows the image obtained using Maximum Likelihood classification, along with the classes of interest. The training statistics of the classes selected and the classification accuracy as obtained from the confusion matrix are given in Table 6.2 and Table 6.3 respectively.

Table 6.2 Training statistics of the classes for Maximum Likelihood Classification

S.No	Class	Band	Mean	StdDev	Nr	Pred	Total
1	Salt Encrustated Soil	1	78.2	6.0	18	80	95
		2	55.1	3.4	21	57	95
		3	80.7	3.6	17	83	95
		4	70.6	2.8	16	67	95
2	Young/fresh plain sand	1	53.3	2.4	18	51	100
		2	41.5	2.9	17	39	100
		3	71.2	5.7	13	68	100
		4	69.9	4.4	17	72	100
3	Older plain sand	1	43.0	1.2	35	43	111
		2	29 9	1.1	44	29	111
		3	50.4	1.5	29	49	111
		4	54.0	1.1	40	54	111
4	Fixed sand plains	1	38.3	1.7	75	38	353
		2	24.7	1.9	77	24	353
		3	38.1	4.2	40	40	353
		4	42.1	4.9	36	45	353
5	Vegetation area	1	34.8	1.3	35	34	113
		2	20.3	1.4	32	20	113
		3	25.0	3.3	27	23	113
		4	51.1	1.8	30	52	113
6	Lake green algae	1	44.1	1.9	106	45	351
		2	37.5	2.2	118	38	351
		3	34.5	2.5	85	36	351
		4	23.4	2.7	67	26	351
7	Lake red algae	1	33.3	0.6	147	33	267
		2	18.6	1.0	98	18	267
		3	30.8	7.1	36	24	267
		4	14.6	0.5	149	15	267
8	Shallow lake	1	48.2	1.0	133	48	372
		2	32.9	0.7	217	33	372
		3	40.8	1.6	119	42	372
		4	19.6	1.8	93	21	372
9	Medium depth	1	45.6	0.6	206	46	344
		2	29.7	0.5	230	30	344
		3	32.0	0.8	172	32	344
		4	14.0	0.7	233	14	344

S.No	Class	Band	Mean	StdDev	Nr	Pred	Total
10	Deep lake	1	41.3	0.9	86	41	220
		2	26.7	1.1	102	26	220
		3	28.0	2.1	63	26	220
		4	13.3	0.7	114	13	220
11	Shallow salty area	1	65.7	0.7	93	66	151
		2	47.1	0.7	79	47	151
		3	68.0	1.1	61	69	151
		4	49.4	3.7	97	48	151
12	Open scrub	1	45.9	1.5	103	46	354
		2	31.4	1.3	149	32	354
		3	50.6	2.4	71	51	354
		4	58.7	2.3	63	58	354

StdDev: Standard deviation

Nr: Number of training pixels with predominant value

Pred: Predominant value

Total: Total number of training pixels of the class

The observations that emerge from the land cover map obtained in this classification stage are as follows:

(a) Sparsely distributed vegetation cover in the image can be observed in green color. It is noticed mostly in the low-lying areas, in the regions receiving water from drainage of Aravalli hills, along the palaeo-channel zones. Open scrub is shown in red color.

(b) The entire lake is divided into three categories based on depth shallow part (light blue), medium depth (grey), deep part (dark blue) and two categories based on algae as green algae spread area (green), red algae spread area (orange).

(c) Salt encrusted lands are shown in cyan color. These are distributed around the Sambhar lake and some parts of the stretch of Mendha and Rupangarh rivers. There are some other areas with shallow water and some salt concentration they are essentially the salt pans around the Sambhar lake and some drying up parts of Phulera lake shown as blue-green shade.

(d) The sand deposits are classified as of three types based on their state of activity, degree of mobility etc., a) Young/fresh sand plains (yellow), b) Older sand plains

Table 6.3 Confusion matrix showing classification accuracy

	(1)	(2)	(3)	(4)	(5)	(6)	(7)	(8)	(9)	(10)	(11)	(12)	Accuracy
(1)	278	0	0	0	0	0	0	0	0	0	0	0	**1.0**
(2)	22	264	0	0	0	0	0	0	0	0	0	4	**0.91**
(3)	0	0	75	0	0	0	0	0	0	0	0	0	**1.0**
(4)	0	0	0	196	11	0	0	0	0	0	0	2	**0.94**
(5)	0	0	0	0	183	0	0	0	0	0	0	0	**1.0**
(6)	0	0	66	19	0	341	0	0	121	35	0	53	**0.54**
(7)	0	0	0	0	0	0	356	0	1	0	0	0	**0.99**
(8)	0	0	0	2	0	0	38	211	0	0	0	0	**0.84**
(9)	0	0	0	0	0	0	0	0	335	0	0	0	**1.0**
(10)	0	0	0	0	0	0	0	0	0	182	0	0	**1.0**
(11)	23	0	0	0	0	0	0	0	0	0	238	0	**0.91**
(12)	0	0	0	3	0	0	0	0	0	0	0	243	**0.98**
REL	**0.86**	**1**	**0.53**	**0.89**	**0.94**	**1**	**0.9**	**1**	**0.73**	**0.84**	**1**	**0.8**	

REL – Reliability

(1) Salt encrusted soil
(2) Young/fresh plain sand
(3) Older plain sand
(4) Fixed sand plains
(5) Sparse vegetation
(7) Lake green algae
(8) Lake red algae
(9) Shallow lake
(10) Deep lake
(11) Shallow-salty area

(a) Average Reliability = 87.41 %
(b) Average Accuracy = 92.58 %
(c) Overall Accuracy = 87.88 %

(brown), c) Fixed sand plains (pink). Younger sand plains are distributed mostly around the Sambhar lake in the Mendha and Rupangarh basins. They are mobilized by both fluvial and aeolian activity. Older sand plains are not much disturbed by either aeolian or fluvial activity. They are distributed mostly on the northeast, east and southeast side of Sambhar lake and also partly along the leeward sides of the hills. Fixed sand plains have a higher moisture content and are fixed by sparse vegetation cover. They are stabilized plains in terms of mobility. These are distributed mostly in the low-lying areas, leeward sides of hills, areas receiving drainage from Aravalli hills etc. These are generally located farther away from the center of Sambhar lake.

6.3 Results on Thresholding of Edge Images

The edge images generated by sobel, kirshf, LoG and Frei-Chen filters consisted of many spurious edges making the visual interpretation of the lineaments very difficult from them. Thresholding techniques were applied on these edge images so as to get rid of the spurious edges (details of thresholding criteria are given in Appendix – 2). The output of the threshold values obtained on these images is given in Table-6.4.

Table 6.4 Results of Thresholding on Band3 of IRS-1B LISS III

Edge Filter Name	Grey Level Value		Global Threshold Value	No. of Parts 'n'	Threshold Value		Successful Thresholds Out of 'n^2'	Mean	Median	Mode
	Min	Max			Min	Max				
Sobel	0	255	63	8	51	83	64	63	63	64
				16	34	105	256	63	63	65
				32	29	108	1020	63	64	64
				64	28	123	4031	64	64	65
Kirsh	0	255	83	8	66	99	64	84	86	88
				16	7	104	255	84	87	87
				32	1	117	1003	84	86	85
				64	1	136	3573	81	84	85
LoG	127	184	136	8	134	138	64	136	136	136
				16	128	139	256	136	136	136
				32	128	144	1018	135	136	136
				64	128	150	4028	135	136	136
Freichen	0	192	11	8	8	11	64	11	11	11
				16	1	34	256	11	11	11
				32	1	40	1018	11	10	9
				64	1	42	4032	10	10	9

Some observations that emerge out of these results are given below:

a) There is no significant difference in value of the global threshold and the mean, median and mode of all the individual local thresholds.

b) As the number of parts into which the image is split is increased, the size of the individual part gets reduced and the frequency histogram of these parts becomes more complex. Thus, the total number of parts in the image for which thresholding is successful in the image falls down proportionately.

c) Various combinations arose between the candidate thresholds satisfying valley check condition and the successful thresholds among them satisfying the neighbourhood condition (refer Appendix – 2) for each individual part of the image while adopting local thresholding.

Table 6.5 Various combinations of candidate and successful thresholds arising while carrying thresholding on each individual part of the image.

No. of Candidate Thresholds	No. of Successful Thresholds	Threshold Adopted
=1	=1	No ambiguity
=1	=0	Single Candidate Threshold
>1	=1	No ambiguity
>1	=0	Mean of all candidate thresholds
>1	>1	Mean of all successful thresholds
=0	=0	Not possible

d) Local thresholding is found appropriate for edge images giving widely distributed thresholds for its individual parts. In the remaining cases, global thresholding is felt sufficient. The image should be divided into those many parts such that there exists atleast one candidate threshold for each of the individual parts. Else, thresholding is not successful.

6.4 Discussions

Based on the information derived from various thematic layers, interpretations have been made regarding the tectono-geomorphic evolution of Sambhar lake. The tectonic/structural evolution of the lake explains the formation of the lake depression. The manifestation of the geomorphic processes on the satellite images provides clues as to how the lake depression has been maintained all through the geologic times. The

paleohydrologic conditions derived from the satellite maps provide evidence for the source of water and sediment into the lake which were further modified through neotectonic activity in the region. A detailed discussion of these ideas is presented next.

6.4.1 Structural Evolution of Sambhar Lake

The area around Sambhar lake is strongly influenced by tectonic activity, which is manifested in the overall geomorphic expression of the area. The drag effects on the Mendha and Rupangarh river (Fig-6.1 and -6.2), characteristic linear stretches of Mendha river labeled as 'D' in Plate-15, swarms of structurally controlled palaeochannels (Fig-6.5), lineament-controlled river diversions, ponding and formation of salt lakes across disorganized channels, truncated hill fronts with fault scarps, shattering and dragging of ridges with rotational effects to form transverse wind gaps (Plate-14), tearing phenomena on the east of Sambhar lake etc., are only some of the features strongly suggestive of tectonic activity in the area. A number of faults have been reported in this terrain. The drainage pattern on either side of the lake manifests a number of faults (Fig-6.1 and –6.2). The broken hills of the Aravalli range also indicate faulting activity (Fig-6.3).

Some of the major lineaments identified in the present work are confirmed with the earlier findings of Sinha-Roy (1986) and Dassarma (1988) respectively. The lineaments shown in blue and green colors in Plate-18 are the ones mapped by Sinha-Roy and those in green color are identified by Dassarma. In the present work, many new lineaments have been identified (shown as Blue color in Plate-18) as a result of detailed investigations through digitally enhanced satellite images. Sobel, Frei-Chen, LoG edge images obtained after thresholding with Otsu's (1979) algorithm, *Band1/Band2* image and PCA3 contributed significantly for obtaining these lineaments.

The statistical analysis of the direction of lineaments in the study area through a Rose diagram indicates that most of the lineaments in the terrain are oriented in NE-SW, NW-SE direction and east direction (Fig-6.4).

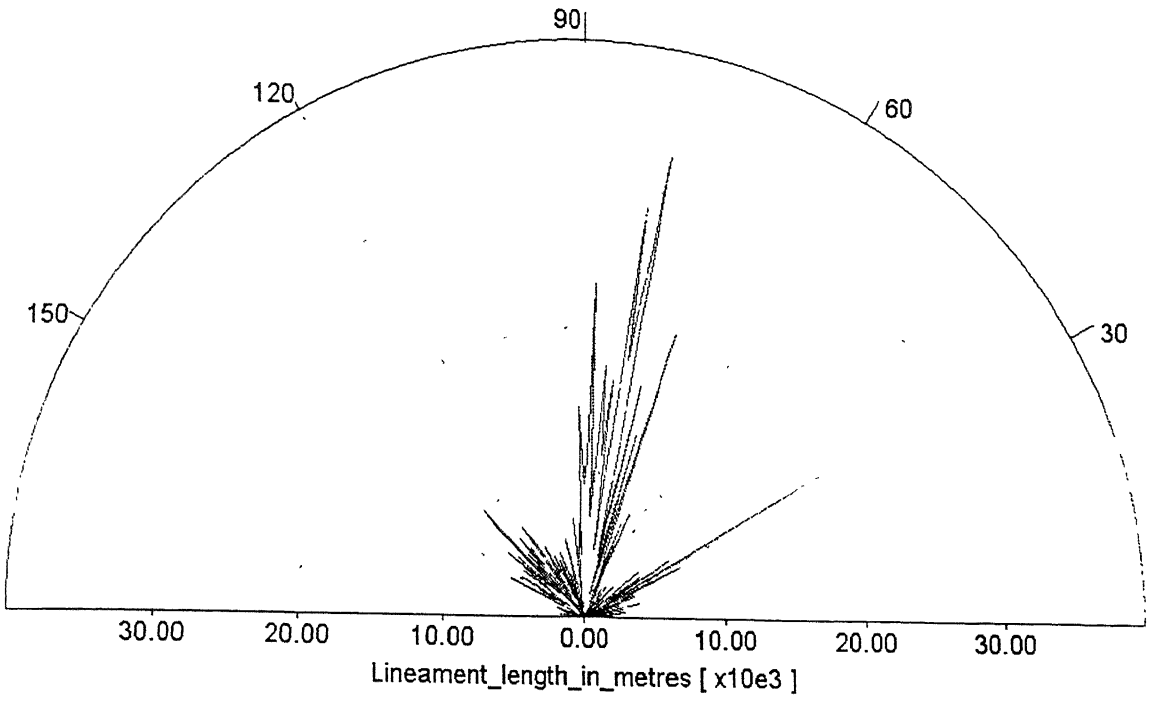

Fig 6.4 Rose diagram

Many parallel lineaments are noticed in each of the aforementioned directions, which intersect each other. From plate-18 it is clearly observed that Sambhar lake is located at the intersection of many lineaments, which supports the findings of Dassarma (1988) and Sinha-Roy (1986). A striking feature in the spatial distribution of the Sambhar lake is that this lake is confined within a narrow belt bounded by the NW-SE trending depression in the basement rocks, which is further segmented by NE-SW running sets of lineament faults. It is clearly observed from the sliced DTM (Plate-11) that an elongated depression ('Mendha stepped graben' of Dassarma, 1988) extends from the northeast to southwest of Sambhar lake and the lake is spread across this depression.

It seems likely that the differential movement along the major lineaments caused rotation of some of the blocks along reactivated faults, ripping open in the process linear depression to form the Sambhar lake basin. The ongoing investigations in the Sambhar lake basin indicate the absence of sediments earlier than Quaternary, which provides stratigraphic evidence for recent movements. Periodic impulses can be seen in terms of sequential faulting in Mendha and Rupangarh river stretch as seen in (Fig-6.1 and -6.2). Further, conspicuous wind gaps, transverse to the Aravalli mountain range between Sambhar lake and Kantli river is observed on Plate-14, where a series of NE-SW and NW-SE lineaments intersect each other (Plate-18).

The lineaments indicated by Mendha stepped graben are curvilinear. The orientation of the Mendha river, slight curvilinearity shown by the Aravalli hills and the wind gaps on the northwest of Sambhar lake indicate clock wise rotation of the crustal block east of the Aravalli orographic axes. Slight curvilinearity of the Aravalli hills on the top left of Plate -7, set of curvilinear faults converging on the northeast side of the lake and diverging on the southwest side (Plate-5), tearing phenomena to the east of Sambhar lake (Plate-14) as converging towards the east and diverging towards the lake confirm such a rotation. Due to this rotation, Sambhar lake could have originated as a pull-apart structural depression. Sinha-Roy (1986) suggests the same idea that the Sambhar originated as a pull-apart structural depression due to strike-slip faulting along curvilinear planes. The rotational process has also pulled apart a series of marginal depressions in the eastern fringes of the gaps to form some other smaller lakes with linear boundaries. A smaller lake to the south of the Sambhar lake, also presents a similar situation, albeit on a smaller scale.

But, when we consider the lineaments in NW-SE direction which are transverse to the previously mentioned curvilinear lineaments (Plate-18), it would seem that some blocks bounded by faults could have formed which might have subsided or rotated to form the present Sambhar basin. Besides this, these faults cutting the convex side of the NE-SW curvilinear faults could have helped in creating a splitting or tearing phenomenon due to which the lake basin got elongated in NE-SW direction. This is in line with the idea of Dassarma (1988), that the pull-apart depression at Sambhar could be due to rotational movements of the fault-bounded blocks.

The distribution pattern of lake Sediments in the Sambhar basin provides indication of deposition in a recent to sub-recent graben formed over a fluvial channel (Sundaram and Pareek, 1995). Hence, it is felt that a NE-SW trending rhombic depression was formed due to the fault bounded blocks and these blocks might have rotated in clockwise direction because of curvilinear strike slip faulting.

6.4.2 Geomorphologic Evolution of Sambhar Lake

After the formation of the Sambhar lake depression through tectonic processes, the lake basin and the surrounding areas have been continuously modified by a variety of aeolian, fluvial and lacustrine processes operating through geologic times. The present-day geomorphology of the region clearly reflects the dominance of wind action in recent times. The surface water processes assume importance only during the monsoon period. The effect of present day lacustrine process is marginal as the lake is shallow in nature; maximum depth being slightly more than 1 m during the monsoon, and is practically devoid of any current and tidal action. The aforementioned processes and landforms are discussed separately in view of the geomorphic-evolution of the Sambhar lake.

6.4.2.1 Wind Deflation

The Aravalli range on the eastern side of the Sambhar lake has breached transversely to form a number of wind gaps. Two major wind gaps are located on the northwest and southwest side of Sambhar lake (Plate-14). As discussed earlier, role of rotational movement of the crustal blocks may have been responsible for the formation of these conspicuous wind gaps, transverse to the Aravalli mountain range between Sambhar lake and Kantli river.

Sambhar lake falls exactly at the intersection of the aforementioned wind gaps, and the depth of the lake is greater at the intersection point. The wind moving from the wind gaps had a concentrated effect on the Sambhar basin and it deflated the sediments in that region. The deflated sand settled farther away from the wind gaps when the wind velocity reduced sufficiently for it to settle. Various aeolian deposits can be clearly observed from the land cover map (Plate-23). Most of the sand deposits were found on the northeast and southeast of Sambhar lake. Thus, this wind deflation process has helped in maintaining the structural depression of the Sambhar lake.

Drainage Map of Sambhar Terrain

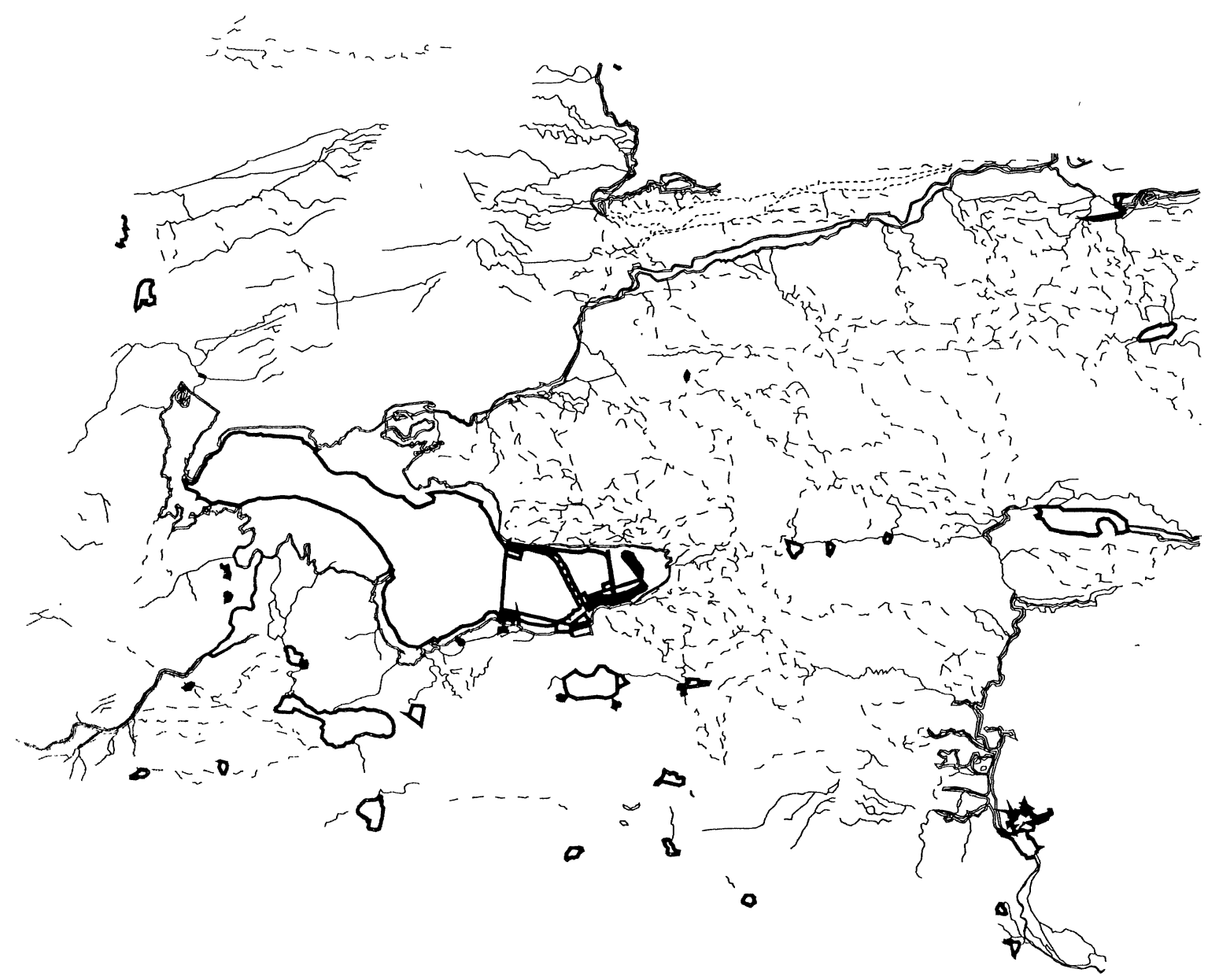

6.4.2.2 Palaeohydrology of the Sambhar Lake Catchment

In general, the paleodrainage map prepared from the satellite image indicates a strong fluvial activity in the geological past, in contrast to the present-day climate. The sub-surface expression of these 'phantom drainage' can be picked up on processed satellite images. Most of the buried channels are distributed on the northeastern side of the Sambhar lake, arising from the Mendha river and finally linking the lakes and other low-lying areas (Plate-20 and Fig-6.5). A group of them are also observed to the southeast of the Sambhar lake. Most of these buried/phantom channels are aligned along the lineaments in this area. Few of the buried channels are also found to originate from the Rupangarh river and show linkage with some lakes around (Plate-19). It seems likely that the Sambhar lake is receiving considerable contribution of water from its northeast and southeast side through these phantom channels. Apart from the above discussed palaeo-channels there are some of them present in the southern and eastern side of the lake which do not seem to be related to either of the two major drainage systems of the area (Fig-6.5). These are showing almost E-W trend, and the one parallel to the southern edge of the Sambhar lake has two small lakes within its channel (Plate-7). These are found to have connections with the Bandi river on the eastern side of the Sambhar lake. Dassarma (1988) speculated the existence of some palaeo-channels showing initial dominance of NE-SW lineaments in this region and the present work provides a very clear evidence for the same.

Further, the presence of fractures, faults and other lineaments would also encourage sub-surface contribution of water into the Sambhar lake. Plate-21 shows some such connections along the lineaments and fractures.

6.4.2.3 Neotectonics

Further modifications in the Sambhar lake basin may have been brought about by the neotectonic activities in the area, the numerous evidence for which have already been presented in previous sections. The drainage system in this area is found to be of centripetal type and also it is structurally controlled as suggested by their drainage patterns.

Amongst the two major rivers, the Mendha channel flowing in NNE direction is wider than that of the Rupangarh and is found to be narrowing down towards the lake. It is approaching the lake in a straight course from NE direction while its intermediate

course follows an N-S alignment and suddenly aligns itself in NW direction just before entering into the Sambhar lake due to a fault at that place. The Mendha is maintaining a straight course throughout the area suggesting a strong structural control (labeled as 'D' in Plate-15). Throughout its course, the Mendha is observed to move along three major parallel lineaments aligned in NE-SW direction (Plate-5). Its movement from one lineament to the other lineament gives a stepped like appearance. It seems that the cause for the connectivity between each of the aforementioned parallel lineaments could be because of sloping of the lineament-bounded blocks towards southeast. The stream along the uppermost lineament seems to have got abandoned because of this phenomenon. Also, the channel joining Mendha as seen on the top at the middle of Plate-7 seems to have got disrupted because of a major lineament occurring almost transverse to its flow. Near the bridge the channel of the Mendha is found to be choked up by sand dunes of barchan type and the satellite image shows that the Mendha channel disappears into the ground here. However, the river is reactivated during the monsoon period and has even caused flash floods several times in the historic record.

In contrast to the straight course of the Mendha, the Rupangarh has a cumulative expression of meandering and sudden drag effects prior to draining into the lake (Fig-6.2). This river is narrow and is furthering narrowing down before joining the lake.
It is oriented more or less in SSW direction as a whole. It gives a stepped like appearance because of faulting at two places along NW-SE direction thus resulting in some drag effect on this channel (Fig-6.2). This kind of drainage pattern suggests the neo-tectonic activity in periodic pulses.

It is therefore likely that the drainage got highly disrupted because of the presence of two sets of parallel lineaments running in NE-SW and NW-SE direction (Plate-18). The drainage moving along the lineaments may have been instrumental in reactivating some of the older faults. These neotectonic activities may have significantly affected the water and sediment discharge into the Sambhar lake at different geologic times. Detailed stratigraphic studies of the lake deposits may reveal more information in this regard.

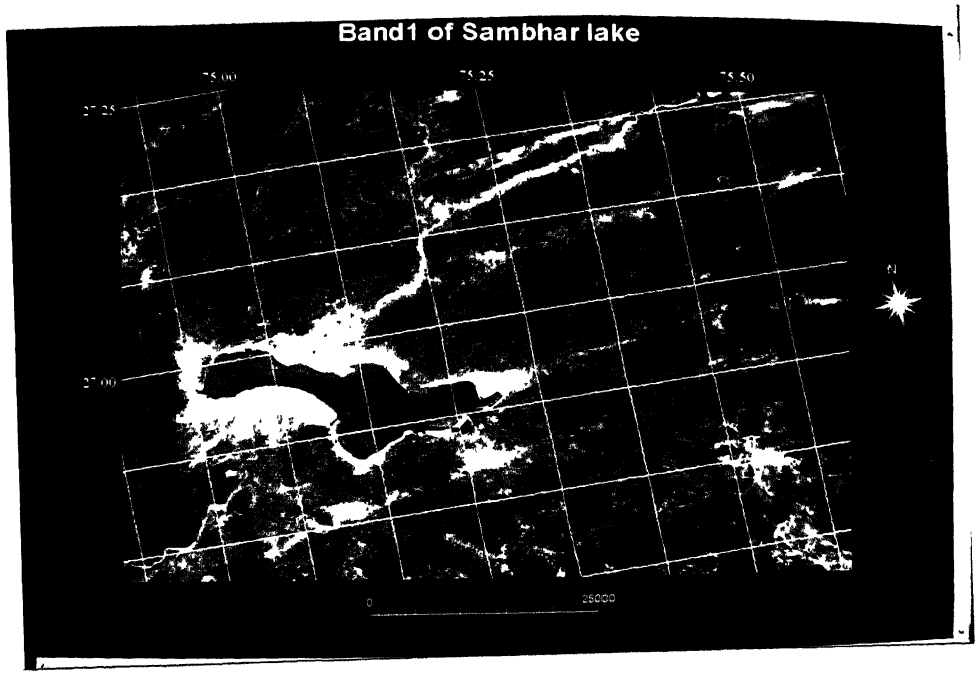

Plate-1 Contrast stretched image of Band1

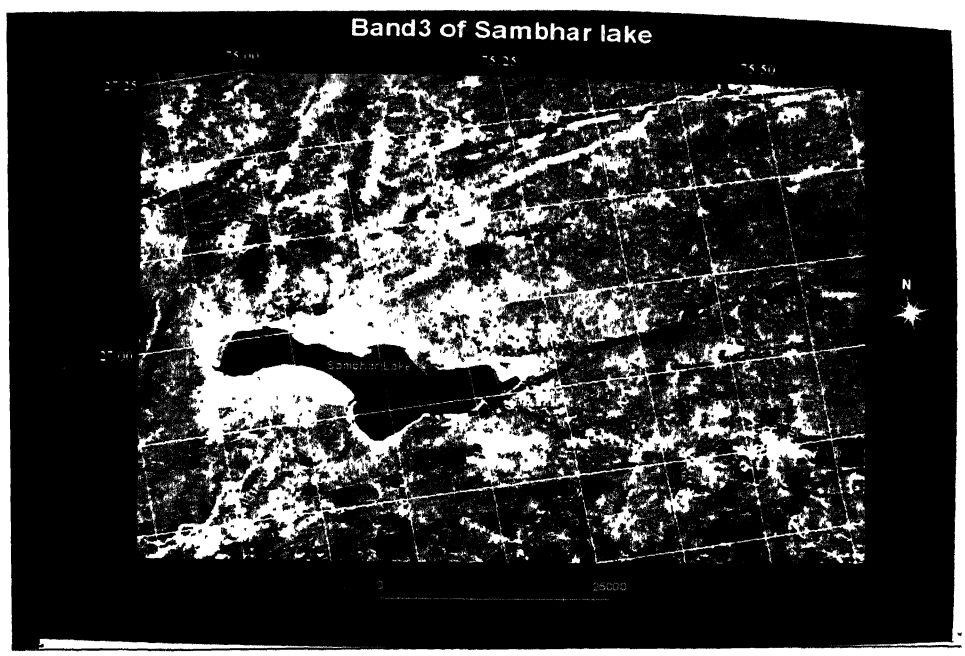

Plate-2 Contrast stretched image of Band3

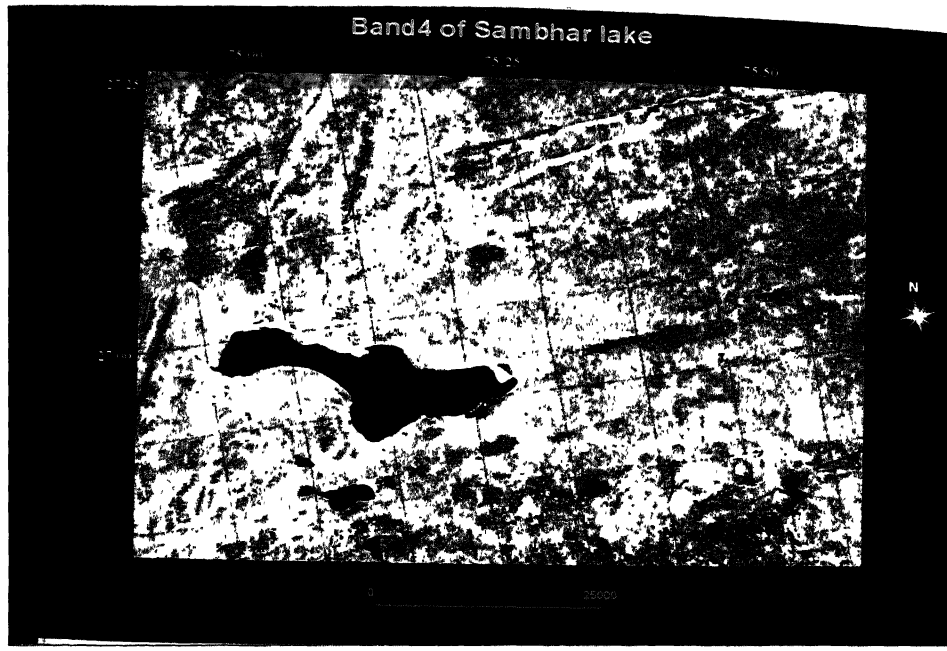

Plate-3 Contrast stretched image of Band4

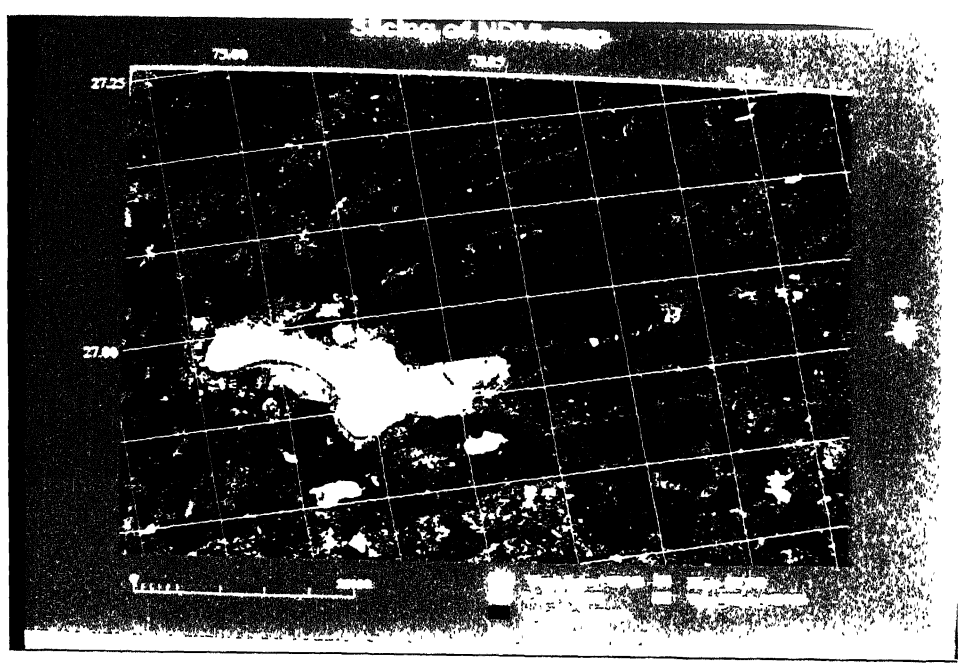

Plate-4 Slicing of NDVI map

Plate-5 Band ratioed image of 'Band1/Band2'

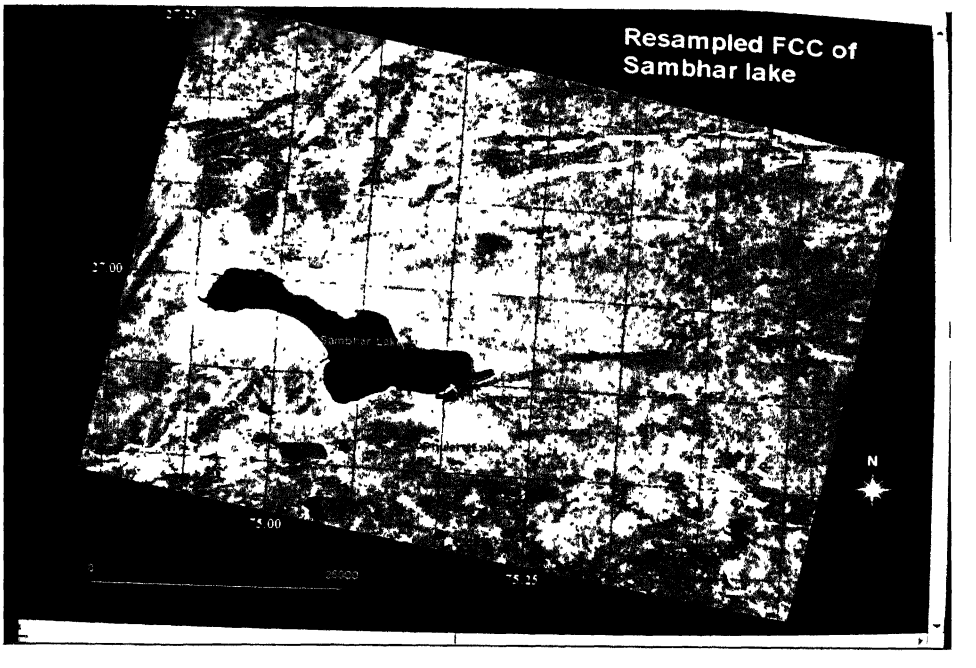

Plate-6 Resampled image of standard FCC

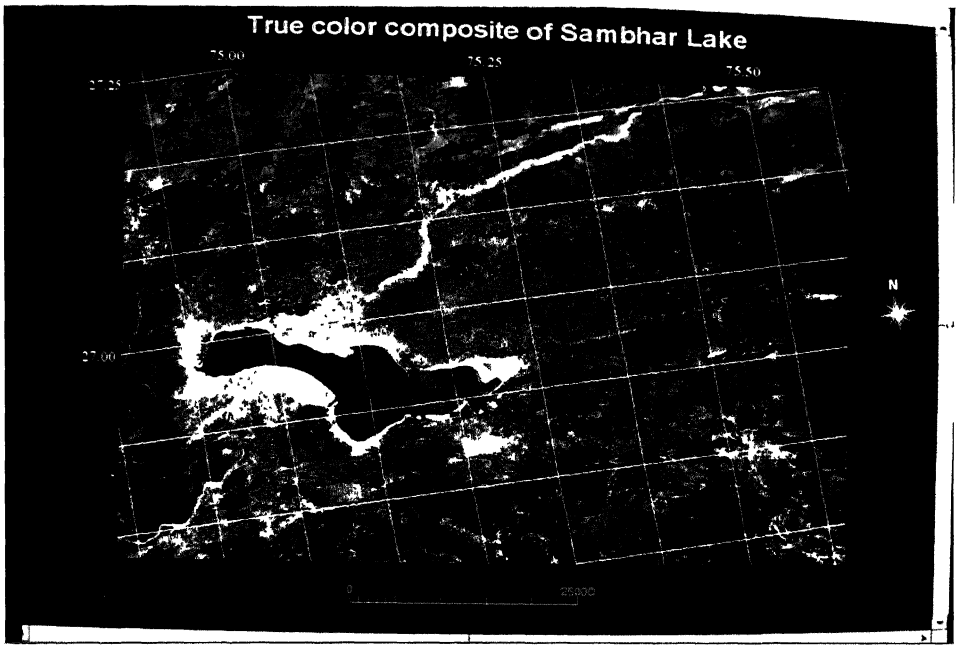

Plate-7 True Color Composite

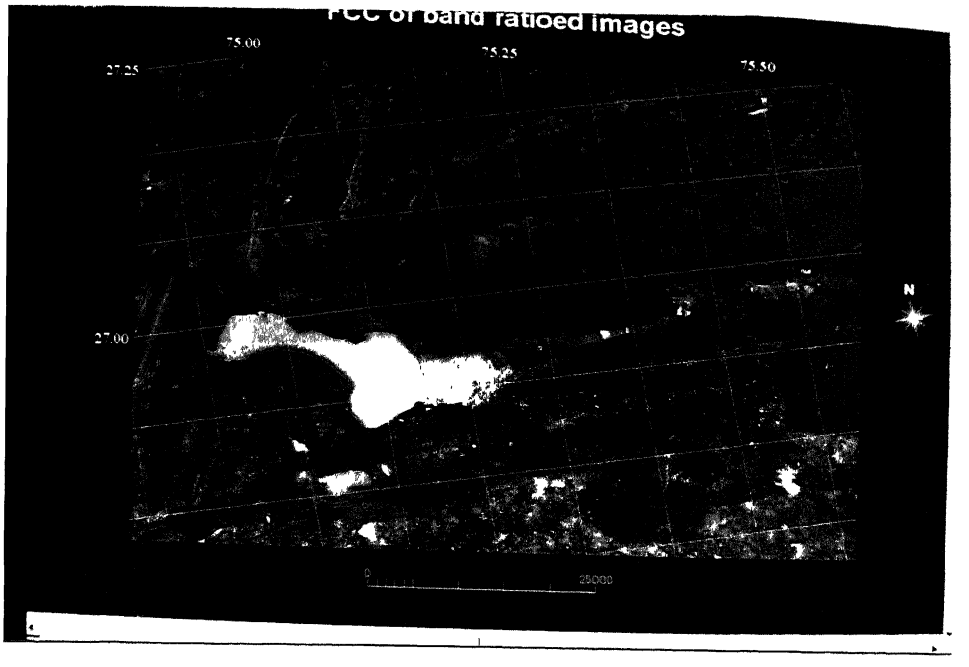

Plate-8 FCC by loading Band1/Band2, Band2/Band3, Band3/Band4 on R,G, B planes

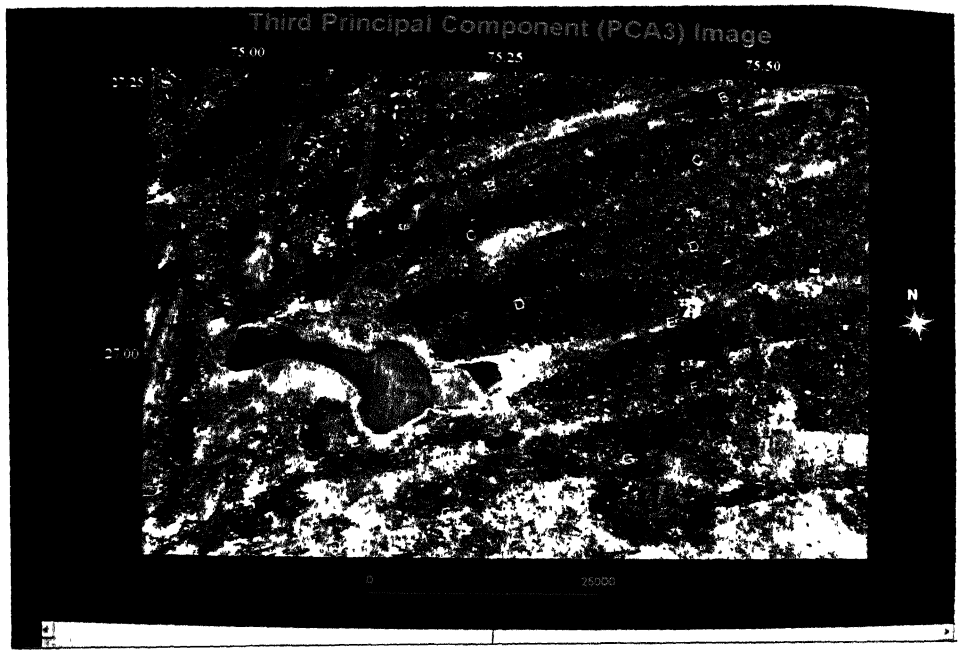

Plate-9 Image of third principal component

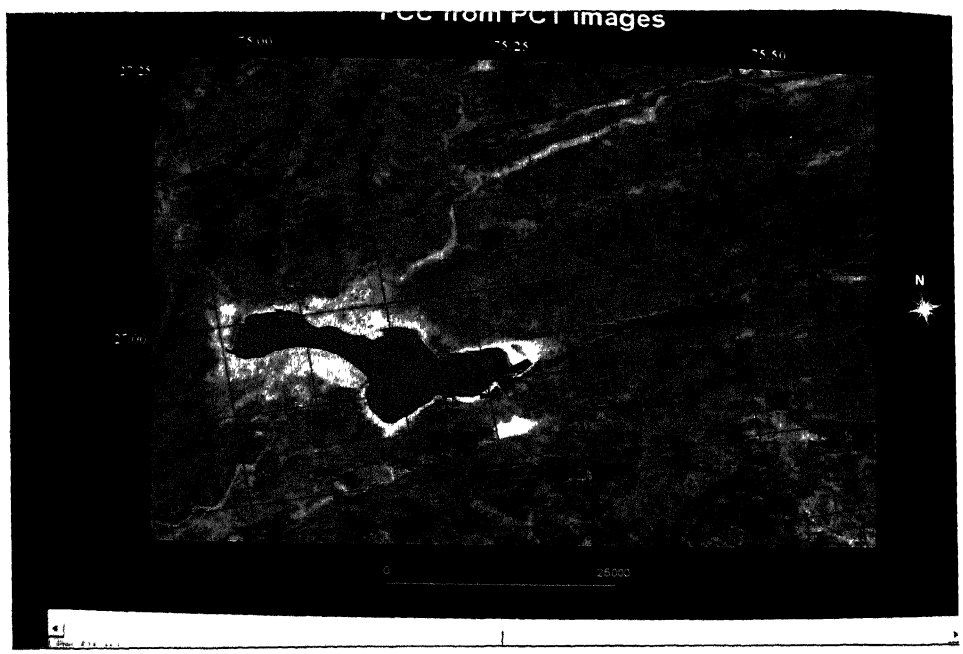

Plate-10 FCC by loading PCA -1, -2, -3 on R, G, B planes overlaid by high moisture zones

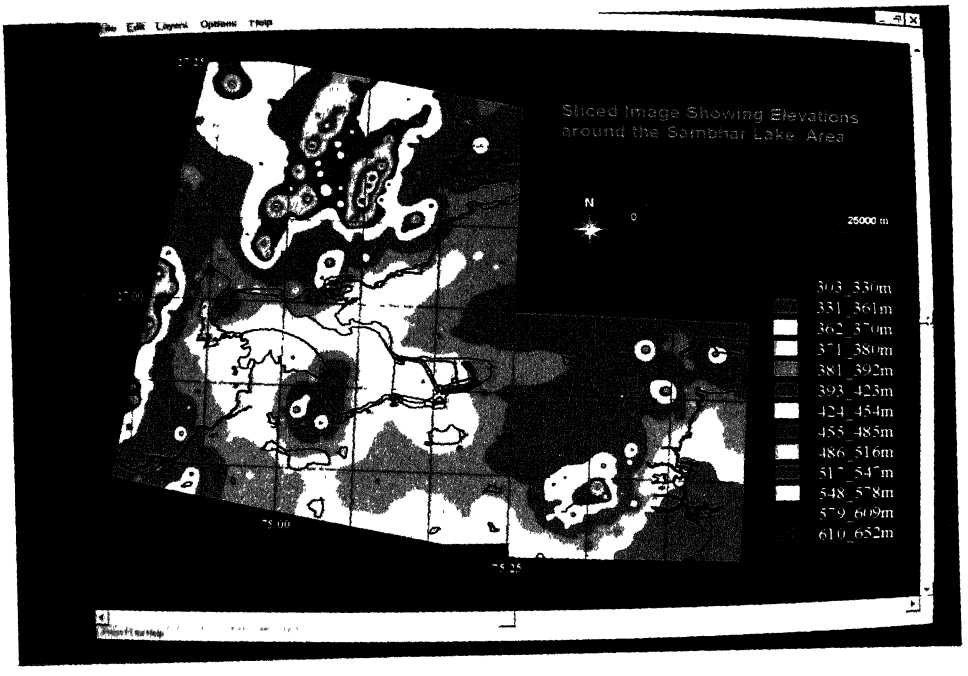

Plate-11 Slicing of DTM

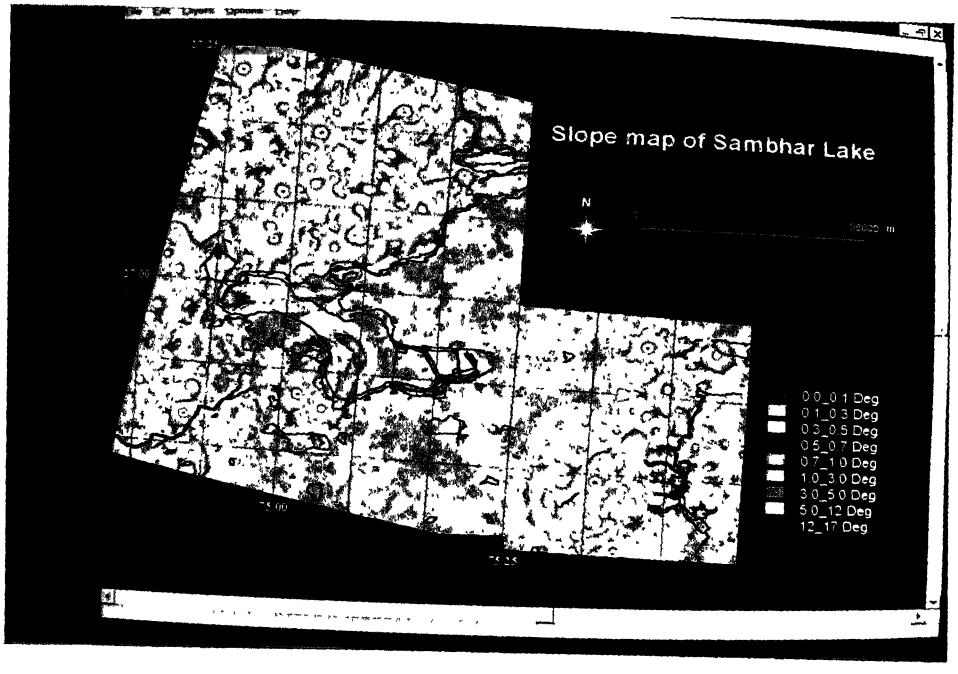

Plate-12 Slicing of slope map

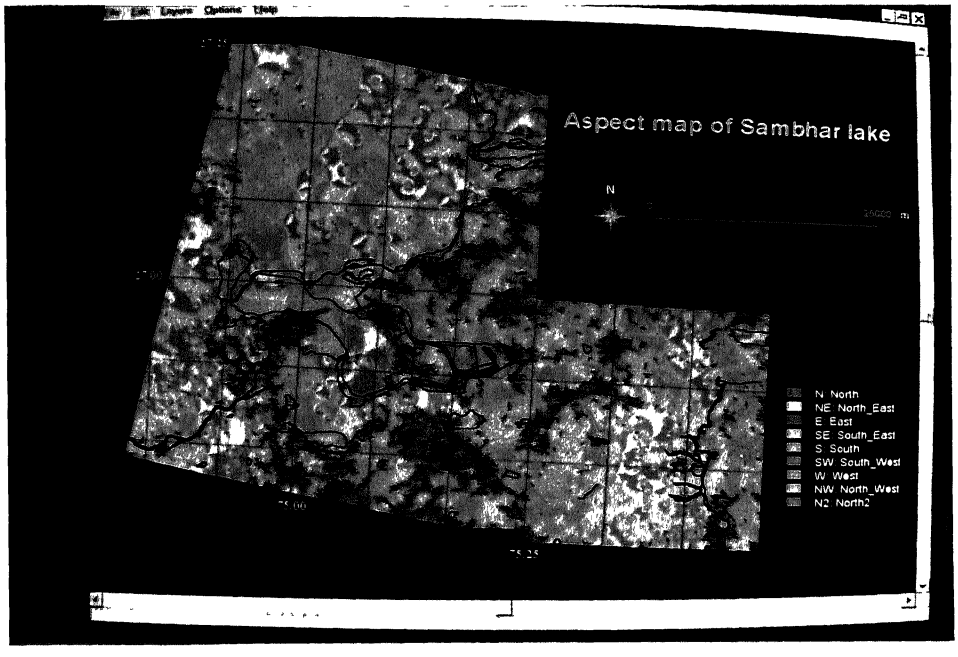

Plate-13 Aspect map showing various slope directions on the terrain

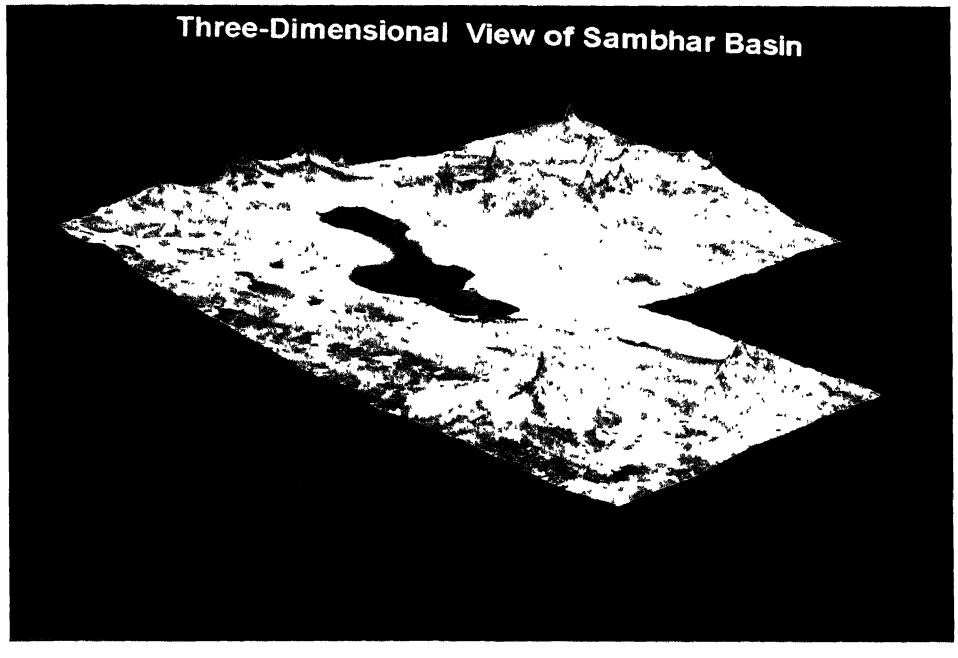

Plate-14 Three-dimensional view of the Sambhar terrain

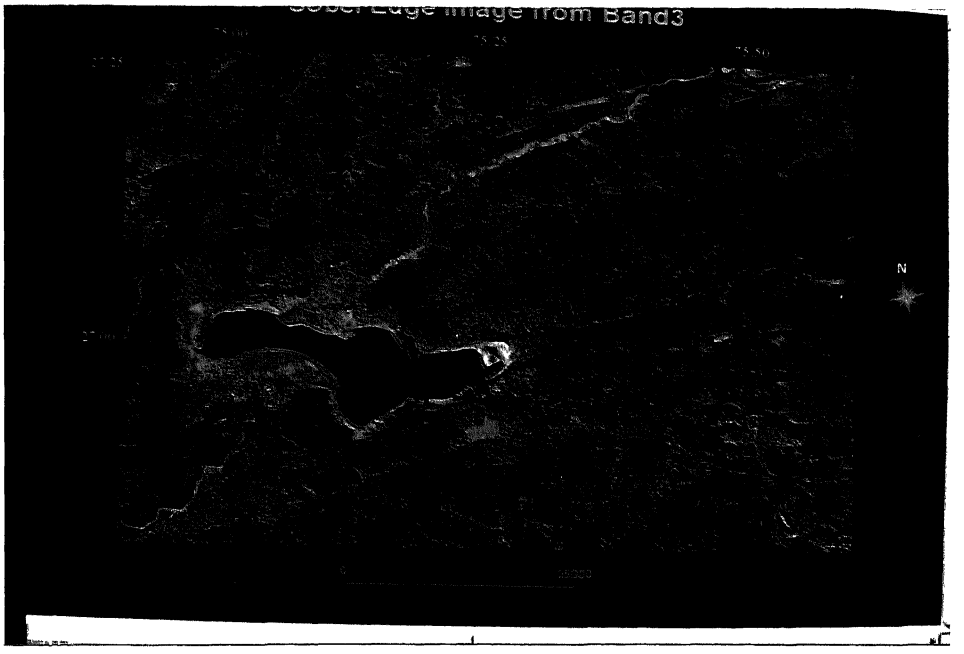

Plate-15 Sobel edge filter applied on Band3

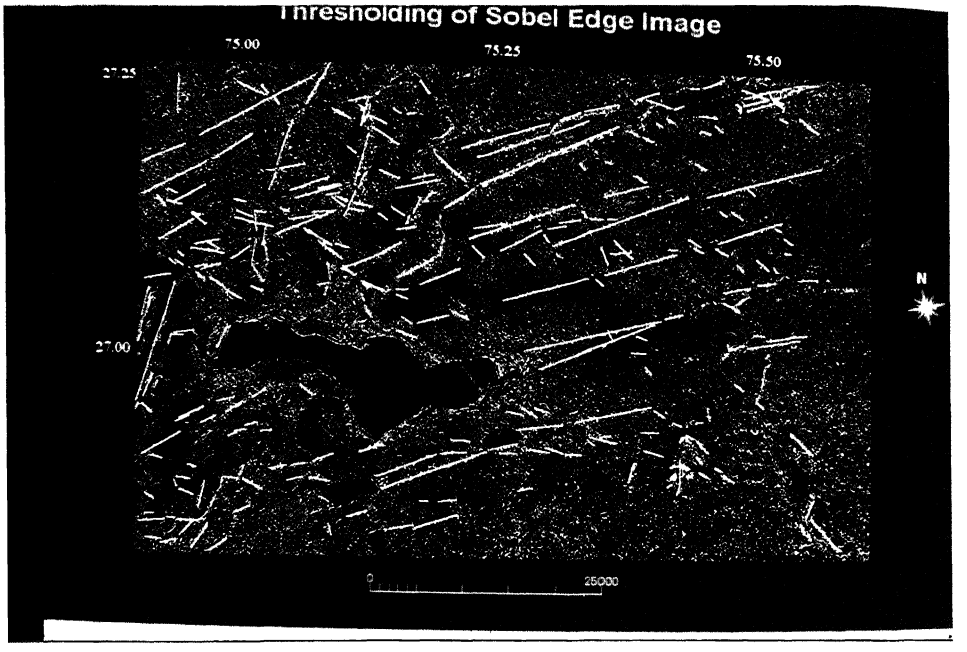

Plate-16 Sobel edge image after local thresholding, with lineaments overlaid

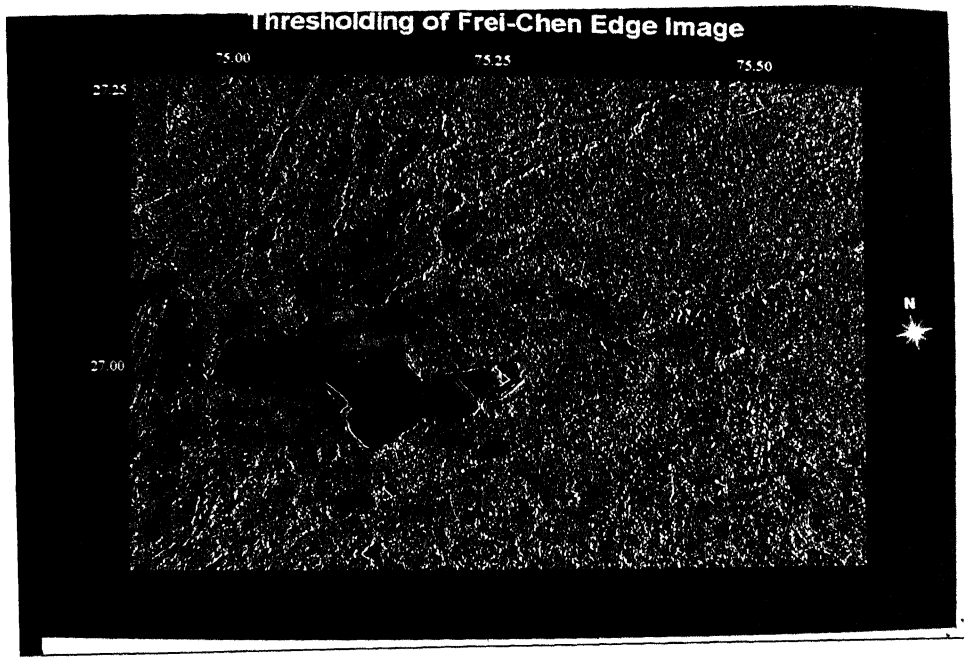

Plate-17 Frei-Chen edge image after local thresholding

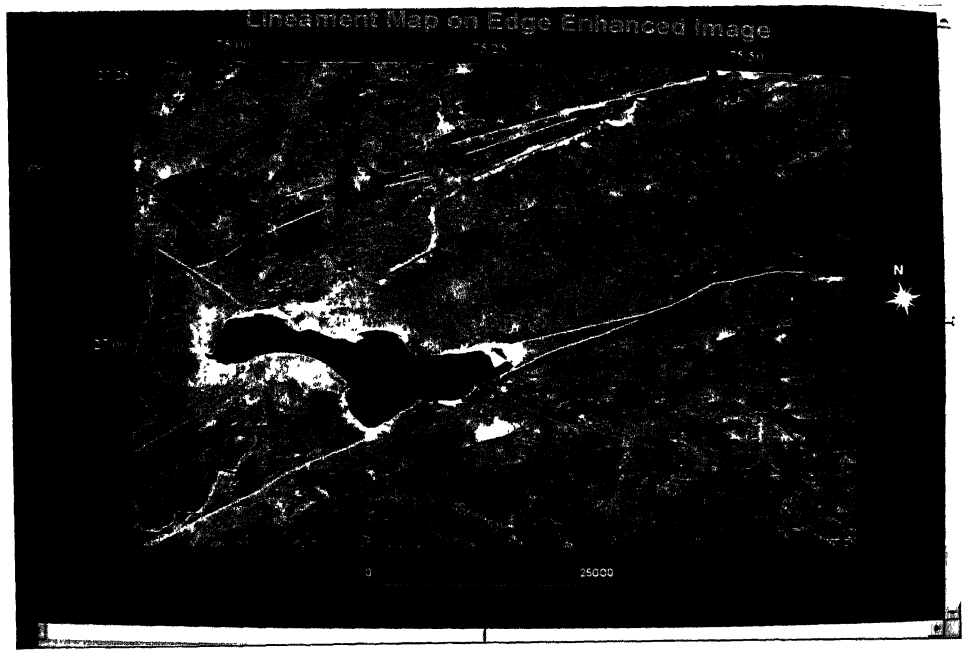

Plate-18 Lineament map of Sambhar terrain

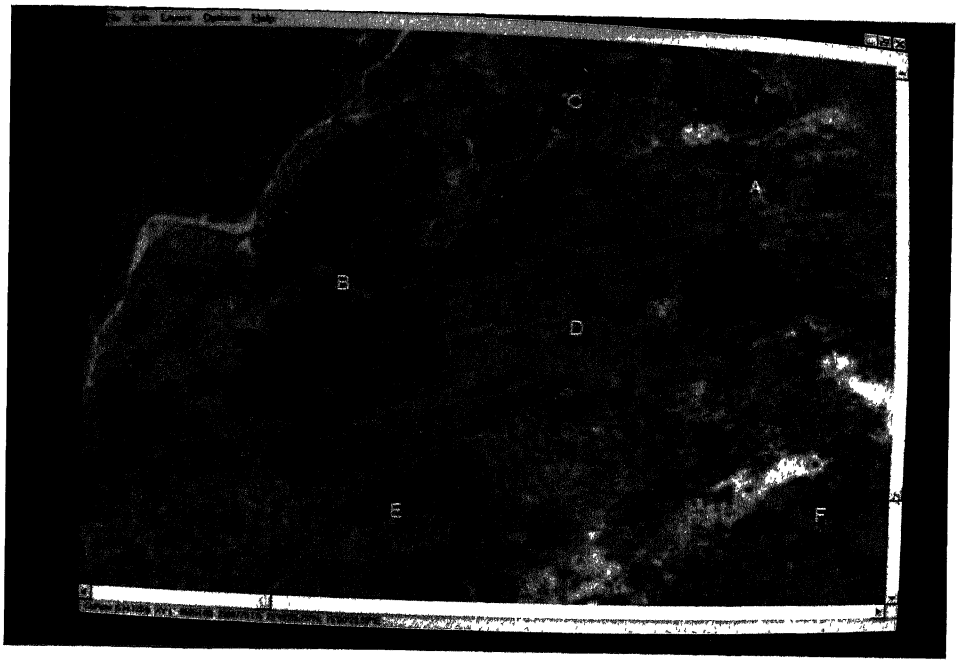

Plate-19 Palaeo-channels on the southeast of Rupangarh river

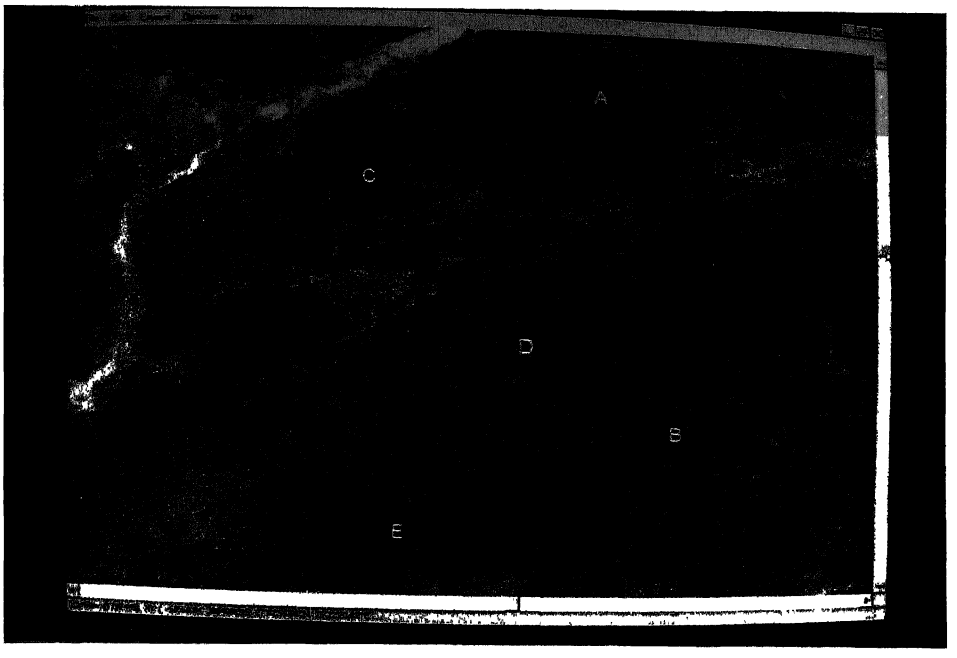

Plate-20 Palaeo-channels below the Mendha river

Plate-21 Palaeo-channels on the northeast and southeast of Sambhar lake

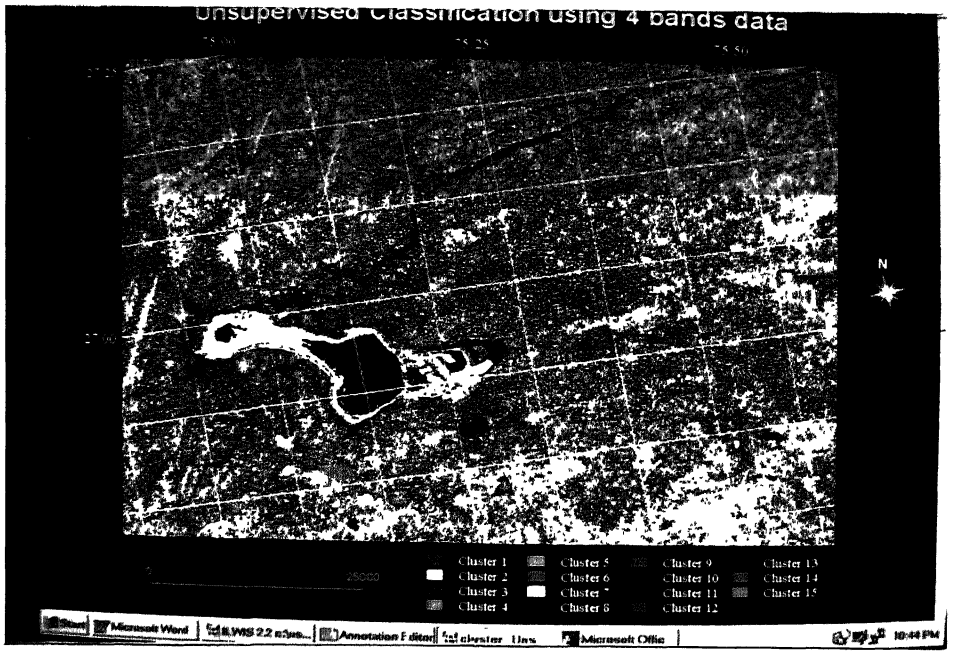

Plate-22 Unsupervised classification with all the four bands data

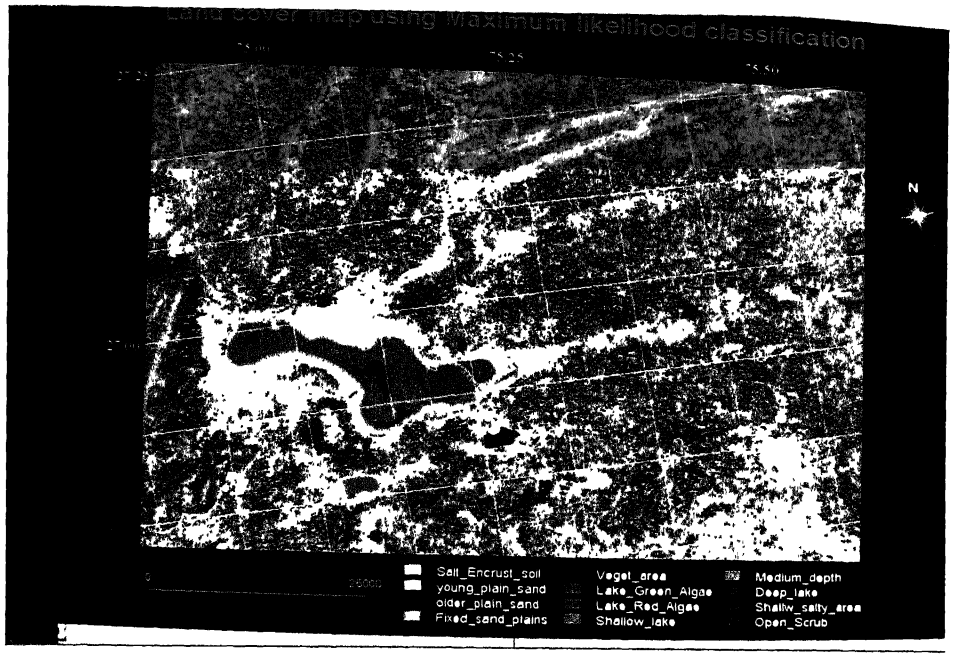

Plate-23 Land cover map using Maximum Likelihood classification

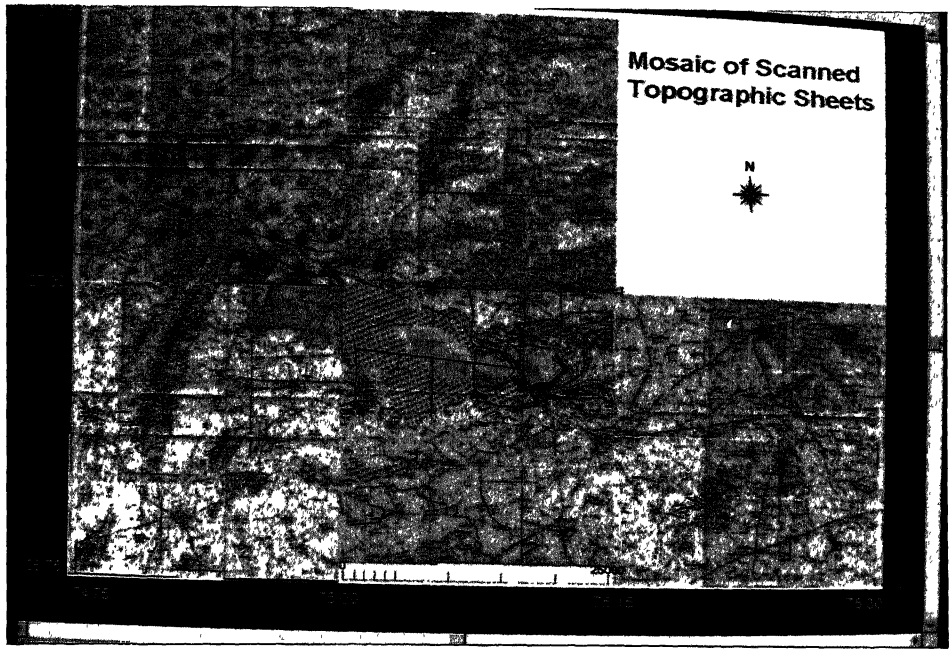

Plate-24 Mosaic of Scanned topographic sheets

SUMMARY AND CONCLUSIONS

The focus of this work has been to study the physical aspects of evolution of the Sambhar lake. Remote sensing concepts along with some advanced image processing techniques like thresholding were used to generate diverse information about the Sambhar terrain. This includes mainly the topographic parameters (height, slope, aspect etc), the aeolian and fluvial landforms (buried channels, sand dunes, other active drainage, fluvial deposits etc) and structural aspects (lineaments, faults). The information obtained in this way was interpreted in a GIS environment in the light of the past research in this area to understand the various processes that could have been responsible in the physical evolution of the Sambhar lake.

The main important physical aspects of evolution of the Sambhar lake are (a) development of an elongated depression, (b) maintenance of such a depression subsequently, and (c) source of water and sediment for the depression to form a lake. The first aspect concerns itself with the 'tectono' part and the remaining two aspects are related to the 'Geomorphic' part.

From the lineament map of the Sambhar lake region and the Rose diagram generated, it is observed that the lake is located at the intersection of many lineaments oriented in NE-SW and NW-SE directions. Apart from the major lineaments identified by Dassarma (1988) and Sinha-Roy (1986), the present work has mapped many other major and minor lineaments by adopting some advanced techniques like thresholding of digital satellite data. It seems likely that the intersecting lineaments could have created a fault-bounded rhombic block in the present Sambhar lake position, which is clearly evident from the elongated depression as visualized in the sliced DTM image (Plate). Also, the lineaments in NE-SW directions are observed to be slightly curvilinear due to strike-slip faulting along curvilinear planes and were converging towards NE. Besides this, the presence of wind gaps as observed from three-dimensional view of DTM, slight curvilinearity of Aravalli hills, orientation of the

Mendha river, a tearing type of fracture on the east of Sambhar lake etc., indicate clock wise rotation of the crustal block east of the Aravalli orographic axes.

Thus, due to this rotational process, the earlier mentioned Rhombic block could have been subjected to some pull-apart force along with some simultaneous subsidence or rotation in the downward direction, thus causing the present depression of the Sambhar lake. The rotational process has also pulled apart a series of marginal depressions in the eastern fringes of the gaps to form some other smaller lakes with linear boundaries. A smaller lake to the south of the Sambhar lake, also presents a similar situation to that of Sambhar lake, albeit on a smaller scale. It may be emphasized that although many of the findings were speculated by earlier workers, the present work has attempted to provide definite proofs from the analysis of remote sensing data.

Further, the most important geomorphic process responsible for maintaining such a large depression as the Sambhar lake seems to be deflation. Two wind gaps are clearly observed on the northwest and southwest of the Sambhar lake in the three-dimensional view of the terrain that was generated. The high wind flowing from the west along the gap in the Aravallis initiated the deflation process excavating a hollow in this quaternary sand. The presence of huge sand dunes and sand mounds along the eastern periphery of the lake as observed from the land cover map supports this interpretation. Moreover, Sambhar lake was found to be located at the intersection of the wind gaps. Thus, the central portion of the Sambhar lake depression receives a concentrated effect from the wind coming in both the directions. Hence, greater depths are observed in those portions.

Although the present-day lake receives most of its surface water discharge from the Rupangarh and Menda rivers, the present work has established a strong sub-surface contribution through 'phantom drainage' into the Sambhar lake. The present work gives a detailed methodology along with some special interpretation clues for extracting the buried channels. The buried/phantom channels identified in the present work are mostly distributed on the NE and SE of the Sambhar lake. There are some paleochannels present in the southern and eastern side of the lake which do not seem to be related to either of the two major drainage systems of the area. These are showing almost E-W trend, and the one parallel to the southern edge of the Sambhar

lake has two small lakes within its channel. These are found to have connections with the Bandi river on the eastern side of the Sambhar lake. Most of the buried/phantom channels are found to be aligned along the lineaments in this area. Further, the presence of fractures, faults and other lineaments would also encourage sub-surface contribution of water into the Sambhar lake.

The present work has been a humble attempt to answer some of the intriguing problems related to the physical evolution of the sambhar lake. However, there is scope for further detailed work in this area. Some of the issues which can be picked by furture workers are as follows:

(i) Thorough field surveys and checks are required to identify the presence of various Phantom channels. Microwave remote sensing data products may be useful to get more details of subsurface features (i.e., buried lineaments and palaeochannel information).

(ii) Detailed investigation on the lake sediments gives more clear idea of the source of water, sediment etc. and to work out the chemical evolution of the Sambhar lake, which may be strongly liked to the physical evolution.

(iii) Detailed stratigraphic studies through deep drilling and geophysical surveys in the lake region to understand the sedimentation history and tectonic influences on basin-scale sedimentation.

REFERENCES

Aggarwal, S. C., 1975. Pachbadra and Didwana Salt Sources. – Gov. India Press, Delhi, 206 p.

Aggarwal, S. C., 1951. Sambhar lake salt source. Govt. of India publication, New Delhi. 365p.

Allen, J. R. L., 1968. Principles of Physical Sedimentology.- George Allen and Unwin, London, 272p.

Amal Kar., 1990. "A Stream trap hypothesis for the evolution of some saline lakes in the Indian desert"(eds Sen, A. K. and Kar, A.), *Saline lakes in the Indian desert*, Scientific Publishers, Jodhpur, pp. 37-47.

Amal Kar., 1994. "Sand Dunes and their mobility in Jaisalmer District" (eds Dikshit, K. R., Vishwas, S. K. and Kaul, M. N.), *India: Geomorphological Diversity*, Rawat Publications, Jaipur, pp. 395-418.

Biswas, R. K., Chattopadhyay, G. S. and Subrata Sinha, 1982. "Some observations on the salinity problems of the inland lakes of Rajasthan". Records: Geological Survey of India. Misc. Pub. 49.

Blatt, H., Middleton, G. V. and Murry, R., 1980. *Origin of sedimentary rocks*, 2nd ed. Englewood Cliffs, NJ: Prentice Hall.

Bloom, A. L., 1969. *The surface of earth*, Prentice-Hall, Inc., Englewood Cliffs, New Jercy.

Chandra, P. K. and Chowdhary, L. R., 1997. Bull. ONGC.,Dehradun, v.6, pp. 37-50.

Chansarkar, R. A., 1994. "Morphological Variation in Aeolian Landforms and its Significance" (eds Dikshit, K. R., Vishwas, S. K. and Kaul, M. N.), *India: Geomorphological Diversity*, Rawat Publications, Jaipur, pp. 355-369.

Chatopadhyay, G. S., 1978. Geomorphological review a part of Mendha river catchment with special emphasis on desertification problem in H.S. Mann (ed.) *Arid Zone Research and Development*, Scientific Publishers, Jodhpur, pp. 31-34.

Dassarma, D. C., 1988. "Post Orogenic deformation of the Pre-Cambrian Crust In North-Eastern Rajasthan, In. Precambrian of the Aravalli Mountain, Rajasthan, India", Geol. Soc. of India, Bangalore; Memoir 7, pp. 109-120.

Dregne, H. E., 1986. "Desertification of Arid Lands." In. Physics of Desertification, F. El-Baz and M.H.A. Hassan, eds. Martinus Nijhoff Publishers, Dordrecht, pp. 4-34.

Ghose, B., S. Singh & A. Kar., 1977. "Desertification around the Thar - a geomorphological interpretation", Ann. Arid Zone, v. 16(3), pp. 290-301.

Ghose, B., 1964. "Geomorphological aspects of the formation of salt basins in western Rajasthan", Proc. Symp. Problems of Indian Arid Zone, Minist. Educ. Gov. India and UNESCO, Cazri, Jodhpur, pp. 79-83.

Godbole, N. N., 1952. " The salinity of the Sambhar lake", Bull. Nat. Inst. Sci. Ind., 1, pp. 89-93.

Gopal, B. and Sharma, K. P., 1994. Sambhar lake Rajasthan (Ramsar site of India), WWF publication.

Gupta, R. P., 1991. *Remote Sensing Geology*, Springer-verlag, Berlin Heidelberg.

Hacket. C. A., 1989. Salt in Rajputana. Rec. Geol. Surv. India. v. 13, 197p.

Haralick, R. M., Sternberg, S. R. and Zhaung, X., 1987. " Image analysis using mathematical morphology", *IEEE Trans., Pattern Analysis and Machine Intelligence*, PAMI-6(1), 58-68.

Heron. A. M., 1917. The geology of northeastern Rajputana. Memoir Geol. Surv. India. v.45. 128p.

Kar, A., 1989.*Geog. Rev. India*, v. 51, pp. 48-99.

Kitler and Illingworth, J., 1985. "On threshold selection using clustering criteria", *IEEE Trans. Systems, Man and Cybernetics*, SMC-15(5), pp.652-655.

Lillesand, Thomas M. and Kiefeer, Ralph. W., 1994. *Remote Sensing and Image Interpretation*, 3rd ed. John Wiley & Sons.

Mather, P. M., 1987. *Computer processing of remotely sensed images*, John Wiley & Sons, NY.

Mokhopadhya, D. and Dasgupta, S., 1978. "Delhi-preDelhi relations near Bandar, Central Rajasthan", *Indian Jour. of Earth Sci.*, v. 7, pp.64-75.

Otsu, N., 1979. "A threshold selection method from grey-level-histograms", *IEEE Trans., Systems, Man and Cybernetics,* SMC-21 3 , pp. 660-674.

Raju, A. T. R., 1968. Bull. Am. Assoc. Petrol. Geol., v. 52, pp. 2422-2437.

Reeves, C. C., 1968. *Introduction to Palaeolimnology, Development in Sedimentology*, Elisevier publishing company.

Reeves, C. C. and Judy, A. Reeves, 1996. The Ogallala Aquifer (of the Southern High Plains). Lubbock, TX : Estacado Books.

Roy, A. B., 1999. "Evolution of saline lakes in Rajasthan", *Current Science*, v. 76, pp. 290-295.

Roy, A. B. and Das, A. R., 1985 " A study of time relations between movements, Metamorphism and Granite emplacement in the middle proterozoic Delhi Supergroup Rocks of Rajasthan", *Jour. Geol. Soc. India*, v. 26, pp.229-236.

Roy, J. N. and Sen, S., 1983. " Post neogen tectonism along the Aravalli range, Rajasthan, India", v. 24, pp.229-236.

Sen, A. K. and Ramalingam, 1976. Report on the geology of the area around Sambhar lake, Jaipur and Nagaur districts, Rajasthan, Progress report, G.S.I (Unpub.).

Sen, D. and Sen, S., 1983. " Post neogen tectonics along Aravalli range, Rajasthan, India", *Tectono Physics*, v. 93, pp.75-98.

Sharma, H. S., " Geomorphological Aspects of the Processes of Desertification – A case study of Sambhar Lake and Environs " (ed Sharma, H. S.), *Indian Geomorphology.*, pp. 57-66.

Singh, G., Joshi, R. D. and Singh, A. B., 1972. "Stratigraphic and radiocarbon evidence for the age and development of three salt lake deposits in Rajasthan, India. - Quat. Res. 2 4 , pp.496-505.

Singh, S., 1994."Geomorphology of the Indian desert" (eds Dikshit, K. R., Vishwas, S. K. and Kaul, M. N.), *India: Geomorphological Diversity*, Rawat Publications, Jaipur, pp. 370-394.

Singh, S. P., 1988. "Stratigraphy and Sedimentation pattern in the proterozoic Delhi Supergroup, Northwestern India, In. Pre. Cambrian of Aravalli Mountain Rajasthan, India", *Geol. Soc. of India*, Memoir 7, pp.193-206.

Sinha-Roy, S., 1988. Proceedings of the International Symposium on Neotectonics in South Asia, Dehradun, India, 7, 109-120.

Sundaram, R. M. and Suresh Pareek., 1995. "Quarternary Facies and Palaeoenvironment in North and East of Sambhar Lake, Rajasthan", *Journal Geological Society of India*, v. 46, pp. 387-392.

Tiwari, K. C., and Gangadhar, K., 1997. Abstract, Discussion on 'Drainage evolution of northwestern India with particular reference to the lost Saraswati', MS University, Baroda, p. 41.

Wasson, R. J., Rajaguru, S. N., Misra, V. N., Aggarwal, D. P., Dhir, R. P., Singhvi, A. K. and Kameswara Rao, K., 1983. " Geomorphology, late Quarternary stratigraphy and palaeoclimatolog of the Thar dunefield ", *Z. Geomorph N. F.*, v. 45, pp. 117-151.

EDGE FILTERS

Edges are extracted by convolving the image ($F(i, j)$) with some edge filters in different directions to calculate first the directional gradients. For instance, the gradients in row and column direction can be calculated as below

$$G_R(i,j) = F(i,j) \otimes H_R(i,j)$$
$$G_C(i,j) = F(i,j) \otimes H_C(i,j)$$

Where, $G_R(i,j)$ and $G_C(i,j)$ are the row and column gradients while $H_R(i,j)$ and $H_C(i,j)$ are defined in the table below for few types of masks.

The spatial gradient amplitude, $G(i, j)$, at location (i, j) is given by

$$G(i,j) = \left[G_R(i,j)^2 + G_C(i,j)^2\right]^{1/2}$$

The approximations of this for computational efficiency are as follows

$$G(i,j) = |G_R(i,j)| + |G_C(i,j)|$$

$$G(i,j) = Max\{|G_R(i,j)|, |G_C(i,j)|\}$$

Operator	Row Gradient($H_R(i,j)$)	Column Gradient($H_C(i,j)$)
Prewitt	$\frac{1}{3}\begin{bmatrix} 1 & 0 & -1 \\ 1 & 0 & -1 \\ 1 & 0 & -1 \end{bmatrix}$	$\frac{1}{3}\begin{bmatrix} -1 & -1 & -1 \\ 0 & 0 & 0 \\ 1 & 1 & 1 \end{bmatrix}$
Sobel	$\frac{1}{4}\begin{bmatrix} 1 & 0 & -1 \\ 2 & 0 & -2 \\ 1 & 0 & -1 \end{bmatrix}$	$\frac{1}{4}\begin{bmatrix} -1 & -2 & -1 \\ 0 & 0 & 0 \\ 1 & 2 & 1 \end{bmatrix}$
Frei-Chen	$\frac{1}{2+\sqrt{2}}\begin{bmatrix} 1 & 0 & -1 \\ \sqrt{2} & 0 & -\sqrt{2} \\ 1 & 0 & -1 \end{bmatrix}$	$\frac{1}{2+\sqrt{2}}\begin{bmatrix} -1 & -\sqrt{2} & -1 \\ 0 & 0 & 0 \\ 1 & \sqrt{2} & 1 \end{bmatrix}$

Kirsh Filter

Kirsh filter has eight compass masks computing gradients in eight directions. The image is convolved with all the directional masks given below. Then, the edge gradient as defined by the Kirsh operator is given by

$$G(i,j) = Max\{|G_1(i,j)|,.....,G_m(i,j)|\}$$

Where, $G_m = F(i,j) \otimes H_m(i,j)$ is the gradient in the mth equispaced direction obtained by convolving with a gradient impulse response array H given below.

East	$\begin{bmatrix} 5 & -3 & -3 \\ 5 & 0 & -3 \\ 5 & -3 & -3 \end{bmatrix}$	*West*	$\begin{bmatrix} -3 & -3 & 5 \\ -3 & 0 & 5 \\ -3 & -3 & 5 \end{bmatrix}$
Northeast	$\begin{bmatrix} -3 & -3 & -3 \\ 5 & 0 & -3 \\ 5 & 5 & -3 \end{bmatrix}$	*Southwest*	$\begin{bmatrix} -3 & 5 & 5 \\ -3 & 0 & 5 \\ -3 & -3 & -3 \end{bmatrix}$
North	$\begin{bmatrix} -3 & -3 & -3 \\ -3 & 0 & -3 \\ 5 & 5 & 5 \end{bmatrix}$	*South*	$\begin{bmatrix} 5 & 5 & 5 \\ -3 & 0 & -3 \\ -3 & -3 & -3 \end{bmatrix}$
Northwest	$\begin{bmatrix} -3 & -3 & -3 \\ -3 & 0 & 5 \\ -3 & 5 & 5 \end{bmatrix}$	*Southeast*	$\begin{bmatrix} 5 & 5 & -3 \\ 5 & 0 & -3 \\ -3 & -3 & -3 \end{bmatrix}$

Thresholding Method by Otsu (1979)

It is a non-parametric and unsupervised method of automatic threshold selection for picture segmentation based on maximising the separability of the resulting grey levels. Let a picture has L grey levels {0, 1, 2, 3, - - -, L-1} and let N be total pixels in image with $N = n_0 + n_1 + n_2 + - - - + n_{L-1}$, where n_I is number of pixels with grey level i. Then,

$$p_i = \frac{n_i}{N} \text{ , } p_I \geq 0 \text{ and } \sum_{i=0}^{L-1} p_i = 1 \qquad \text{(A.2.1)}$$

If the image is divided into two regions C_0 and C_1 (background and objects) by a threshold t then C_0 represents all pixels with grey levels [0, 1, 2, 3, - - - t] and C_1 denotes all pixels with grey levels [t+1, t+2, - - -, L-1]. The probabilities of class occurrences and class mean levels are given by

$$\omega_0 = \Pr(C_0) = \sum_{i=0}^{t} p_i = \omega(t) \qquad \text{(A.2.2)}$$

$$\omega_1 = \Pr(C_1) = \sum_{i=t+1}^{L-1} p_i = 1 - \omega(t) \qquad \text{(A.2.3)}$$

$$\mu_0 = \sum_{i=0}^{t} i \Pr(i / C_0) = \sum_{i=0}^{t} i(P_i / \omega_0) = \frac{\mu(t)}{\omega(t)} \qquad \text{(A.2.4)}$$

$$\mu_1 = \sum_{i=t+1}^{L-1} i \Pr(i / C_1) = \sum_{i=t+1}^{L-1} i(P_i / \omega_1) = \frac{\mu_T - \mu(t)}{1 - \omega(t)} \qquad \text{(A.2.5)}$$

where

$$\omega(t) = \sum_{i=0}^{t} p_i \qquad \text{(A.2.6)}$$

$$\mu(t) = \sum_{i=0}^{t} i p_i \qquad \text{(A.2.7)}$$

are the zeroth and the first-order cumulative moments of histogram up to the i^{th} level respectively and

$$\mu(t) = \sum_{i=0}^{L-1} i p_i \tag{A.2.8}$$

is the mean of picture. For any choice of t, following conditions should be satisfied:

$$\omega_0 \mu_0 + \omega_1 \mu_1 = \mu_T \text{ , and } \omega_0 + \omega_1 = 1 \tag{A.2.9}$$

The class variances are given by:

$$\sigma_0^{\,2} = \sum_{i=0}^{t} (i - \mu_0)^2 \Pr(i / C_0) = \sum_{i=0}^{t} (i - \mu_0)^2 (p_i / \omega_0) \tag{A.2.10}$$

$$\sigma_1^{\,2} = \sum_{i=t+1}^{L-1} (i - \mu_1)^2 \Pr(i / C_1) = \sum_{i=t+1}^{L-1} (i - \mu_1)^2 (p_i / \omega_1) \tag{A.2.11}$$

Otsu introduced following criterion functions to evaluate the goodness of the threshold at level t:

$$\lambda = \frac{\sigma_b^{\,2}}{\sigma_w^{\,2}} \tag{A.2.12}$$

$$\kappa = \frac{\sigma_T^{\,2}}{\sigma_w^{\,2}} \tag{A.2.13}$$

$$\eta = \frac{\sigma_b^{\,2}}{\sigma_T^{\,2}} \tag{A.2.14}$$

where

$$\sigma_w^{\,2} = \omega_0 \sigma_0^{\,2} + \omega_1 \sigma_1^{\,2} \tag{A.2.15}$$

$$\sigma_b^{\,2} = \omega_0 (\mu_0 - \mu_T)^2 + \omega_1 (\mu_1 - \mu_T)^2 + \omega_0 \omega_1 (\mu_1 - \mu_0)^2 \tag{A.2.16}$$

$$\sigma_T^{\,2} = \sum_{i=1}^{L} (i - \mu_T)^2 p_i \tag{A.2.17}$$

$\sigma_w^{\,2}$, $\sigma_b^{\,2}$ and $\sigma_T^{\,2}$ are called within class, between class, and the total class variance of grey levels. The problem becomes to find out a threshold t such that one of the objective

functions from Equations A.2.15-A.2.17 are maximized. Also, the discriminating criterion of maximizing λ, κ, and η are equivalent to one another as,

$$\kappa = \lambda + 1 \tag{A.2.18}$$

$$\eta = \frac{\lambda}{\lambda + 1} \tag{A.2.19}$$

because

$$\sigma_w^{\,2} + \sigma_b^{\,2} = \sigma_T^{\,2} \tag{A.2.20}$$

In all these expressions $\sigma_w^{\,2}$ and $\sigma_b^{\,2}$ are functions of threshold level t but $\sigma_T^{\,2}$ is independent of t. Also $\sigma_w^{\,2}$ is based on the second order statistics (class variances) and $\sigma_b^{\,2}$ is based on the first order statistics (class means). On these basis η is selected as the simplest criterion function to get the optimal threshold. The optimal threshold t^* that maximizes η or equivalently maximizes $\sigma_b^{\,2}$ is selected following a sequential search by using the expression:

$$\sigma_b^{\,2} = \frac{[\mu_T \omega(t) - \mu(t)]^2}{\omega(t)(1-\omega(t))} \tag{A.2.21}$$

and optimal threshold t^* is:

$$s_b^{\,2}(t^*) = Max s_b^{\,2}(t^*);\ 1 \le t \le L\text{-}1 \tag{A.2.21}$$

The range of t over which maximum is sought is restricted to,

$$S^* = \{t; w_0 w_1 = w(t)[1 - w(t)] \ge 0,\ or\ 0 < w(t) < 1\} \tag{A.2.23}$$

* is termed effective range of histogram. From definition of $\sigma_b^{\,2}$, it takes a minimum alue of zero for such values of t as

$$t \in S - S^* = \{t; \omega(t) = 0 \text{ or } 1\} \tag{A.2.24}$$

making all pixels either C_1 or C_0 and takes a positive and bounded value for $t \in S^*$.

Kitler and Illingworth (1985) found that Otsu's method performs significantly well for range of applications. However, their experiments revealed that this method breaks down for certain populations which occur quite frequently in nature. Otsu proposed a criterion function $J_0(t)$ defined as (see Equation A.2.21 also):

$$J_0(t) = N_1(T)N_2(T) \times \frac{[\mu_1(T) - \mu_2(T)]^2}{N_1(T) + N_2(T)} \qquad \text{(A.2.25)}$$

Where $\mu_i(T), i = 1, 2$, is mean of i^{th} population and $N_i(T)$ is the number of pixels constituting it. The function $J_0(T)$ behaves well; i.e. it has just one maximum that corresponds to a good threshold value if the objective function $J_0(T)$ is unimodal. But it has been observed by Kittler and Illingworth (1985) that the objective function $J_0(T)$ may be multimodal. It means that its global maximum is not guaranteed to give a correct threshold. As the population sizes of the background and object become greatly dissimilar, the criterion function becomes bimodal with the second mode centered near the mean grey level of large population. The exact range of population size ratios over which $J_0(T)$ is bimodal will depend upon the increasing population imbalance. The second mode grows in size while the first mode diminishes until at very large disparities the objective function once more appears unimodal.

These findings suggest that it is not enough to find the global maximum. One should analyse all possible local peaks of threshold. Having found the local peaks, one should determine which peak is associated with good threshold. Kittler and Illingworth (1985) proposed following algorithm for this:

(a) select candidate threshold, T_i, using $J_0(T)$.

(b) find mean of two populations obtained at threshold T_i,

say they are μ_{i1} and μ_{i2}.

(c) the candidate threshold should satisfy following conditions:

$$h(T_1) < h(\mu_{i1}),\ h(T_1) < h(\mu_{i2}) \tag{A.2.26}$$

where $h(g)$ represents frequency of histogram at grey level g. However, if the histogram is noisy then it is more reliable to check for this condition:

$$\sum_{j=-1}^{1} h(T_i + j) < \sum_{j=-1}^{1} h(\mu_{i1} + j) \tag{A.2.27}$$

$$\sum_{j=-1}^{1} h(T_i + j) < \sum_{j=-1}^{1} h(\mu_{i2} + j) \tag{A.2.28}$$

It may well be the case that for bimodal criterion function, $J_0(T)$, both candidate thresholds satisfy above conditions implying that both thresholds are likely to be valid. Alternatively, one can say that it is not possible to binarize the image without loosing the meaningful information. Equations A.2.27 and A.2.28 represents *valley check* conditions which is very useful even if the objective function has only one mode as it may arise out of various conditions. For example, for images with bimodal histogram the valley check will be satisfied, confirming that binarization is possible. However, if none of the conditions is satisfied, it implies that histogram is either unimodal or bimodal, with the relative populations size of one of the modes very large. Hence, a more sophisticated approach is needed for such situations.

In case of a histogram of edge magnitudes, one gets a unimodal histogram and objective function, however, only one valley check condition will be satisfied, hence suggesting that image may be thresholdable but the point of maximum of objective function will not necessarily be a good threshold. (Additional information using grey level thinning method will enhance the separability of edge. Anonedge modes in histogram and convert the histogram in bimodal form (Kittler and Illingworth, 1985) thereby enabling to find a good threshold.